Identification and Interaction Analysis of Molecular Markers in Pancreatic Ductal Adenocarcinoma by Integrated Bioinformatics Analysis and Molecular Docking Experiments

Basavaraj Vastrad[1] , Chanabasayya Vastrad [*2], Anandkumar Tengli[3]

1. Department of Biochemistry, Basaveshwar College of Pharmacy, Gadag, Karnataka 582103, India.

2. Biostatistics and Bioinformatics,Chanabasava Nilaya, Bharthinagar, Dharwad, Karanataka 580001, India.

3. Department of Pharmaceutical Chemistry, JSS College of Pharmacy, Mysuru and JSS Academy of Higher Education & Research, Mysuru- 570015, Karnataka, India.

* Chanabasayya Vastrad

channu.vastrad@gmail.com

Ph: +919480073398

Chanabasava Nilaya, Bharthinagar,

Dharwad 580001 , Karanataka, India

Abstract

The current investigation aimed to mine therapeutic molecular targets that play an key part in the advancement of pancreatic ductal adenocarcinoma (PDAC). The expression profiling by high throughput sequencing dataset profile GSE133684 dataset was downloaded from the Gene Expression Omnibus (GEO) database. Limma package of R was used to identify differentially expressed genes (DEGs). Functional enrichment analysis of DEGs were performed. Protein-protein interaction (PPI) networks of the DEGs were constructed. An integrated gene regulatory network was built including DEGs, microRNAs (miRNAs), and transcription factors. Furthermore, consistent hub genes were further validated. Molecular docking experiment was conducted. A total of 463 DEGs (232 up regulated and 231 down regulated genes) were identified between very early PDAC and normal control samples. The results of Functional enrichment analysis revealed that the DEGs were significantly enriched in vesicle organization, secretory vesicle, protein dimerization activity, lymphocyte activation, cell surface, transferase activity, transferring phosphorus-containing groups, hemostasis and adaptive immune system. The PPI network and gene regulatory network of up regulated genes and down regulated genes were established, and hub genes were identified. The expression of hub genes (CCNB1, FHL2, HLA-DPA1 and TUBB1) were also validated to be differentially expressed among PDAC and normal control samples. Molecular docking experiment predicted the novel inhibitory molecules for CCNB1 and FHL2. The identification of hub genes in PDAC enhances our understanding of the molecular mechanisms underlying the progression of this disease. These genes may be potential diagnostic biomarkers and/or therapeutic molecular targets in patients with PDAC.

Keywords: pancreatic ductal adenocarcinoma; bioinformatics analysis; biomarker; enrichment analysis; differentially expressed genes

Introduction

Pancreatic ductal adenocarcinoma (PDAC) is one of the most prevalent cancers in the world and primary tumor of the pancreas [1]. PDAC is a global burden ranking 15th in terms of incidence and fourth in terms of mortality [2]. Despite new developments in multimodal therapy its overall 5-year survival rate remains less than 8% [3]. PDAC treatment commonly includes surgery, radiation, chemotherapy and immunotherapy [4]. However, PDAC remains common and malignant due to recurrence and metastasis, and ultimately key cause of PDAC associated death [5]. Therefore, there is a vital need to advance new diagnostic strategies and therapeutic agents to upgrade the prognosis of patients with PDAC.

The molecular mechanisms of PDAC tumorigenesis and development remain imprecise. It is therefore key to identify novel genes and pathways that are linked with PDAC tumorigenesis and patient prognosis, which may not only help to illuminate the underlying molecular mechanisms involved, but also to disclose novel diagnostic markers and therapeutic targets. Oji et al [6] demonstrated that the over expression of WT1 is linked with prognosis in patients with PDAC. A previous investigation reported that phosphoinositide 3-kinase signaling pathway is linked with development of PDAC [7]. Expression profiling by high throughput sequencing can promptly uncover gene expression on a global basis and are specially useful in identifying for differentially expressed genes (DEGs) [8]. A huge amount of data has been generated through the use of microarrays and the majority of such data has been deposited and saved in public databases. Previous investigations concerning PDAC gene expression profiling have diagnosed hundreds of DEGs [9].

The aim of this investigation was to identify hub genes and pathways in PDAC using bioinformatics methods. Our investigation contributes predictable biomarkers for early detection and prognosis, as well as effective drug targets for treating PDAC.

Materials and methods

Sequencing data

PDAC expression profiling by high throughput sequencing dataset in this investigation was downloaded from the GEO database (https://www.ncbi.nlm.nih.gov/gds/) [10]. The DEGs were considered by 1 independent PDAC dataset, GSE133684 [11] with 284 PDAC and 117 normal samples. The GSE133684 expression profiling by high throughput sequencing data was based on the GPL20795 HiSeq X Ten (Homo sapiens) platform..

Identification of DEGs

The Limma package of R language were used to normalize and convert the raw data to expression profiles [12]. The limma package of R language was used for DEGs between PDAC and normal control samples [12]. The P-value was adjusted by the Benjamini-Hochberg method [13]. An adjusted P-value <0.05 and |log2 fold change (FC) | >1 were considered as threshold values for DEGs identification. The ggplot2 package and gplots package of R language was used to generate volcano plot and heat map. The identified DEGs were preserved for further bioinformatics analysis.

GO analysis and pathway enrichment analysis of DEGs

The GO repository (http://geneontology.org/) [14] consists of a massive set of annotation terms and is generally used for annotating genes and identifying the distinctive biological aspects for expression profiling by high throughput sequencing data. The REACTOME database (https://reactome.org/) [15] contains data on known genes and their biochemical functions and is used for identifying functional and metabolic pathways. By performing the GO and REACTOME enrichment analysis at the functional level, we can boost a better understanding of the roles of these DEGs in the induction and in the advancement of PDAC. The ToppGene (ToppFun) (https://toppgene.cchmc.org/enrichment.jsp) [16] is an online resource that add tools for functional annotation and bioinformatics analysis. Both GO categories and REACTOME pathway enrichment analysis were implemented using ToppGene to inform the functions of these DEGs. P<0.05 was considered to indicate a statistically significant difference.

Protein-protein interaction (PPI) network construction and module analysis

The online database IID interactome (http://iid.ophid.utoronto.ca//) [17] was used to construct a PPI network of the proteins encoded by DEGs. Then, Cytoscape software (Version 3.8.1) [18] was applied to perform protein interaction association network analysis and analyze the interaction correlation of the candidate proteins encoded by the DEGs in PDAC. Next, the Network Analyzer Cytoscape plug-in was applied to calculate node degree [19], betweenness centrality [20], stress centrality [21], closeness centrality [22]. Finally, the PEWCC1 (http://apps.cytoscape.org/apps/PEWCC1) [23] module for Cytoscape was used to collect the significant modules in the PPI network complex.

Construction of miRNA-DEG regulatory network

The miRNet database (https://www.mirnet.ca/) [24] is a database, containing miRNAs involved in various diseases. The miRNAs related to PDAC were searched from miRNet database. Through getting the intersection of the miRNAs and the DEGs, the miRNA-DEG regulatory relationships were selected. Finally, miRNA-DEG regulatory network was built using Cytoscape software.

Construction of TF-DEG regulatory network

The NetworkAnalyst database (https://www.networkanalyst.ca/) [25] is a database, containing TFs involved in various diseases. The TFs related to PDAC were searched from TF database. Through getting the intersection of the TFs s and the DEGs, the TF-DEG regulatory relationships were selected. Finally, TFs -DEG regulatory network was built using Cytoscape software.

Hub genes validation

After hub genes identified from expression profiling by high throughput sequencing dataset, UALCAN (http://ualcan.path.uab.edu/analysis.html) [26] was used to validate the selected up regulated and down regulated hub genes. UALCAN is an online tool for gene expression analysis between PDAC and normal data from The Cancer Genome Atlas (TCGA). It adds data such as gene expression, tumor staging, and survival period for PDAC. cBioPortal is an online platform (http://www.cbioportal.org) [27] for gene alteration of hub genes analysis from TCGA. Human protein atlas is an online database (HPA, www.proteinatlas.org) [28] for protein expression analysis between PDAC and

normal data from TCGA. TIMER is an online platform (https://cistrome.shinyapps.io/timer/) [29] for immune infiltration analysis from TCGA. To explore diagnostic biomarkers of PDAC, we used the above hub genes as candidates to find their diagnostic value based on generalized linear model (GLM) [30]. The pROC in R was used for Receiver operating characteristic (ROC) curve analysis [30]. In brief, half of the samples (PDAC = 142, controls = 59) were aimlessly distributed as the training set and remaining data were used as the test set, which were used to set up a model. An ROC curve analysis was tested to calculate the specificity and sensitivity of the GLM prediction model. The area under the curve (AUC) was figure out to determine the diagnostic efficiency of the classifier.

RT-PCR analysis

TRI Reagent® (Sigma, USA) was used to extract total RNA from the culture cells of PDAC (CRL-2549™) and normal (CRL-2989™) according to the manufacturer's protocol. Reverse transcription cDNA kit (Thermo Fisher Scientific, Waltham, MA, USA) and random primers were used to synthesize cDNA. Quantitative real-time PCR (qRT-PCR) was conducted on the 7 Flex real-time PCR system (Thermo Fisher Scientific, Waltham, MA, USA). The reaction guideline included a denaturation program (5 min at 95 °C), followed by an amplification and quantification program over 40 cycles (15 s at 95°C and 45 s at 65°C). Each sample was tested in triplicates. Table 1 depicts the primer sequences of hub genes. The expression level was resolved as a ratio between the hub genes and the internal control β-actin in the same mRNA sample, and determined by the comparative CT method [31]. Levels of CCNB1, FHL2, HLA-DPA1 and TUBB1 expression were determined by the $2^{-\Delta\Delta Ct}$ method.

Molecular docking experiment

The module SYBYL-X 2.0 perpetual software were used for Surflex-Docking of the designed molecules. The molecules were sketched by using ChemDraw Software and imported and saved in sdf. format using openbabel free software. The protein structures of CyclinB1 (CCNB1) its co-crystallisedprotein of PDB code 4Y72, 5H0V and Four and half LIM domains 2 (FHL2) its NMR structure of proteins 2D8Z and 2EHE was retrieved from Protein Data Bank [32-34]. Together

with the TRIPOS force field, GasteigerHuckel (GH) charges were added to all designed derivatives for the structure optimization process.In addition, energy minimization was carried outusing MMFF94s and MMFF94 algorithm process. Protein processing was carried out after the incorporation of protein.The co-crystallized ligand and all water molecules were removed from the crystal structure; more hydrogens were added and the side chain was set. TRIPOS force field was used for the minimization of structure. The compounds' interaction efficiency with the receptor was represented by the Surflex-Dock score in kcal / mol units. The interaction between the protein and the ligand, the best pose was incorporated into the molecular area. The visualisation of ligand interaction with receptor is done by using discovery studio visualizer.

Results

Identification of DEGs

We analyzed the DEGs of GSE133684 by using the limma package. We used $p < 0.05$ and $|logFC| \geq 1$ as the cutoff criteria. We screened 463 DEGs, including 232 up regulated genes and 231 down regulated genes in PDAC samples compared with normal control samples and are listed in Table 2. We identified all the DEGs which were shown in the above volcano map according to the value of |logFC| is shown in Fig. 1 and then displayed the DEGs on a heatmap is shown in Fig. 2.

GO analysis and pathway enrichment analysis of DEGs

To symbolize the function of the DEGs and to identify important candidate pathways, GO functional enrichment analysis and REACTOME pathway enrichment analysis were performed. The results of GO categories analysis including biological processes (BP), cellular components (CC) and molecular functions (MF) are listed in Table 3. Firstly, the up regulated genes were annotated with the BP category, including vesicle organization and secretion, whereas the down regulated genes were annotated with the GO terms, including lymphocyte activation and regulation of cell death. Secondly, the up regulated genes were annotated with the GO terms of the CC category, namely secretory vesicle and whole membrane, whereas the down regulated genes were annotated with the GO terms, including cell surface and intrinsic component of plasma membrane.

Thirdly, the up regulated genes were annotated with the GO terms of the MF category, such as protein dimerization activity and signaling receptor binding, whereas the down regulated genes were annotated with the GO terms, including transferase activity, transferring phosphorus-containing groups and drug binding. As shown in Table 4, the significantly enriched REACTOME pathways of the up regulated genes with $P<0.05$ were hemostasis and cell cycle, whereas down regulated genes with $P<0.05$ were adaptive immune system and transmembrane transport of small molecules.

Protein-protein interaction (PPI) network construction and module analysis

After all the DEGs were uploaded to the online IID interactome database, the PPI network with 6188 nodes and 13153 edges was constructed using the Cytoscape software (Fig. 3A). Hub DEGs with the node degree, betweenness centrality, stress centrality and closeness centrality were obtained and are listed in Table 5. Among them, CCNB1 and FHL2 were the major up regulated genes, while HLA-DPA1 and TUBB1 were the major down regulated genes. Then, two significant module that fulfilled the cut-off criteria, namely, PEWCC1 scores >3 and number of nodes >5, was screened (Fig. 3B and Fig. 3C). The FGB, FGA, FGG, EEF1A1, RPL13A, ITGA4, RPL27A, RPL23A and RPL10 genes were identified in these modules. GO analysis of these genes showed that they were annotated with vesicle organization, regulation of cell death and lymphocyte activation. In addition, the REACTOME enrichment analysis suggested that these genes were mainly involved in hemostasis, innate immune system, disease and adaptive immune system.

Construction of miRNA-DEG regulatory network

The regulatory network of miRNA-DEG and predicted targets is presented in Fig. 4A. Notably, MAP1B targeted 202 miRNAs, including hsa-mir-4461; CCNB1 targeted 94 miRNAs, including hsa-mir-3928-3p; AHNAK targeted 256 miRNAs, including hsa-mir-2682-5p; KMT2D targeted 209 miRNAs, including hsa-mir-1202 and top 20 are listed in Table 6. As a group, a total of 257 of the 463 DEGs were contained in the miRNA-DEG regulatory network.

Construction of TF-DEG regulatory network

The regulatory network of TF-DEG and predicted targets is presented in Fig. 4B. Notably, EZH2 targeted 45 TFs, including SOX2; TPM1 targeted 40 TFs, including MYC; AHNAK targeted 58 TFs, including KLF4, TXNIP targeted 51 TFs, including TP63 and top 20 are listed in Table 6. As a group, a total of 259 of the 463 DEGs were contained in the TF-DEG regulatory network.

Hub genes validation

All of the hub genes were validated in TCGA data. Hub genes contributed to the survival period in patients with PDAC, we analyzed the overall survival (OS) for each hub gene by UALCAN (Fig. 5). The results showed that the high expression of CCNB1 and FHL2 mRNA level were associated with the worse OS in patients with PDAC, while low expression of HLA-DPA1 and TUBB1 mRNA level were associated with the worse OS in patients with PDAC. As shown in Fig. 6, the expression of the up regulated hub genes CCNB1 and FHL2 in PDAC were significantly elevated compared with normal, while expression of the down regulated hub genes HLA-DPA1 and TUBB1 in PDAC were significantly decreased compared with normal. The expression of each hub gene in PDAC patients was analyzed according to the individual cancer stage. As shown in Fig. 7, the expression of CCNB1 and FHL2 were higher in patients with all individual cancer stages than that in normal, which revealed that these up regulated hub genes might be associated with tumor progression positively, where as the expression of HLA-DPA1 and TUBB1 were lower in patients with all individual cancer stages than that in normal, which revealed that these down regulated hub genes might be associated with tumor progression positively. We used cBioportal tool to explore the specific mutation of hub genes in PDAC dataset with 184 samples. From the OncoPrint, percentages of alterations in CCNB1, FHL2, HLA-DPA1 and TUBB1 genes among lung cancer ranged from 0% to 2.3% in individual genes (CCNB1, 0%; FHL2, 0.6%; HLA-DPA1, 2.3%; TUBB1, 2.3%) and is shown in Fig. 8. In addition, we used the ‘HPA’ to examine the protein expression levels of CCNB1 and FHL2, and observed that the protein expression levels of the these hub genes were noticeably up regulated in PDAC compared with normal tissues, whereas protein expression levels of HLA-DPA1 and TUBB1, and observed that the protein expression levels of the these hub genes were noticeably down regulated in PDAC compared with normal tissues (Fig. 9). The association of CCNB1, FHL2, HLA-DPA1 and TUBB1 expression level with immune infiltration abundance in PDAC

was evaluated using TIMER database. CCNB1 and FHL2 expression were negatively correlated with infiltration degree of B cells, CD8+ T cells, macrophage, neutrophil, and dendritic cells, where as HLA-DPA1 and TUBB1 were positively correlated with infiltration degree of B cells, CD8+ T cells, macrophage, neutrophil, and dendritic cells and is shown in Fig. 10. As these 4 genes are prominently expressed in PDAC, we performed a ROC curve analysis to evaluate their sensitivity and specificity for the diagnosis of PDAC. As shown in Fig. 11, CCNB1, FHL2, HLA-DPA1 and TUBB1 achieved an AUC value of >0.70, demonstrating that these genes have high sensitivity and specificity for PDAC diagnosis. The results suggested that CCNB1, FHL2, HLA-DPA1 and TUBB1 can be used as biomarkers for the diagnosis of PDAC.

RT-PCR analysis

Next, in order to verify the results of previous bioinformatics analysis, the gene expression levels of CCNB1, FHL2, HLA-DPA1 and TUBB1 were detected by RT-PCR. As shown in Fig 12, CCNB1 and FHL2 mRNA expression levels were significantly up regulated in the PDAC compared to normal, and HLA-DPA1 and TUBB1 mRNA level were down regulated compared to normal, which was consistent with the results of bioinformatics analysis.

Molecular docking experiment

The docking simulation was performed in the present study to recognize the active site conformation andsignificant interactions, which are responsible for complex stability with ligand receptor. Novel molecules containing alkylating group and purine heterocyclic ring were designed and performed docking studies using Sybyl X 2.1 drug design software. Molecules containing alkylating group is designed due to non-specific alkylation of physiologically important groupings and purine heterocyclic ring is incorporated due to structural similarity of purine derivatives and to compete for the synthesis of proteins. The proteins which are over expressed in pancreatic duct adenocarcinoma are selected for docking studies. The two proteins of each over expressedcyclin B1 (CCNB1)its co-crystallised protein of PDB code 4Y72, 5H0V and Four and half LIM domains 2 (FHL2) of NMR structure of proteins 2D8Z and 2EHE were selected for docking. The investigation of designed molecules was performed to identify the potential molecule. The most

of the designed molecules obtained C-score greater than 5 and are active having the c-score greater than 5 are said to be an active, among total of 48 designed molecules few molecules have excellent good binding energy (C-score) greater than 8 respectively. Few of the designed molecules IM 11 & PU 42, shown good binding score of 7.83& 8.57 and the molecules IM 13, TZ 23, TZ 27, TZ 37, PU 41, PU 43 & PU 49 have good binding score 8.013, 8.523, 8.235, 8.800, 10.338, 10.891& 9.411 with CCNB1 PDB code 1H0V and 4Y72 respectively and are shown in Fig. 13. Molecules of IM 09, IM 10, IM & 18 shown good binding score of 7.14, 7.75 & 7.80 and the molecules IM 8 and TZ 24 with binding score 6.24 and 6.32 with FHL2 of PDB code 2D8Z and 2EQQ respectively, the values are depicted in Table 7. The molecule IM 8has highest binding score its interaction with protein 1H0V and hydrogen bonding and other bonding interactions with amino acids are depicted by 3D and 2D shown in Fig. 14 and Fig. 15.

Discussion

Due to the high heterogeneity of PDAC, PDAC was still a disease with high rates of pervasiveness and fatality. With surgery as the main, the other treatments including radiotherapy, chemotherapy, targeted therapy, and gene therapy as a additive to the finite treatment measures of PDAC, the 5-year survival rate was still less than 8% [35]. Therefore, the early diagnosis and effective treatment of PDAC is crucially required, which may be achieved via the identification of the DEGs between PDAC and normal control, and by considerate the underlying molecular mechanism. Microarray and high throughput sequencing analysis can screen a massive number of genes in the human genome for farther functional analysis, and can be extensively used to screen biomarkers for early diagnosis and unique therapeutic targets. Therefore, they may help the diagnosis of PDAC in the early stages and the advancement of targeted treatment, thus developing prognosis.

The current investigation systematically applied integrated bioinformatics methods to identify novel biomarkers that serve roles in the advancement PDAC. The data extracted from the GEO dataset contained 31 pairs of lung cancer and normal samples. A total of 232 up regulated and 231 down regulated genes in PDAC, when compared with normal control samples, were identified using bioinformatics analysis, indicating that the incidence and advancement of PDAC. The results of the DEGs may provide potential biomarkers for the diagnosis of

PDAC. DAP (death associated protein) [36], KRT8 [37], IGFBP2 [38], KRT19 [39], CD44 [40], AHNAK (AHNAK nucleoprotein) [41] and BTG1 [42] are a noticeable factors in the PDAC progression. Wang et al [43] reported that KIF2C induces proliferation, migration, and invasion in gastric cancer patients through the MAPK signaling pathway, but this gene might be associated with development of PDAC. DBN1 expression was significantly increased in breast cancer [44], but this gene might be liable for development of PDAC. MAP1B was reported to lung cancer progression [45], but this gene may be key for advancement of PDAC. BNIP3L down regulation was required to develop breast and ovarian cancer [46], but this down regulation of gene might be involved in progression of PDAC. Yen et al [47] reported that ITGA4 was expressed in oral cancer, but this gene might be novel biomarker for PDAC. Tomsic et al. [48] showed that mutation in SRRM2 was associated with progression of thyroid carcinoma, but alteration in this gene might be key factor for advancement of PDAC. Recent studies have shown that down regulation of IL7R is associated with progression of esophageal squamous cell carcinoma [49], but this gene might be involved in pathogenesis of PDAC. Lee et al [50] found that reduced expression of the HLA-DRA is key factor for development of colorectal cancer, but this gene might be linked with advancement of PDAC. Liu et al. [51] reported that the absence of SESN3 linked with development of hepatocellular carcinoma, but this gene might be associated with progression of PDAC.

Then, GO and REACTOME pathway analyses were used to investigate the interactions of these DEGs. Increasing evidence shows that LAPTM4B [52], CEACAM6 [53], SERPINE2 [54] and VNN1 [55], SPHK1 [56], HRG (histidine rich glycoprotein) [57], VEGFC (vascular endothelial growth factor C) [58], ANXA3 [59], APOA2 [60], LCN2 [61], TIMP1 [62], CD63 [63], CD151 [64], MAL2 [65], ARNTL2 [66], PKD2 [67], E2F1 [68], MMP1 [69], CCR7 [70], NOTCH2 [71], BTLA (B and T lymphocyte associated) [72], TFRC (transferrin receptor) [73], CD4 [74], ATM (ATM serine/threonine kinase) [75], LEF1 [76], CSF1R [77], CTSB (cathepsin B) [78], DUSP2 [79] and NR4A1 [80] are closely associated with progression of PDAC. PTGER3 [81] and MAGI2 [82] are linked with angiogenesis, chemoresistance, cell proliferation and migration in ovary cancer, but these genes might be liable for growth PDAC. Hoagland et al [83] demonstrated that HP (haptoglobin) expression was responsible for progression of

lung cancer, but this gene might be involved in PDAC progression. FGA (fibrinogen alpha chain) was demonstrated to be a lung cancer susceptibility gene through activation of integrin–AKT signaling pathway [84], but this gene might be liable for progression of PDAC. Repetto et al [85] investigated the importance of FGB (fibrinogen beta chain) in the pathogenesis of gastric carcinoma, but this gene might be responsible for progression of PDAC. PLA2G4A [86], FGG (fibrinogen gamma chain) [87] and TYMS (thymidylatesynthetase) [88] have been demonstrated to be up regulated in cancer, but these genes might be liable for progression of PDAC. RAB32 [89], SEPTIN4 [90], TPM2 [91], ACOT7 [92], PRTFDC1 [93], CABLES1 [94], HLA-DMB [95], PTPRC (protein tyrosine phosphatase receptor type C) [96], CD5 [97], CD6 [97], MS4A1 [98], CD22 [99], CD27 [100], MRC2 [101], CLEC2D [102], EEF1A1 [103] and APOB (apolipoprotein B) [104] played a predominant role in the cancer progression, but these genes might be associated with development of PDAC. Jung et al [105] found that SMPD1 stimulates the drug resistance in colorectal cancer, but this gene might be linked with development of PDAC. Liu et al. [106], Yang et al [107], Song et al [108], Seachrist et al [109], Zhu et al [110], Wu et al [111], Wang et al [112], Yi et al [113], Lan et al [114] and Appert-Collin et al [115] revealed that PADI4, MAOB (monoamine oxidase B), TRPC6, BCL11A, CXCR5, TCF7, POU2F2, SLC4A1, STK17B and LRP1 were associated with cancer cell invasion, but these genes might be liable for progression of PDAC. Kairouz et al [116], Diez-Bello et al [117], Xue et al [118], Abo-Elfadl et al [119], Li et al [120] and Zhao et al [121] reported that GRB14, TRPC6, ZFPM2, TNFRSF13B, ADAM19 and PIK3IP1enhance the cancer cell proliferation, but this gene might be involved in advancement of PDAC. Leite et al [122], Feng et al [123], Wang et al [124], Zhong et al [125], Yokoyama-Mashima et al [126], Guo et al [127], Lawson et al [128] and Wang et al [129] demonstrated that low levels of HLA-DPA1, FGL2, CBLB (Cbl proto-oncogene B), NCKAP1L, DYRK2, OGT (O-linked N-acetylglucosamine (GlcNAc) transferase), CAMK1D and RNF213 are linked with progression of cancer, but these genes might be essential for progression of PDAC. Polymorphic genes such as RORA (RAR related orphan receptor A) [130], IGF2R [131] and ZBTB20 [132] are contribute to progression of cancer, but these genes might be crucial for advancement of PDAC. Hope et al. [133] identified that the VCAN (versican) was central role in immune cell infiltration in cancer, but this gene may be associated with immune cell infiltration in PDAC.

Construction of PPI network and modules of DEGs may be helpful for understanding the relationship of developmental PDAC. Bai et al [134] reported that CCNB1 plays a positive role in proliferation of cancer cells, but this gene might be involved in development of PDAC. FHL2 [135] and RPL10 [136] are associated with progression of PDAC. Further investigation is required in order to clarify the underlying biological mechanisms of novel biomarkers HLA-DPA1, TUBB1, RPL13A, RPL27A and RPL23A on PDAC.

The miRNA-DEG regulatory network and TF-DEG regulatory network were constructed to explore the molecular mechanism of PDAC. The EZH2 [137], KMT2D [138], TXNIP (thioredoxin interacting protein) [139], TP63 [140], SOX2 [141], MYC [142] and KLF4 [143] genes are associated with PDAC. TPM1 [144] and hsa-mir-1202 [145] have been associated with cancer risk, but these genes and miRNAs might be responsible for progression of PDAC. Hsa-mir-4461, hsa-mir-3928-3p and hsa-mir-2682-5p might be considered as novel biomarkers for progression of PDAC.

In conclusion, we aim to identify DEGs by bioinformatics analysis to find the potential biomarkers which may be involved in the advancement of PDAC. The investigation contributes a set of useful DEGs for future studies into molecular mechanisms and biomarkers of PDAC. And the application of data mining and integration is accessible for prediction of PDAC advancement. Nevertheless, further molecular biological analyses are recommended to certify the function of the DEGs in PDAC.

Conflict of interest

The authors declare that they have no conflict of interest.

Ethical approval

This article does not contain any studies with human participants or animals performed by any of the authors.

Informed consent

No informed consent because this study does not contain human or animals participants.

Availability of data and materials

The datasets supporting the conclusions of this article are available in the GEO (Gene Expression Omnibus) (https://www.ncbi.nlm.nih.gov/geo/) repository. [(GSE133684) (https://www.ncbi.nlm.nih.gov/geo/query/acc.cgi?acc=GSE133684]

Consent for publication

Not applicable.

Competing interests

The authors declare that they have no competing interests.

Authors

Basavaraj Vastrad ORCID ID: 0000-0003-2202-7637

Chanabasayya Vastrad ORCID ID: 0000-0003-3615-4450

Anandkumar Tengli ORCID ID: 0000-0001-8076-928X

Acknowledgement

I thank Shenglin Huang, Fudan University, Shanghai, China, very much, the author who deposited their microarray dataset, GSE133684, into the public GEO database.

Author Contributions

Basavaraj Vastrad - Writing original draft, and review and editing

Anandkumar Tengli - Writing original draft and investigation

Chanabasayya Vastrad - Software and investigation

References

1. Thiruvengadam, S.S.; Chuang, J.; Huang, R.; Girotra, M.; Park, W.G. Chronic pancreatitis changes in high-risk individuals for pancreatic ductal adenocarcinoma. *Gastrointest. Endosc* **2019**,89,842-851.e1. doi:10.1016/j.gie.2018.08.029

2. Al-Hawary, M.M.; Kaza, R.K.; Azar, S.F.; Ruma, J.A.; Francis, I.R. Mimics of pancreatic ductal adenocarcinoma. *Cancer. Imaging* **2013**,13,342-349. doi:10.1102/1470-7330.2013.9012
3. Siegel, R.L.; Miller, K.D.; Jemal, A. Cancer statistics, 2018. CA. *Cancer. J. Clin* **2018**,68,7-30. doi:10.3322/caac.21442
4. Adamska, A.; Domenichini, A.; Falasca, M. Pancreatic Ductal Adenocarcinoma: Current and Evolving Therapies. *Int. J. Mol. Sci* **2017**,18,1338. doi:10.3390/ijms18071338
5. Tsuchiya, N.; Matsuyama, R.; Murakami, T.; Yabushita, Y.; Sawada, Y.U, Kumamoto, T.; Endo, I. Risk Factors Associated With Early Recurrence of Borderline Resectable Pancreatic Ductal Adenocarcinoma After Neoadjuvant Chemoradiation Therapy and Curative Resection. *Anticancer. Res* **2019**,39,4431-4440. doi:10.21873/anticanres.13615
6. Oji, Y.; Nakamori, S.; Fujikawa, M.; Nakatsuka, S.; Yokota, A.; Tatsumi, N.; Abeno, S.; Ikeba, A.; Takashima, S.; Tsujie, M.; et al. Overexpression of the Wilms' tumor gene WT1 in pancreatic ductal adenocarcinoma. *Cancer. Sci.* **2004**,95,583-587. doi:10.1111/j.1349-7006.2004.tb02490.x
7. Murthy, D.; Attri, K.S.; Singh, P.K. Phosphoinositide 3-Kinase Signaling Pathway in Pancreatic Ductal Adenocarcinoma Progression, Pathogenesis, and Therapeutics. *Front. Physiol* **2018**,9,335. doi:10.3389/fphys.2018.00335
8. Reddy, R.R.S, Ramanujam, M.V. High Throughput Sequencing-Based Approaches for Gene Expression Analysis. *Methods. Mol. Biol* **2018**,1783,299-323. doi:10.1007/978-1-4939-7834-2_15
9. Gu, Y.; Feng, Q.; Liu, H.; Zhou, Q.; Hu, A.; Yamaguchi, T.; Xia, S.; Kobayashi, H. Bioinformatic evidences and analysis of putative biomarkers in pancreatic ductal adenocarcinoma. *Heliyon* **2019**,5,e02378. doi:10.1016/j.heliyon.2019.e02378
10. Clough, E.; Barrett, T. The Gene Expression Omnibus Database. *Methods. Mol. Biol* **2016**,1418,93□110. doi:10.1007/978-1-4939-3578-9_5
11. Yu, S.; Li, Y.; Liao, Z.; Wang, Z.; Wang, Z.; Li, Y.; Qian, L.; Zhao, J.; Zong, H.; Kang, B.; et al. Plasma extracellular vesicle long RNA profiling identifies a diagnostic signature for the detection of pancreatic ductal adenocarcinoma. *Gut* **2020**,69,540-550. doi:10.1136/gutjnl-2019-318860

12. Ritchie, M.E.; Phipson, B.; Wu, D.; Hu, Y.; Law, C.W.; Shi, W.; Smyth, G.K. limma powers differential expression analyses for RNA-sequencing and microarray studies. *Nucleic. Acids. Res* **2015**,43,e47. doi:10.1093/nar/gkv007
13. Ferreira, J.A. The Benjamini-Hochberg method in the case of discrete test statistics. *Int. J. Biostat* **2007**,3. doi:10.2202/1557-4679.1065
14. Thomas, P.D. The Gene Ontology and the Meaning of Biological Function. *Methods. Mol. Biol* **2017**,1446,15□24. doi:10.1007/978-1-4939-3743-1_2
15. Fabregat, A.; Jupe, S.; Matthews, L.; Sidiropoulos, K.; Gillespie, M.; Garapati, P.; Haw, R.; Jassal, B.; Korninger, F.; May, B.; et al. The Reactome Pathway Knowledgebase. *Nucleic. Acids. Res* **2018**,46,D649–D655. doi:10.1093/nar/gkx1132
16. Chen, J.; Bardes, E.E.; Aronow, B.J.; Jegga, A.G. ToppGene Suite for gene list enrichment analysis and candidate gene prioritization. *Nucleic. Acids. Res* **2009**,37,W305-W311. doi:10.1093/nar/gkp427
17. Kotlyar, M.; Pastrello, C.; Malik, Z.; Jurisica, I. IID 2018 update: context-specific physical protein-protein interactions in human, model organisms and domesticated species. *Nucleic. Acids. Res* **2019**,47,D581-D589. doi:10.1093/nar/gky1037
18. Shannon, P.; Markiel, A.; Ozier, O.; Baliga, N.S, Wang, J.T.; Ramage, D.; Amin, N.; Schwikowski, B.; Ideker, T. Cytoscape: a software environment for integrated models of biomolecular interaction networks. *Genome. Res* **2003**,13(,2498-2504. doi:10.1101/gr.1239303
19. Przulj, N.; Wigle, D.A.; Jurisica, I. Functional topology in a network of protein interactions. *Bioinformatics* **2004**,20,340–348. doi:10.1093/bioinformatics/btg415
20. Nguyen, T.P.; Liu, W.C.; Jordán, F. Inferring pleiotropy by network analysis: linked diseases in the human PPI network. *BMC. Syst. Biol* **2011**,5,179. doi:10.1186/1752-0509-5-179
21. Shi, Z.; Zhang, B. Fast network centrality analysis using GPUs. *BMC. Bioinformatics* **2011**,12,149. doi:10.1186/1471-2105-12-149
22. Fadhal, E.; Gamieldien, J.; Mwambene, E.C. Protein interaction networks as metric spaces: a novel perspective on distribution of hubs. *BMC. Syst. Biol* **2014**,8,6. doi:10.1186/1752-0509-8-6

23. Zaki, N.; Efimov, D.; Berengueres, J. Protein complex detection using interaction reliability assessment and weighted clustering coefficient. *BMC. Bioinformatics* **2013**,14,163. doi:10.1186/1471-2105-14-163
24. Fan, Y.; Xia, J miRNet-Functional Analysis and Visual Exploration of miRNA-Target Interactions in a Network Context. *Methods. Mol. Biol* **2018**,1819,215-233. doi:10.1007/978-1-4939-8618-7_10
25. Zhou, G.; Soufan, O.; Ewald, J.; Hancock, R.E.W.; Basu, N.; Xia, J. NetworkAnalyst 3.0: a visual analytics platform for comprehensive gene expression profiling and meta-analysis. *Nucleic. Acids. Res* **2019**,47,W234-W241. doi:10.1093/nar/gkz240
26. Chandrashekar, D.S.; Bashel, B.; Balasubramanya, S.A.H.; Creighton, C.J: Ponce-Rodriguez, I.; Chakravarthi, B.V.S.K.; Varambally, S. UALCAN: A Portal for Facilitating Tumor Subgroup Gene Expression and Survival Analyses. *Neoplasia* **2017**,19,649-658. doi:10.1016/j.neo.2017.05.002
27. Gao, J.; Aksoy, B.A.; Dogrusoz, U.; Dresdner, G.; Gross, B.; Sumer, S.O.; Sun, Y.; Jacobsen, A.; Sinha R.; Larsson E.; et al. Integrative analysis of complex cancer genomics and clinical profiles using the cBioPortal. *Sci Signal.* **2013**,6,pl1. doi:10.1126/scisignal.2004088
28. Uhlen, M.; Oksvold, P.; Fagerberg, L.; Lundberg, E.; Jonasson, K.; Forsberg, M.; Zwahlen, M.; Kampf, C.; Wester, K.; Hober, S.; et al. Towards a knowledge-based Human Protein Atlas. *Nat. Biotechnol* **2010**,28,1248-1250. doi:10.1038/nbt1210-1248
29. Li, T.; Fan, J.; Wang, B.; Traugh, N.; Chen Q.; Liu J.S.; Li B.; Liu X.S. TIMER: A Web Server for Comprehensive Analysis of Tumor-Infiltrating Immune Cells. *Cancer. Res* **2017**,77,e108–e110. doi:10.1158/0008-5472.CAN-17-0307
30. Robin, X.; Turck, N.; Hainard, A.; Tiberti, N.; Lisacek, F.; Sanchez, J.C.; Müller, M. pROC: an open-source package for R and S+ to analyze and compare ROC curves. *BMC. Bioinformatics* **2011**,12,77. doi:10.1186/1471-2105-12-77
31. Livak, K.J.; Schmittgen, T.D. Analysis of relative gene expression data using real-time quantitative PCR and the 2(-Delta Delta C(T)) Method. *Methods* **2001**,25,402–408. doi:10.1006/meth.2001.1262
32. El-Saadi M.W.; Williams-Hart T.; Salvatore B.A.; Mahdavian E. Use of in-silico assays to characterize the ADMET profile and identify potential

therapeutic targets of fusarochromanone, a novel anti-cancer agent. *In. Silico. Pharmacol* **2015**,3,6. doi:10.1186/s40203-015-0010-5

33. Li, J.; Ma, X.; Liu, C.; Li, H.; Zhuang, J.; Gao, C.; Zhou, C.; Liu, L.; Wang, K.; Sun C. Exploring the Mechanism of Danshen against Myelofibrosis by Network Pharmacology and Molecular Docking. Evid. Based. Complement. *Alternat. Med.* **2018**,2018,8363295. doi:10.1155/2018/8363295
34. Ruddarraju, R.R.; Murugulla, A.C.; Kotla, R.; Tirumalasetty, M.C.B.; Wudayagiri, R.; Donthabakthuni, S.; Maroju, R. Design, synthesis, anticancer activity and docking studies of theophylline containing 1,2,3-triazoles with variant amide derivatives. *Medchemcomm* **2016**,8,176-183. doi:10.1039/c6md00479b
35. Moffitt, R.A.; Marayati, R.; Flate, E.L.; Volmar, K.E.; Loeza, S.G.; Hoadley, K.A.; Rashid, N.U.; Williams, L.A.; Eaton, S.C.; Chung, A.H.; et al. Virtual microdissection identifies distinct tumor- and stroma-specific subtypes of pancreatic ductal adenocarcinoma. *Nat. Genet* **2015**,47,1168-1178. doi:10.1038/ng.3398
36. Dansranjavin, T.; Möbius, C.; Tannapfel, A.; Bartels, M.; Wittekind, C.; Hauss, J.; Witzigmann, H. E-cadherin and DAP kinase in pancreatic adenocarcinoma and corresponding lymph node metastases. *Oncol. Rep* **2006**,15,1125-1131.
37. Treiber, M.; Schulz, H.U.; Landt, O.; Drenth, J.P.; Castellani, C.; Real, F.X.; Akar, N.; Ammann, R.W.; Bargetzi, M.; Bhatia, E.; et al. Keratin 8 sequence variants in patients with pancreatitis and pancreatic cancer. *J. Mol. Med (Berl)* **2006**,84,1015-1022. doi:10.1007/s00109-006-0096-7
38. Liu, H.; Li, L.; Chen, H.; Kong, R.; Pan, S.; Hu, J.; Wang, Y.; Li, Y.; Sun B. Silencing IGFBP-2 decreases pancreatic cancer metastasis and enhances chemotherapeutic sensitivity. *Oncotarget* **2017**,8,61674-61686. doi:10.18632/oncotarget.18669
39. Yao, H.; Yang, Z.; Liu, Z.; Miao, X.; Yang, L.; Li, D.; Zou, Q.; Yuan, Y. Glypican-3 and KRT19 are markers associating with metastasis and poor prognosis of pancreatic ductal adenocarcinoma. *Cancer. Biomark* **2016**,17,397-404. doi:10.3233/CBM-160655
40. Huynh, D.L.; Koh, H.; Chandimali, N.; Zhang, J.J.; Kim, N.; Kang, T.Y.; Ghosh, M.; Gera, M.; Park, Y.H.; Kwon, T.; et al. BRM270 Inhibits the Proliferation of CD44 Positive Pancreatic Ductal Adenocarcinoma Cells via

Downregulation of Sonic Hedgehog Signaling. *Evid. Based. Complement Alternat. Med.* **2019**,2019,8620469. doi:10.1155/2019/8620469

41. Zhang, Z.; Liu, X.; Huang, R.; Liu, X.; Liang, Z.; Liu, T. Upregulation of nucleoprotein AHNAK is associated with poor outcome of pancreatic ductal adenocarcinoma prognosis via mediating epithelial-mesenchymal transition. *J. Cancer* **2019**,10,3860-3870. doi:10.7150/jca.31291
42. Huang, Y.; Zheng, J.; Tan, T.; Song, L.; Huang, S.; Zhang, Y.; Lin, L.; Liu, J.; Zheng P.; Chen X.; et al. BTG1 low expression in pancreatic ductal adenocarcinoma is associated with a poorer prognosis. *Int. J. Biol. Markers.* **2018**,33,189-194. doi:10.5301/ijbm.5000310
43. Wang, P.B.; Chen, Y.; Ding, G.R.; Du, H.W.; Fan, H.Y. Keratin 18 induces proliferation, migration, and invasion in gastric cancer via the MAPK signalling pathway. *Clin. Exp. Pharmacol. Physiol.* **2020**,10.1111/1440-1681.13401. doi:10.1111/1440-1681.13401
44. Alfarsi, L.H.; El Ansari, R.; Masisi, B.K.; Parks, R.; Mohammed, O.J.; Ellis, I.O.; Rakha, E.A.; Green, A.R. Integrated Analysis of Key Differentially Expressed Genes Identifies DBN1 as a Predictive Marker of Response to Endocrine Therapy in Luminal Breast Cancer. *Cancers. (Basel).* **2020**,12,1549. doi:10.3390/cancers12061549
45. Tessema, M.; Yingling, C.M.; Picchi, M.A.; Wu, G.; Liu, Y.; Weissfeld, J.L.; Siegfried, J.M.; Tesfaigzi, Y.; Belinsky, S.A. Epigenetic Repression of CCDC37 and MAP1B Links Chronic Obstructive Pulmonary Disease to Lung Cancer. *J. Thorac. Oncol* **2015**,10,1181-1188. doi:10.1097/JTO.0000000000000592
46. Lai, J.; Flanagan, J.; Phillips, W.A.; Chenevix-Trench, G.; Arnold, J. Analysis of the candidate 8p21 tumour suppressor, BNIP3L, in breast and ovarian cancer. *Br. J. Cancer* **2003**,88,270-276. doi:10.1038/sj.bjc.6600674
47. Yen, C.Y.; Huang, C.Y.; Hou, M.F.; Yang, Y.H.; Chang, C.H.; Huang, H.W.; Chen, C.H.; Chang, H.W. Evaluating the performance of fibronectin 1 (FN1), integrin α4β1 (ITGA4), syndecan-2 (SDC2), and glycoprotein CD44 as the potential biomarkers of oral squamous cell carcinoma (OSCC). *Biomarkers* **2013**,18,63-72. doi:10.3109/1354750X.2012.737025
48. Tomsic, J.; He, H.; Akagi, K.; Liyanarachchi, S.; Pan, Q.; Bertani, B.; Nagy, R.; Symer, D.E.; Blencowe, B.J.; de la Chapelle, A. A germline mutation in

SRRM2, a splicing factor gene, is implicated in papillary thyroid carcinoma predisposition. *Sci. Rep* **2015**,5,10566. doi:10.1038/srep10566

49. Kim, M.J.; Choi, S.K.; Hong, S.H.; Eun, J.W.; Nam, S.W.; Han, J.W.; You, J.S. Oncogenic IL7R is downregulated by histone deacetylase inhibitor in esophageal squamous cell carcinoma via modulation of acetylated FOXO1. *Int. J. Oncol* **2018**,53,395-403. doi:10.3892/ijo.2018.4392
50. Lee, J.; Li, L.; Gretz, N.; Gebert, J.; Dihlmann, S. Absent in Melanoma 2 (AIM2) is an important mediator of interferon-dependent and -independent HLA-DRA and HLA-DRB gene expression in colorectal cancers. *Oncogene* **2012**,31,1242-1253. doi:10.1038/onc.2011.320
51. Liu, Y.; Kim, H.G.; Dong, E.; Dong, C.; Huang, M.; Liu, Y.; Liangpunsakul, S, Dong, X.C. Sesn3 deficiency promotes carcinogen-induced hepatocellular carcinoma via regulation of the hedgehog pathway. *Biochim. Biophys. Acta. Mol. Basis. Dis* **2019**,1865,2685-2693. doi:10.1016/j.bbadis.2019.07.011
52. Yang, Z.; Senninger, N.; Flammang, I.; Ye, Q.; Dhayat, S.A. Clinical impact of circulating LAPTM4B-35 in pancreatic ductal adenocarcinoma. *J. Cancer. Res. Clin. Oncol* **2019**,145,1165-1178. doi:10.1007/s00432-019-02863-w
53. Pandey, R.; Zhou, M.; Islam, S.; Chen, B.; Barker, N.K.; Langlais, P.; Srivastava, A.; Luo, M.; Cooke, L.S.; Weterings, E.; et al. Carcinoembryonic antigen cell adhesion molecule 6 (CEACAM6) in Pancreatic Ductal Adenocarcinoma (PDA): An integrative analysis of a novel therapeutic target. *Sci. Rep* **2019**,9,18347. doi:10.1038/s41598-019-54545-9
54. Neesse, A.; Wagner, M.; Ellenrieder, V.; Bachem, M.; Gress, T.M.; Buchholz, M. Pancreatic stellate cells potentiate proinvasive effects of SERPINE2 expression in pancreatic cancer xenograft tumors. *Pancreatology* **2007**,7,380-385. doi:10.1159/000107400
55. Kang, M.; Qin, W.; Buya, M.; Dong, X.; Zheng, W.; Lu, W.; Chen, J.; Guo, Q.; Wu, Y. VNN1, a potential biomarker for pancreatic cancer-associated new-onset diabetes, aggravates paraneoplastic islet dysfunction by increasing oxidative stress. *Cancer. Lett* **2016**,373,241-250. doi:10.1016/j.canlet.2015.12.031
56. Li, J.; Wu, H.; Li, W.; Yin, L.; Guo, S.; Xu, X.; Ouyang, Y.; Zhao, Z.; Liu, S.; Tian, Y.; et al Downregulated miR-506 expression facilitates pancreatic

cancer progression and chemoresistance via SPHK1/Akt/NF-κB signaling. *Oncogene* **2016**,35,5501-5514. doi:10.1038/onc.2016.90

57. Chen, X.L.; Xie, K.X.; Yang, Z.L.; Yuan, L.W. Expression of FXR and HRG and their clinicopathological significance in benign and malignant pancreatic lesions. *Int. J. Clin. Exp. Pathol* **2019**,12,2111-2120.
58. Guo, J.; Lou, W.; Ji, Y.; Zhang, S. Effect of CCR7, CXCR4 and VEGF-C on the lymph node metastasis of human pancreatic ductal adenocarcinoma. *Oncol. Lett* **2013**,5,1572-1578. doi:10.3892/ol.2013.1261
59. Wan, Y.C.E.; Liu, J.; Zhu, L.; Kang, T.Z.E.; Zhu, X.; Lis, J.; Ishibashi, T.; Danko, C.G.; Wang, X.; Chan, K.M. The H2BG53D oncohistone directly upregulates ANXA3 transcription and enhances cell migration in pancreatic ductal adenocarcinoma. *Signal. Transduct. Target. Ther* **2020**,5,106. doi:10.1038/s41392-020-00219-2
60. Sato, Y.; Kobayashi, T.; Nishiumi, S.; Okada, A.; Fujita, T.; Sanuki, T.; Kobayashi, M.; Asahara, M.; Adachi, M.; Sakai, A.; et al. Prospective Study Using Plasma Apolipoprotein A2-Isoforms to Screen for High-Risk Status of Pancreatic Cancer. *Cancers (Basel)* **2020**,12,E2625. doi:10.3390/cancers12092625
61. Gumpper, K.; Dangel, A.W.; Pita-Grisanti, V.; Krishna, S.G.; Lara, L.F.; Mace, T.; Papachristou, G.I.; Conwell, D.L.; Hart, P.A.; Cruz-Monserrate, Z. Lipocalin-2 expression and function in pancreatic diseases. *Pancreatology* **2020**,20,419-424. doi:10.1016/j.pan.2020.01.002
62. D'Costa, Z.; Jones, K.; Azad, A.; van Stiphout, R.; Lim, S.Y.; Gomes, A.L.; Kinchesh, P.; Smart, S.C.; Gillies McKenna, W.; Buffa, F.M.; et al. Gemcitabine-Induced TIMP1 Attenuates Therapy Response and Promotes Tumor Growth and Liver Metastasis in Pancreatic Cancer. *Cancer. Res.* **2017**,77,5952-5962. doi:10.1158/0008-5472.CAN-16-2833
63. Buscail, E.; Chauvet, A.; Quincy, P.; Degrandi, O.; Buscail, C.; Lamrissi, I.; Moranvillier, I.; Caumont, C.; Verdon, S.; Brisson, A.; et al. CD63-GPC1-Positive Exosomes Coupled with CA19-9 Offer Good Diagnostic Potential for Resectable Pancreatic Ductal Adenocarcinoma. *Transl. Oncol* **2019**,12,1395-1403. doi:10.1016/j.tranon.2019.07.009
64. Zhu, G.H.; Huang, C.; Qiu, Z.J.; Liu, J.; Zhang, Z.H.; Zhao, N.; Feng, Z.Z.; Lv, X.H. Expression and prognostic significance of CD151, c-Met, and

integrin alpha3/alpha6 in pancreatic ductal adenocarcinoma. *Dig. Dis. Sci* **2011**,56,1090-1098. doi:10.1007/s10620-010-1416-x

65. Eguchi, D.; Ohuchida, K.; Kozono, S.; Ikenaga, N.; Shindo, K.; Cui, L.; Fujiwara, K.; Akagawa, S.; Ohtsuka, T.; Takahata, S.; et al. MAL2 expression predicts distant metastasis and short survival in pancreatic cancer. *Surgery* **2013**,154,573-582. doi:10.1016/j.surg.2013.03.010
66. Wang, Z.; Liu, T.; Xue, W.; Fang, Y.; Chen, X.; Xu, L.; Zhang, L.; Guan, K.; Pan, J.; Zheng, L.; et al. ARNTL2 promotes pancreatic ductal adenocarcinoma progression through TGF/BETA pathway and is regulated by miR-26a-5p. *Cell. Death. Dis* **2020,**11,692. doi:10.1038/s41419-020-02839-6
67. Yuan, J.; Rozengurt, E. PKD, PKD2, and p38 MAPK mediate Hsp27 serine-82 phosphorylation induced by neurotensin in pancreatic cancer PANC-1 cells. *J. Cell. Biochem* **2008**,103,648-662. doi:10.1002/jcb.21439
68. Schild, C.; Wirth, M.; Reichert, M.; Schmid, R.M.; Saur, D.; Schneider, G.; PI3K signaling maintains c-myc expression to regulate transcription of E2F1 in pancreatic cancer cells. *Mol. Carcinog* **2009**,48,1149-1158. doi:10.1002/mc.2056
69. Chen, Y.; Peng, S.; Cen, H.; Lin, Y.; Huang, C.; Chen, Y.; Shan, H.; Su, Y.; Zeng, L. MicroRNA hsa-miR-623 directly suppresses MMP1 and attenuates IL-8-induced metastasis in pancreatic cancer. *Int. J. Oncol* **2019**,55,142-156. doi:10.3892/ijo.2019.4803
70. Wang, L.; Zhao, X.Y.; Zhu, J.S.; Chen, N.W.; Fan, H.N.; Yang, W.; Guo, J.H. CCR7 regulates ANO6 to promote migration of pancreatic ductal adenocarcinoma cells via the ERK signaling pathway. *Oncol. Lett* **2018**,16,2599-2605. doi:10.3892/ol.2018.8962
71. Mazur, P.K.; Einwächter, H.; Lee, M.; Sipos, B.; Nakhai, H.; Rad, R.; Zimber-Strobl, U.; Strobl, L.J.; Radtke, F.; Klöppel, G.; et al. Notch2 is required for progression of pancreatic intraepithelial neoplasia and development of pancreatic ductal adenocarcinoma. *Proc. Natl. Acad. Sci. U. S. A.* **2010**,107,13438-13443. doi:10.1073/pnas.1002423107
72. Bian, B.; Fanale, D.; Dusetti, N.; Roque, J.; Pastor, S.; Chretien, A.S.; Incorvaia, L.; Russo, A.; Olive, D.; Iovanna, J.; et al. Prognostic significance of circulating PD-1, PD-L1, pan-BTN3As, BTN3A1 and BTLA in patients

with pancreatic adenocarcinoma. *Oncoimmunology* **2019**,8,e1561120. doi:10.1080/2162402X.2018.1561120

73. Ryschich, E.; Huszty, G.; Knaebel, H.P.; Hartel, M.; Büchler, M.W.; Schmidt, J. Transferrin receptor is a marker of malignant phenotype in human pancreatic cancer and in neuroendocrine carcinoma of the pancreas. *Eur. J. Cancer* **2004**,40,1418-1422. doi:10.1016/j.ejca.2004.01.036
74. Sonntag, K.; Hashimoto, H.; Eyrich, M.; Menzel, M.; Schubach, M.; Döcker, D.; Battke, F.; Courage, C.; Lambertz, H.; Handgretinger, R.; et al. Immune monitoring and TCR sequencing of CD4 T cells in a long term responsive patient with metastasized pancreatic ductal carcinoma treated with individualized, neoepitope-derived multipeptide vaccines: a case report. *J. Transl. Med* **2018**,16,23. doi:10.1186/s12967-018-1382-1
75. Hutchings, D.; Jiang, Z.; Skaro, M.; Weiss, M.J.; Wolfgang, C.L.; Makary, M.A.; He, J.; Cameron, J.L.; Zheng, L.; Klimstra, D.S.; et al Histomorphology of pancreatic cancer in patients with inherited ATM serine/threonine kinase pathogenic variants. *Mod. Pathol* **2019**,32,1806-1813. doi:10.1038/s41379-019-0317-6
76. Singhi, A.D.; Lilo, M.; Hruban, R.H.; Cressman, K.L.; Fuhrer, K.; Seethala, R.R. Overexpression of lymphoid enhancer-binding factor 1 (LEF1) in solid-pseudopapillary neoplasms of the pancreas. *Mod. Pathol* **2014**,27,1355-1363. doi:10.1038/modpathol.2014.40
77. Zhu, Y.; Knolhoff, B.L.; Meyer, M.A.; Nywening, T.M.; West, B.L.; Luo, J.; Wang-Gillam, A.; Goedegebuure, S.P.; Linehan, D.C.; DeNardo, D.G. CSF1/CSF1R blockade reprograms tumor-infiltrating macrophages and improves response to T-cell checkpoint immunotherapy in pancreatic cancer models. *Cancer. Res* **2014**,74,5057-5069. doi:10.1158/0008-5472.CAN-13-3723
78. Dumartin, L.; Whiteman, H.J.; Weeks, M.E.; Hariharan, D.; Dmitrovic, B.; Iacobuzio-Donahue, C.A.; Brentnall, T.A.; Bronner, M.P.; Feakins, R.M.; Timms, J.F.; et al AGR2 is a novel surface antigen that promotes the dissemination of pancreatic cancer cells through regulation of cathepsins B and D. *Cancer. Res* **2011**,71,7091-7102. doi:10.1158/0008-5472.CAN-11-1367
79. Wang, C.A.; Chang, I.H.; Hou, P.C.; Tai, Y.J.; Li, W.N.; Hsu, P.L.; Wu, S.R.; Chiu, W.T.; Li, C.F.; Shan, Y.S.; et al. DUSP2 regulates extracellular

vesicle-VEGF-C secretion and pancreatic cancer early dissemination. *J. Extracell. Vesicles* **2020**,9,1746529. doi:10.1080/20013078.2020.1746529

80. Yoon, K.; Lee, S.O.; Cho, S.D.; Kim, K.; Khan, S.; Safe ,S. Activation of nuclear TR3 (NR4A1) by a diindolylmethane analog induces apoptosis and proapoptotic genes in pancreatic cancer cells and tumors. *Carcinogenesis* **2011**,32,836-842. doi:10.1093/carcin/bgr040
81. Rodriguez-Aguayo, C.; Bayraktar, E.; Ivan, C.; Aslan, B.; Mai, J.; He, G.; Mangala, L.S.; Jiang, D.; Nagaraja, A.S.; Ozpolat, B.; et al. PTGER3 induces ovary tumorigenesis and confers resistance to cisplatin therapy through up-regulation Ras-MAPK/Erk-ETS1-ELK1/CFTR1 axis. *EBioMedicine* **2019**,40,290-304. doi:10.1016/j.ebiom.2018.11.045
82. Chang, H.; Zhang, X.; Li, B.; Meng, X. MAGI2-AS3 suppresses MYC signaling to inhibit cell proliferation and migration in ovarian cancer through targeting miR-525-5p/MXD1 axis. *Cancer. Med* **2020**,9,6377-6386. doi:10.1002/cam4.3126
83. Hoagland, L.F.; Campa, M.J.; Gottlin, E.B.; Herndon, J.E.; Patz, E.F. Haptoglobin and posttranslational glycan-modified derivatives as serum biomarkers for the diagnosis of nonsmall cell lung cancer. *Cancer* **2007**,110,2260-2268. doi:10.1002/cncr.23049
84. Wang, M.; Zhang, G.; Zhang, Y.; Cui, X.; Wang, S.; Gao, S.; Wang, Y.; Liu, Y.; Bae, J.H.; Yang, W.H.; et al. Fibrinogen Alpha Chain Knockout Promotes Tumor Growth and Metastasis through Integrin-AKT Signaling Pathway in Lung Cancer. *Mol. Cancer. Res* **2020**,18,943-954. doi:10.1158/1541-7786.MCR-19-1033
85. Repetto, O.; Maiero, S.; Magris, R.; Miolo, G.; Cozzi, M.R.; Steffan, A.; Canzonieri, V.; Cannizzaro, R.; De Re, V. Quantitative Proteomic Approach Targeted to Fibrinogen β Chain in Tissue Gastric Carcinoma. *Int. J. Mol. Sci* **2018**,19,759. doi:10.3390/ijms19030759
86. Bazhan, D.; Khaniani, M.S. Supplementation with omega fatty acids increases the mRNA expression level of PLA2G4A in patients with gastric cancer. *J. Gastrointest. Oncol* **2018**,9,1176-1183. doi:10.21037/jgo.2018.08.12
87. Duan, S.; Gong, B.; Wang, P.; Huang, H.; Luo, L.; Liu, F. Novel prognostic biomarkers of gastric cancer based on gene expression microarray:

COL12A1, GSTA3, FGA and FGG. *Mol. Med. Rep* **2018**,18,3727-3736. doi:10.3892/mmr.2018.9368

88. Lee, S.W.; Chen, T.J.; Lin, L.C.; Li, C.F.; Chen, L.T.; Hsing, C.H.; Hsu, H.P.; Tsai, C.J.; Huang, H.Y.; Shiue, Y.L. Overexpression of thymidylate synthetase confers an independent prognostic indicator in nasopharyngeal carcinoma. *Exp. Mol. Pathol* **2013**,95,83-90. doi:10.1016/j.yexmp.2013.05.006
89. Shibata, D.; Mori, Y.; Cai, K.; Zhang, L.; Yin, J.; Elahi, A.; Hamelin, R.; Wong, Y.F.; Lo, W.K.; Chung T.K.; et al. RAB32 hypermethylation and microsatellite instability in gastric and endometrial adenocarcinomas. *Int. J. Cancer* **2006**,119,801-806. doi:10.1002/ijc.21912
90. Zhao, X.; Feng, H.; Wang, Y.; Wu, Y.; Guo, Q.; Feng, Y.; Ma, M.; Guo, W.; Song, X.; Zhang, Y.; et al. Septin4 promotes cell death in human colon cancer cells by interacting with BAX. *Int. J. Biol. Sci* **2020**,16,1917-1928. doi:10.7150/ijbs.44429
91. Zhang, J.; Zhang, J.; Xu, S.; Zhang, X.; Wang, P.; Wu, H.; Xia, B.; Zhang, G.; Lei, B.; Wan, L.; et al. Hypoxia-Induced TPM2 Methylation is Associated with Chemoresistance and Poor Prognosis in Breast Cancer. *Cell. Physiol. Biochem* **2018**,45,692-705. doi:10.1159/000487162
92. Feng, H.; Liu, X. Interaction between ACOT7 and LncRNA NMRAL2P via Methylation Regulates Gastric Cancer Progression. *Yonsei. Med. J* **2020**,61,471-481. doi:10.3349/ymj.2020.61.6.471
93. Suzuki, E.; Imoto, I.; Pimkhaokham, A.; Nakagawa, T.; Kamata, N.; Kozaki, K.I.; Amagasa, T.; Inazawa, J. PRTFDC1, a possible tumor-suppressor gene, is frequently silenced in oral squamous-cell carcinomas by aberrant promoter hypermethylation. *Oncogene* **2007**,26,7921-7932. doi:10.1038/sj.onc.1210589
94. Sakamoto, H.; Friel, A.M.; Wood, A.W.; Guo, L.; Ilic, A.; Seiden, M.V.; Chung, D.C.; Lynch, M.P.; Serikawa, T.; Munro, E.; et al. Mechanisms of Cables 1 gene inactivation in human ovarian cancer development. *Cancer. Biol. Ther* **2008**,7,180-188. doi:10.4161/cbt.7.2.5253
95. Callahan, M.J.; Nagymanyoki, Z.; Bonome, T.; Johnson, M.E.; Litkouhi, B.; Sullivan, E.H.; Hirsch, M.S.; Matulonis, U.A.; Liu, J.; Birrer, M.J.; et al. Increased HLA-DMB expression in the tumor epithelium is associated with increased CTL infiltration and improved prognosis in advanced-stage serous

ovarian cancer. *Clin. Cancer. Res* **2008**,14,7667-7673. doi:10.1158/1078-0432.CCR-08-0479

96. Wu, Y.; Han, J.; Vladimirovna, K.E.; Zhang, S.; Lv, W.; Zhang, Y.; Jamaspishvili, E.; Sun, J.; Fang, Q.; Meng, J.; et al. Upregulation Of Protein Tyrosine Phosphatase Receptor Type C Associates To The Combination Of Hashimoto's Thyroiditis And Papillary Thyroid Carcinoma And Is Predictive Of A Poor Prognosis. *Onco. Targets. Ther* **2019**,12,8479-8489. doi:10.2147/OTT.S226426
97. Moreno-Manuel, A.; Jantus-Lewintre, E.; Simões, I.; Aranda, F.; Calabuig-Fariñas, S.; Carreras, E.; Zúñiga, S.; Saenger, Y.; Rosell, R.; Camps, C.; et al. CD5 and CD6 as immunoregulatory biomarkers in non-small cell lung cancer. *Transl. Lung. Cancer. Res* **2020**,9,1074-1083. doi:10.21037/tlcr-19-445
98. Wright, C.M.; Savarimuthu Francis, S.M.; Tan, M.E.; Martins, M.U.; Winterford, C.; Davidson, M.R.; Duhig, E.E.; Clarke, B.E.; Hayward, N.K.; et al. MS4A1 dysregulation in asbestos-related lung squamous cell carcinoma is due to CD20 stromal lymphocyte expression. *PLoS. One* **2012**,7,e34943. doi:10.1371/journal.pone.0034943
99. Tuscano, J.M.; Kato, J.; Pearson, D.; Xiong, C.; Newell, L.; Ma, Y.; Gandara, D.R.; O'Donnell, R.T. CD22 antigen is broadly expressed on lung cancer cells and is a target for antibody-based therapy. *Cancer. Res* **2012**,72,5556-5565. doi:10.1158/0008-5472.CAN-12-0173
100. Nielsen, J.S.; Sahota, R.A.; Milne, K.; Kost, S.E.; Nesslinger, N.J.; Watson, P.H.; Nelson, B.H. CD20+ tumor-infiltrating lymphocytes have an atypical CD27- memory phenotype and together with CD8+ T cells promote favorable prognosis in ovarian cancer. *Clin. Cancer. Res* **2012**,18,3281-3292. doi:10.1158/1078-0432.CCR-12-0234
101. Gai, X.; Tu, K.; Lu, Z.; Zheng, X. MRC2 expression correlates with TGFβ1 and survival in hepatocellular carcinoma. *Int. J. Mol. Sci* **2014**,15,15011-15025. doi:10.3390/ijms150915011
102. Mathew, S.O.; Chaudhary, P.; Powers, S.B.; Vishwanatha, J.K.; Mathew, P.A. Overexpression of LLT1 (OCIL, CLEC2D) on prostate cancer cells inhibits NK cell-mediated killing through LLT1-NKRP1A (CD161) interaction. *Oncotarget* **2016**,7,68650-68661. doi:10.18632/oncotarget.11896

103. Joung, E.K.; Kim, J.; Yoon, N.; Maeng, L.S.; Kim, J.H.; Park, S.; Kang, K.; Kim, J.S.; Ahn, Y.H.; Ko, Y.H.; et al. Expression of EEF1A1 Is Associated with Prognosis of Patients with Colon Adenocarcinoma. *J. Clin. Med* **2019**,8,1903. doi:10.3390/jcm8111903

104. Yang, D.D.; Chen, Z.H.; Wang, D.S.; Yu, H.E.; Lu, J.H.; Xu, R.H.; Zeng, Z.L. Prognostic value of the serum apolipoprotein B to apolipoprotein A-I ratio in metastatic colorectal cancer patients. *J. Cancer* **2020**,11,1063-1074. doi:10.7150/jca.3565

105. Jung, J.H.; Taniguchi, K.; Lee, H.M.; Lee, M.Y.; Bandu, R.; Komura, K.; Lee, K.Y.; Akao, Y.; Kim, K.P. Comparative lipidomics of 5-Fluorouracil-sensitive and -resistant colorectal cancer cells reveals altered sphingomyelin and ceramide controlled by acid sphingomyelinase (SMPD1). *Sci. Rep* **2020**,10,6124. doi:10.1038/s41598-020-62823-0

106. Liu, M.; Qu, Y.; Teng, X.; Xing, Y.; Li, D.; Li, C.; Cai, L.; PADI4□mediated epithelial□mesenchymal transition in lung cancer cells. *Mol. Med. Rep* **2019**,19,3087-3094. doi:10.3892/mmr.2019.9968

107. Yang, Y.C.; Chien, M.H.; Lai, T.C.; Su, C.Y.; Jan, Y.H.; Hsiao, M.; Chen, C.L. Monoamine Oxidase B Expression Correlates with a Poor Prognosis in Colorectal Cancer Patients and Is Significantly Associated with Epithelial-to-Mesenchymal Transition-Related Gene Signatures. *Int. J. Mol. Sci* **2020**,21,2813. doi:10.3390/ijms21082813

108. Song, Y.; Liu, G.; Liu, S.; Chen, R.; Wang, N.; Liu, Z.;, Zhang, X.; Xiao, Z.; Liu, L. Helicobacter pylori upregulates TRPC6 via Wnt/β-catenin signaling to promote gastric cancer migration and invasion. *Onco. Targets. Ther* **2019**,12,5269-5279. doi:10.2147/OTT.S201025

109. Seachrist, D.D.; Hannigan, M.M.; Ingles, N.N.; Webb, B.M.; Weber-Bonk, K.L.; Yu, P.; Bebek, G.; Singh, S.; Sizemore, S.T.; Varadan, V.; et al. The transcriptional repressor BCL11A promotes breast cancer metastasis. *J. Biol. Chem* **2020**,295,11707-11719. doi:10.1074/jbc.RA120.014018

110. Zhu, Z.; Zhang, X.; Guo, H.; Fu, L.; Pan, G.; Sun, Y. CXCL13-CXCR5 axis promotes the growth and invasion of colon cancer cells via PI3K/AKT pathway. *Mol. Cell. Biochem* **2015**,400,287-295. doi:10.1007/s11010-014-2285-y

111. Wu, B.; Chen, M.; Gao, M.; Cong, Y.; Jiang, L.; Wei, J.; Huang, J. Down-regulation of lncTCF7 inhibits cell migration and invasion in

colorectal cancer via inhibiting TCF7 expression. *Hum. Cell* **2019**,32,31-40. doi:10.1007/s13577-018-0217-y

112. Wang, S.M.; Tie, J.; Wang, W.L.; Hu, S.J.; Y+in, J.P.; Yi, X.F.; Tian, Z.H.; Zhang, X.Y.; Li, M.B.; Li, Z.S.; et al. POU2F2-oriented network promotes human gastric cancer metastasis. *Gut* **2016**,65,1427-1438. doi:10.1136/gutjnl-2014-308932

113. Yi, T.; Zhou, X.; Sang, K.; Huang, X.; Zhou, J.; Ge, L. Activation of lncRNA lnc-SLC4A1-1 induced by H3K27 acetylation promotes the development of breast cancer via activating CXCL8 and NF-kB pathway. *Artif. Cells. Nanomed. Biotechnol* **2019**,47,3765-3773. doi:10.1080/21691401.2019.1664559

114. Lan, Y.; Han, J.; Wang, Y.; Wang, J.; Yang, G.; Li, K.; Song, R.; Zheng, T.; Liang, Y.; Pan, S.; et al. STK17B promotes carcinogenesis and metastasis via AKT/GSK-3β/Snail signaling in hepatocellular carcinoma. *Cell. Death. Dis* **2018**,9,236. doi:10.1038/s41419-018-0262-1

115. Appert-Collin, A.; Bennasroune, A.; Jeannesson, P.; Terryn, C.; Fuhrmann, G.; Morjani, H.; Dedieu, S. Role of LRP-1 in cancer cell migration in 3-dimensional collagen matrix. *Cell. Adh. Migr* **2017**,11,316-326. doi:10.1080/19336918.2016.1215788

116. Kairouz, R.; Parmar, J.; Lyons, R.J.; Swarbrick, A.; Musgrove, E.A.; Daly, R.J. Hormonal regulation of the Grb14 signal modulator and its role in cell cycle progression of MCF-7 human breast cancer cells. *J. Cell. Physiol* **2005**,203,85-93. doi:10.1002/jcp.20199

117. Diez-Bello, R.; Jardin, I.; Lopez, J.J.; El Haouari, M.; Ortega-Vidal, J.; Altarejos, J.; Salido, G.M.; Salido, S.; Rosado, J.A. (-)□Oleocanthal inhibits proliferation and migration by modulating Ca2+ entry through TRPC6 in breast cancer cells. *Biochim. Biophys. Acta. Mol. Cell. Res.* **2019**,1866,474-485. doi:10.1016/j.bbamcr.2018.10.010

118. Xue, M.; Tao, W.; Yu, S.; Yan, Z.; Peng, Q.; Jiang, F.; Gao, X. lncRNA ZFPM2-AS1 promotes proliferation via miR-18b-5p/VMA21 axis in lung adenocarcinoma. *J. Cell. Biochem* **2020**,121,313-321. doi:10.1002/jcb.29176

119. Abo-Elfadl, M.T.; Gamal-Eldeen, A.M.; Ismail, M.F.; Shahin, N.N. Silencing of the cytokine receptor TNFRSF13B: A new therapeutic target

for triple-negative breast cancer. *Cytokine* **2020**,125,154790. doi:10.1016/j.cyto.2019.154790

120. Li, J.; Xu, X.; Wei, C.; Liu, L.; Wang, T. Long noncoding RNA NORAD regulates lung cancer cell proliferation, apoptosis, migration, and invasion by the miR-30a-5p/ADAM19 axis. *Int. J. Clin. Exp. Pathol* **2020**,13,1-13.

121. Zhao, J.; Cheng, L. Long non-coding RNA CCAT1/miR-148a axis promotes osteosarcoma proliferation and migration through regulating PIK3IP1. *Acta. Biochim. Biophys. Sin (Shanghai)* **2017**,49,503-512. doi:10.1093/abbs/gmx041

122. Leite, F.A.; Lira, R.C.; Fedatto, P.F.; Antonini, S.R.; Martinelli, C.E .; de Castro, M.; Neder, L.; Ramalho, L.N.; Tucci, S.; Mastelaro, M.J.; et al. Low expression of HLA-DRA, HLA-DPA1, and HLA-DPB1 is associated with poor prognosis in pediatric adrenocortical tumors (ACT). *Pediatr. Blood. Cancer* **2014**,61,1940-1948. doi:10.1002/pbc.25118

123. Feng, Y.; Guo, C.; Wang, H.; Zhao, L.; Wang, W.; Wang, T.; Feng, Y.; Yuan, K.; Huang, G. Fibrinogen-Like Protein 2 (FGL2) is a Novel Biomarker for Clinical Prediction of Human Breast Cancer. *Med. Sci. Monit* **2020**,26,e923531. doi:10.12659/MSM.923531

124. Wang, S.; Xu, L.; Che, X.; Li, C.; Xu, L.; Hou, K.; Fan, Y.; Wen, T.; Qu, X.; Liu, Y. E3 ubiquitin ligases Cbl-b and c-Cbl downregulate PD-L1 in EGFR wild-type non-small cell lung cancer. *FEBS. Lett* **2018**,592,621-630. doi:10.1002/1873-3468.12985

125. Zhong, X.P.; Kan, A.; Ling, Y.H.; Lu, L.H.; Mei, J.; Wei, W.; Li, S.H.; Guo, R.P. NCKAP1 improves patient outcome and inhibits cell growth by enhancing Rb1/p53 activation in hepatocellular carcinoma. *Cell. Death. Dis* **2019**,10,369.. doi:10.1038/s41419-019-1603-4

126. Yokoyama-Mashima, S.; Yogosawa, S.; Kanegae, Y.; Hirooka, S.; Yoshida, S.; Horiuchi, T.; Ohashi, T.; Yanaga, K.; Saruta, M.; Oikawa, T.; et al. Forced expression of DYRK2 exerts anti-tumor effects via apoptotic induction in liver cancer. *Cancer. Lett* **2019**,451,100-109. doi:10.1016/j.canlet.2019.02.046

127. Guo, H.; Zhang, B.; Nairn, A.V.; Nagy, T.; Moremen, K.W.; Buckhaults, P.; Pierce, M. O-Linked N-Acetylglucosamine (O-GlcNAc) Expression Levels Epigenetically Regulate Colon Cancer Tumorigenesis by

Affecting the Cancer Stem Cell Compartment via Modulating Expression of Transcriptional Factor MYBL1. *J. Biol. Chem* **2017**,292,4123-4137. doi:10.1074/jbc.M116.763201

128. Lawson, J.; Dickman, C.; MacLellan, S.; Towle, R.; Jabalee, J.; Lam, S.; Garnis, C. Selective secretion of microRNAs from lung cancer cells via extracellular vesicles promotes CAMK1D-mediated tube formation in endothelial cells. *Oncotarget* **2017**,8,83913-83924. doi:10.18632/oncotarget.19996

129. Wang, X.; Ye, M.; Wu.; M.; Fang, H.; Xiao, B.; Xie, L.; Zhu, X. RNF213 suppresses carcinogenesis in glioblastoma by affecting MAPK/JNK signaling pathway. *Clin. Transl. Oncol* **2020**,22,1506-1516. doi:10.1007/s12094-020-02286-x

130. Taheri, M.; Omrani, M.D.; Noroozi, R.; Ghafouri-Fard, S.; Sayad, A. Retinoic acid-related orphan receptor alpha (RORA) variants and risk of breast cancer. *Breast. Dis* **2017**,37,21-25. doi:10.3233/BD-160248

131. Hoyo, C.; Murphy, S.K.; Schildkraut, J.M.; Vidal, A.C.; Skaar, D.;, Millikan, R.C.; Galanko, J.; Sandler R.S.; Jirtle R.; Keku T. IGF2R genetic variants, circulating IGF2 concentrations and colon cancer risk in African Americans and Whites. *Dis. Markers* **2012**,32,133-141. doi:10.3233/DMA-2011-0865

132. Bai, F.; Xiao, K. Prediction of gastric cancer risk: association between ZBTB20 genetic variance and gastric cancer risk in Chinese Han population. *Biosci. Rep* **2020**,40,BSR20202102. doi:10.1042/BSR20202102

133. Hope, C.; Emmerich, P.B, Papadas, A.; Pagenkopf, A.; Matkowskyj, K.A.; Van De Hey, D.R.; Payne, S.N.; Clipson, L.; Callander, N.S.; Hematti, P.; et al. Versican-Derived Matrikines Regulate Batf3-Dendritic Cell Differentiation and Promote T Cell Infiltration in Colorectal Cancer. *J. Immunol* **2017**,199,1933-1941. doi:10.4049/jimmunol.1700529

134. Bai, X.; Wang, W.; Zhao, P.; Wen, J.; Guo, X.; Shen, T.; Shen, J.; Yang, X. LncRNA CRNDE acts as an oncogene in cervical cancer through sponging miR-183 to regulate CCNB1 expression. *Carcinogenesis* **2020**,41,111-121. doi:10.1093/carcin/bgz166

135. Zienert, E.; Eke, I.; Aust, D.; Cordes, N. LIM-only protein FHL2 critically determines survival and radioresistance of pancreatic cancer cells. *Cancer. Lett* **2015**,364,17-24. doi:10.1016/j.canlet.2015.04.019

136. Yang, J.; Chen, Z.; Liu, N.; Chen, Y. Ribosomal protein L10 in mitochondria serves as a regulator for ROS level in pancreatic cancer cells. *Redox Biol* **2018**,19,158-165. doi:10.1016/j.redox.2018.08.016

137. Xie, F.; Huang, Q.; Wang, C.; Chen, S.; Liu, C.; Lin, X.; Lv, X.; Wang, C. Downregulation of long noncoding RNA SNHG14 suppresses cell proliferation and invasion by regulating EZH2 in pancreatic ductal adenocarcinoma (PDAC). *Cancer. Biomark* **2020**,27,357-364. doi:10.3233/CBM-190908

138. Li, S.S.; Jiang, W.L.; Xiao, W.Q.; Li, K.; Zhang, Y.F.; Guo, X.Y.; Dai, Y.Q.; Zhao, Q.Y.; Jiang, M.J.; Lu, Z.J.; et al. KMT2D deficiency enhances the anti-cancer activity of L48H37 in pancreatic ductal adenocarcinoma. *World. J. Gastrointest. Oncol* **2019**,11,599-621. doi:10.4251/wjgo.v11.i8.599

139. Zhu, G.; Zhou, L.; Liu, H.; Shan, Y.; Zhang, X. MicroRNA-224 Promotes Pancreatic Cancer Cell Proliferation and Migration by Targeting the TXNIP-Mediated HIF1α Pathway. *Cell. Physiol. Biochem* **2018**,48,1735-1746. doi:10.1159/000492309

140. Zhang, K.D.; Hu, B.; Cen, G.; Yang, Y.H.; Chen, W.W.; Guo, Z.Y.; Wang, X.F.; Zhao, Q.; Qiu, Z.J. MiR-301a transcriptionally activated by HIF-2α promotes hypoxia-induced epithelial-mesenchymal transition by targeting TP63 in pancreatic cancer. *World. J. Gastroenterol* **2020**,26,2349-2373. doi:10.3748/wjg.v26.i19.2349

141. Wuebben, E.L.; Wilder, P.J.; Cox, J.L.; Grunkemeyer, J.A.; Caffrey, T.; Hollingsworth, M.A.; Rizzino, A. SOX2 functions as a molecular rheostat to control the growth, tumorigenicity and drug responses of pancreatic ductal adenocarcinoma cells. *Oncotarget* **2016**,7,34890-34906. doi:10.18632/oncotarget.8994

142. Muthalagu, N.; Monteverde, T.; Raffo-Iraolagoitia, X.; Wiesheu, R.; Whyte, D.; Hedley, A.; Laing, S.; Kruspig, B.; Upstill-Goddard R.; Shaw R.; et al. Repression of the Type I Interferon Pathway Underlies MYC- and KRAS-Dependent Evasion of NK and B Cells in Pancreatic Ductal Adenocarcinoma. *Cancer. Discov* **2020**,10,872-887. doi:10.1158/2159-8290.CD-19-0620

143. Wang, Z.; Chen, Y.; Lin, Y.; Wang, X.; Cui, X.; Zhang, Z.; Xian, G.; Qin, C. Novel crosstalk between KLF4 and ZEB1 regulates gemcitabine

resistance in pancreatic ductal adenocarcinoma. *Int. J. Oncol* **2017**,51,1239-1248. doi:10.3892/ijo.2017.4099

144. Hu, L.; Fang, L.; Zhang, Z.P.; Yan, Z.L. TPM1 is a Novel Predictive Biomarker for Gastric Cancer Diagnosis and Prognosis. Clin Lab. **2020**,66,10.7754/Clin.Lab.2019.190235. doi:10.7754/Clin.Lab.2019.190235

145. Chen, H.; Fan, Y.; Xu, W.; Chen, J.; Meng, Y.; Fang, D.; Wang, J. Exploration of miR-1202 and miR-196a in human endometrial cancer based on high throughout gene screening analysis. *Oncol. Rep* **2017**,37,3493-3501. doi:10.3892/or.2017.5596

Tables

Table 1 The sequences of primers for quantitative RT-PCR

Genes	Primers	Length of target fragment, bp
CCNB1	**F:** AATAAGGCGAAGATCAACATGGC	23
	R: TTTGTTACCAATGTCCCCAAGAG	23
FHL2	**F**: GTACAGACTGCTATTCCAACGAG	23
	R: GCACTGCATGGCATGTTGTT	20
HLA-DPA1	**F**: ATGCGCCCTGAAGACAGAATG	21
	R: ACACATGGTCCGCCTTGATG	20
TUBB1	**F**: AACACGGGATCGACTTGGC	19
	R: CTCGGGGCACATATTTCCTAC	21

F: Forward Primers **R: Reverse Primers**

Table 2 The statistical metrics for key differentially expressed genes (DEGs)

Gene Symbol	logFC	p Value	adj.P.Val	t value	Regulation	Gene Name
DAP	0.729809	3.54E-14	2.59E-11	7.862623	Up	death associated protein
MTRNR2L2	1.55786	4.87E-14	3.22E-11	7.816552	Up	MT-RNR2 like 2
ICA1	1.027176	1.66E-13	9E-11	7.636838	Up	islet cell autoantigen 1
KRT8	1.61503	6.94E-13	3.01E-10	7.423576	Up	keratin 8
MAP1LC3B2	1.050642	1.03E-11	3.21E-09	7.008711	Up	microtubule associated protein 1 light chain 3 beta 2
KRT18	1.317775	1.21E-11	3.67E-09	6.984018	Up	keratin 18
DBN1	0.680188	1.71E-11	4.78E-09	6.928904	Up	drebrin 1
MAP1B	0.804673	2.02E-11	5.5E-09	6.902127	Up	microtubule associated protein 1B
IGFBP2	1.26743	2.04E-11	5.5E-09	6.900692	Up	insulin like growth factor binding protein 2
KRT19	1.682062	3.2E-11	8.32E-09	6.828975	Up	keratin 19
ARNTL2	1.064741	3.25E-11	8.42E-09	6.826429	Up	aryl hydrocarbon receptor nuclear translocator like 2
MND1	1.050388	6.48E-11	1.51E-08	6.714983	Up	meiotic nuclear divisions 1
LCN2	1.195504	1.23E-10	2.65E-08	6.610378	Up	lipocalin 2
HP	1.105468	1.98E-10	4.01E-08	6.531824	Up	haptoglobin
GOLIM4	0.730931	1.99E-10	4.01E-08	6.531295	Up	golgi integral membrane protein 4

FGB	1.281458	2.04E-10	4.09E-08	6.526862	Up	fibrinogen beta chain
TCEAL3	0.698058	2.11E-10	4.19E-08	6.521292	Up	transcription elongation factor A like 3
H3P47	0.806164	3.14E-10	5.88E-08	6.455108	Up	H3 histone pseudogene 47
CD27-AS1	1.127104	3.53E-10	6.52E-08	6.435648	Up	CD27 antisense RNA 1
LSMEM1	1.300595	3.94E-10	7.16E-08	6.417125	Up	leucine rich single-pass membrane protein 1
CD63	0.638758	4.97E-10	8.71E-08	6.378004	Up	CD63 molecule
MAOB	1.081308	7.82E-10	1.29E-07	6.301015	Up	monoamine oxidase B
FGG	1.037158	8.4E-10	1.36E-07	6.288927	Up	fibrinogen gamma chain
LOC105370027	1.046446	1.06E-09	1.66E-07	6.248715	Up	uncharacterized LOC105370027
H2BC17	0.973199	1.13E-09	1.75E-07	6.237457	Up	H2B clustered histone 17
ZFPM2	1.167509	1.26E-09	1.93E-07	6.218913	Up	zinc finger protein, FOG family member 2
UBE2Q2P1	0.75226	2.34E-09	3.3E-07	6.111953	Up	ubiquitin conjugating enzyme E2 Q2 pseudogene 1
GTF3C6	0.66658	2.41E-09	3.36E-07	6.107154	Up	general transcription factor IIIC subunit 6
FGA	1.058162	2.56E-09	3.52E-07	6.096366	Up	fibrinogen alpha chain
H4C15	0.646131	3.44E-09	4.5E-07	6.044383	Up	H4 clustered histone 15
TAX1BP3	0.761452	3.74E-09	4.85E-07	6.029641	Up	Tax1 binding protein 3
RET	0.748469	4.44E-09	5.62E-07	5.999495	Up	ret proto-oncogene
HTATIP2	0.696367	4.69E-09	5.87E-07	5.989713	Up	HIV-1 Tat interactive protein 2
MCEMP1	1.055887	7.5E-09	8.94E-07	5.906144	Up	mast cell expressed membrane protein 1
APOB	0.984349	8.66E-09	1.02E-06	5.88037	Up	apolipoprotein B
TPM2	0.808631	9.37E-09	1.09E-06	5.866037	Up	tropomyosin 2
MYL6B	0.735111	9.66E-09	1.12E-06	5.860685	Up	myosin light chain 6B
PRELID2	1.007003	1.01E-08	1.16E-06	5.851789	Up	PRELI domain containing 2
STAC	0.70663	1.08E-08	1.24E-06	5.839882	Up	SH3 and cysteine rich domain
H4C14	0.640786	1.16E-08	1.32E-06	5.826872	Up	H4 clustered histone 14
KLHDC8B	0.931058	1.17E-08	1.32E-06	5.825909	Up	kelch domain containing 8B
HRG	1.25373	1.49E-08	1.63E-06	5.782449	Up	histidine rich glycoprotein
DDAH1	0.960624	2.46E-08	2.46E-06	5.689878	Up	dimethylargininedimethylaminohydrolase 1
C19orf33	1.048033	2.73E-08	2.69E-06	5.670561	Up	chromosome 19 open reading frame 33
FAH	0.995091	3.02E-08	2.92E-06	5.651858	Up	fumarylacetoacetate hydrolase
DCBLD2	0.939546	3.06E-08	2.96E-06	5.649534	Up	discoidin, CUB and LCCL domain containing 2
IFI27L2	0.822377	3.76E-08	3.53E-06	5.611483	Up	interferon alpha inducible protein 27 like 2
PTGES3L	0.989667	3.95E-08	3.7E-06	5.602037	Up	prostaglandin E synthase 3 like
TIMP1	0.829195	4.17E-08	3.89E-06	5.591888	Up	TIMP metallopeptidase inhibitor 1
SNURF	0.743535	4.2E-08	3.91E-06	5.590685	Up	SNRPN upstream reading frame
CMTM2	0.918208	4.76E-08	4.36E-06	5.567227	Up	CKLF like MARVEL transmembrane domain containing 2
MDK	0.797135	6.31E-08	5.6E-06	5.513868	Up	midkine
BCAP31	0.771229	6.77E-08	5.93E-06	5.500637	Up	B cell receptor associated protein 31
RAB32	0.725327	7.54E-08	6.49E-06	5.480174	Up	RAB32, member RAS oncogene family
PCP2	0.848727	7.79E-08	6.64E-06	5.474068	Up	Purkinje cell protein 2
AOPEP	0.665257	9.03E-08	7.61E-06	5.445854	Up	aminopeptidase O (putative)

FKBP1B	1.079675	9.08E-08	7.64E-06	5.444649	Up	FKBP prolylisomerase 1B
UBE2C	0.919203	9.19E-08	7.7E-06	5.442432	Up	ubiquitin conjugating enzyme E2 C
CETN2	0.907963	9.64E-08	7.99E-06	5.433373	Up	centrin 2
TREML3P	0.736245	1.04E-07	8.51E-06	5.418563	Up	triggering receptor expressed on myeloid cells like 3, pseudogene
CLMAT3	0.914772	1.09E-07	8.91E-06	5.409301	Up	colorectal liver metastasis associated transcript 3
TOM1L1	1.010788	1.25E-07	1E-05	5.382976	Up	target of myb1 like 1 membrane trafficking protein
RABAC1	0.685861	1.28E-07	1.02E-05	5.378165	Up	Rab acceptor 1
PTPRN	0.756419	1.8E-07	1.35E-05	5.312969	Up	protein tyrosine phosphatase receptor type N
CCDC9B	0.764226	1.89E-07	1.42E-05	5.302684	Up	coiled-coil domain containing 9B
UNC13B	0.669902	2.49E-07	1.8E-05	5.248667	Up	unc-13 homolog B
APOH	0.937929	2.62E-07	1.88E-05	5.238638	Up	apolipoprotein H
MCM10	0.778282	2.66E-07	1.9E-05	5.236183	Up	minichromosome maintenance 10 replication initiation factor
H2BC11	0.672283	2.8E-07	1.98E-05	5.226015	Up	H2B clustered histone 11
EZH2	0.665264	3E-07	2.1E-05	5.211928	Up	enhancer of zeste 2 polycomb repressive complex 2 subunit
H2AC13	0.672944	3.06E-07	2.14E-05	5.208195	Up	H2A clustered histone 13
NCBP2L	0.690397	3.18E-07	2.2E-05	5.200769	Up	nuclear cap binding protein subunit 2 like
CCNB1	0.69638	3.18E-07	2.2E-05	5.200386	Up	cyclin B1
PKD2	0.747713	3.28E-07	2.25E-05	5.194336	Up	polycystin 2, transient receptor potential cation channel
LOC100130357	0.908199	3.58E-07	2.43E-05	5.176869	Up	uncharacterized LOC100130357
ORM1	0.845653	4.18E-07	2.79E-05	5.145905	Up	orosomucoid 1
CDR2L	0.75789	4.37E-07	2.89E-05	5.137166	Up	cerebellar degeneration related protein 2 like
H2AJ	0.700133	4.63E-07	3.02E-05	5.125431	Up	H2A.J histone
TPM1	0.669813	4.65E-07	3.03E-05	5.124861	Up	tropomyosin 1
ACOT7	0.80117	5.34E-07	3.4E-05	5.097055	Up	acyl-CoA thioesterase 7
AP1M2	0.962099	5.68E-07	3.57E-05	5.084413	Up	adaptor related protein complex 1 subunit mu 2
AVEN	0.668545	6.52E-07	4.05E-05	5.056569	Up	apoptosis and caspase activation inhibitor
DNAH2	0.732007	6.75E-07	4.17E-05	5.049466	Up	dynein axonemal heavy chain 2
TRPC2	0.85544	7.09E-07	4.35E-05	5.039399	Up	transient receptor potential cation channel subfamily C member 2 (pseudogene)
RND3	0.841233	7.53E-07	4.58E-05	5.027115	Up	Rho family GTPase 3
PPP1R14A	0.745833	7.86E-07	4.75E-05	5.018397	Up	protein phosphatase 1 regulatory inhibitor subunit 14A
TGFB3	0.835809	7.9E-07	4.76E-05	5.01733	Up	transforming growth factor beta 3
TPST1	0.819069	8.34E-07	4.99E-05	5.006228	Up	tyrosylproteinsulfotransferase 1
VNN1	0.865209	1.1E-06	6.32E-05	4.949468	Up	vanin 1
MIR1282	1.063689	1.12E-06	6.41E-05	4.945828	Up	microRNA 1282
APOA2	0.724038	1.23E-06	6.93E-05	4.92633	Up	apolipoprotein A2
FAM92A	0.677465	1.25E-06	7.03E-05	4.922308	Up	family with sequence similarity 92 member A
MSANTD3	0.66954	1.29E-06	7.18E-05	4.916615	Up	Myb/SANT DNA binding domain containing 3
GRK4	0.900233	1.37E-06	7.55E-05	4.904444	Up	G protein-coupled receptor kinase 4
TSPAN15	0.802125	1.4E-06	7.7E-05	4.899117	Up	tetraspanin 15

PTGER3	0.731073	1.54E-06	8.36E-05	4.879106	Up	prostaglandin E receptor 3
MITF	0.871653	1.63E-06	8.76E-05	4.867297	Up	melanocyte inducing transcription factor
MMP1	0.771433	1.75E-06	9.33E-05	4.852725	Up	matrix metallopeptidase 1
MAL2	0.749667	1.81E-06	9.62E-05	4.845684	Up	mal, T cell differentiation protein 2 (gene/pseudogene)
CTPS2	0.67219	1.83E-06	9.71E-05	4.843038	Up	CTP synthase 2
LOC101929538	0.711706	1.9E-06	9.98E-05	4.835864	Up	uncharacterized LOC101929538
OR2B6	0.909758	1.94E-06	0.000102	4.831266	Up	olfactory receptor family 2 subfamily B member 6
C20orf96	0.740435	2.13E-06	0.000109	4.811175	Up	chromosome 20 open reading frame 96
MPZL3	0.734878	2.16E-06	0.000111	4.808022	Up	myelin protein zero like 3
LOC101927420	0.734878	2.29E-06	0.000116	4.79601	Up	uncharacterized LOC101927420
EPDR1	0.769808	2.47E-06	0.000125	4.779781	Up	ependymin related 1
FHL2	0.853097	2.75E-06	0.000137	4.756748	Up	four and a half LIM domains 2
LAPTM4B	0.92193	3.02E-06	0.000148	4.736673	Up	lysosomal protein transmembrane 4 beta
ARG2	1.000424	3.03E-06	0.000149	4.735971	Up	arginase 2
ADAM22	0.710055	3.12E-06	0.000152	4.729888	Up	ADAM metallopeptidase domain 22
GPC5	0.6499	3.29E-06	0.000159	4.718778	Up	glypican 5
DERA	0.676038	3.31E-06	0.000161	4.716998	Up	deoxyribose-phosphate aldolase
OXTR	0.917126	3.55E-06	0.00017	4.70246	Up	oxytocin receptor
PROK2	0.789874	3.77E-06	0.000179	4.689155	Up	prokineticin 2
CNN1	0.901951	3.81E-06	0.00018	4.686924	Up	calponin 1
KRT7	0.904375	4.03E-06	0.000188	4.674982	Up	keratin 7
CENPI	0.730063	4.07E-06	0.00019	4.672762	Up	centromere protein I
LINC01684	0.731662	4.19E-06	0.000195	4.666397	Up	long intergenic non-protein coding RNA 1684
KCNMB1	0.752736	4.56E-06	0.000209	4.647801	Up	potassium calcium-activated channel subfamily M regulatory beta subunit 1
LACTB2	0.695963	4.69E-06	0.000215	4.641781	Up	lactamase beta 2
BEST3	0.711771	4.73E-06	0.000216	4.640144	Up	bestrophin 3
C5orf30	0.731538	5.21E-06	0.000236	4.618767	Up	chromosome 5 open reading frame 30
SMPD1	0.834518	5.41E-06	0.000244	4.610568	Up	sphingomyelinphosphodiesterase 1
ANO10	0.657575	5.46E-06	0.000246	4.608531	Up	anoctamin 10
GINS1	0.706019	5.61E-06	0.000252	4.602785	Up	GINS complex subunit 1
TGFB1I1	0.782636	6.07E-06	0.000269	4.585606	Up	transforming growth factor beta 1 induced transcript 1
CABLES1	0.659259	6.29E-06	0.000277	4.577514	Up	Cdk5 and Abl enzyme substrate 1
ROBO1	0.71818	7.03E-06	0.000304	4.552913	Up	roundabout guidance receptor 1
BUB1	0.667318	7.42E-06	0.000319	4.541048	Up	BUB1 mitotic checkpoint serine/threonine kinase
FUNDC1	0.767386	7.66E-06	0.000328	4.533938	Up	FUN14 domain containing 1
CRTC3-AS1	0.751802	7.83E-06	0.000334	4.529039	Up	CRTC3 antisense RNA 1
DMC1	0.841001	7.84E-06	0.000334	4.528894	Up	DNA meiotic recombinase 1
ZSCAN16-AS1	0.738009	8.09E-06	0.000344	4.521862	Up	ZSCAN16 antisense RNA 1
SCARF1	0.676906	8.39E-06	0.000355	4.513776	Up	scavenger receptor class F member 1
ACCSL	0.65649	8.65E-06	0.000365	4.50688	Up	1-aminocyclopropane-1-carboxylate synthase homolog (inactive) like
CXCL3	0.778559	1.03E-05	0.000421	4.468754	Up	C-X-C motif chemokine ligand 3

LINC00892	0.819555	1.05E-05	0.00043	4.462734	Up	long intergenic non-protein coding RNA 892
RNF208	0.841349	1.06E-05	0.000433	4.461088	Up	ring finger protein 208
EAF2	0.668192	1.15E-05	0.000464	4.443023	Up	ELL associated factor 2
LAMB2	0.699363	1.16E-05	0.000468	4.44064	Up	laminin subunit beta 2
LOXL3	0.736971	1.19E-05	0.000477	4.435804	Up	lysyl oxidase like 3
CEACAM6	0.828845	1.22E-05	0.000489	4.429132	Up	CEA cell adhesion molecule 6
HPD	0.801889	1.29E-05	0.00051	4.417691	Up	4-hydroxyphenylpyruvate dioxygenase
TMEM67	0.706644	1.3E-05	0.000511	4.415933	Up	transmembrane protein 67
LINC00534	0.991484	1.3E-05	0.000511	4.415737	Up	long intergenic non-protein coding RNA 534
TYMS	0.660517	1.31E-05	0.000514	4.413975	Up	thymidylatesynthetase
ZGLP1	0.781496	1.36E-05	0.000529	4.405803	Up	zinc finger GATA like protein 1
GNG8	0.74057	1.51E-05	0.000581	4.381524	Up	G protein subunit gamma 8
MT1X	0.78313	1.59E-05	0.000609	4.368771	Up	metallothionein 1X
EVA1B	0.700855	1.71E-05	0.000642	4.352699	Up	eva-1 homolog B
FRMD3	0.658149	1.91E-05	0.000704	4.326801	Up	FERM domain containing 3
ADAMTS1	0.710457	1.94E-05	0.000709	4.324203	Up	ADAM metallopeptidase with thrombospondin type 1 motif 1
ACTR3B	0.733415	2.06E-05	0.00075	4.309603	Up	actin related protein 3B
METTL22	0.69995	2.27E-05	0.00082	4.286931	Up	methyltransferase like 22
WASF1	0.742178	2.34E-05	0.000842	4.280128	Up	WASP family member 1
LINC00548	0.776323	2.51E-05	0.000886	4.264099	Up	long intergenic non-protein coding RNA 548
DTL	0.641962	2.52E-05	0.00089	4.262623	Up	denticleless E3 ubiquitin protein ligase homolog
NT5DC2	0.692809	2.71E-05	0.000939	4.245871	Up	5'-nucleotidase domain containing 2
VEGFC	0.669813	2.88E-05	0.000989	4.231356	Up	vascular endothelial growth factor C
MAGI2	0.735314	2.89E-05	0.00099	4.230904	Up	membrane associated guanylate kinase, WW and PDZ domain containing 2
LINC00211	0.894161	2.93E-05	0.001001	4.227722	Up	long intergenic non-protein coding RNA 211
SPHK1	0.676802	3.04E-05	0.001028	4.219226	Up	sphingosine kinase 1
ZNF529-AS1	0.661567	3.35E-05	0.001114	4.196168	Up	ZNF529 antisense RNA 1
ADAMTS5	0.660099	3.39E-05	0.001123	4.193506	Up	ADAM metallopeptidase with thrombospondin type 1 motif 5
DYNC1I1	0.795012	3.39E-05	0.001124	4.193181	Up	dynein cytoplasmic 1 intermediate chain 1
CCDC3	0.674572	3.42E-05	0.001131	4.191397	Up	coiled-coil domain containing 3
YIF1B	0.743761	3.43E-05	0.001133	4.190185	Up	Yip1 interacting factor homolog B, membrane trafficking protein
PRKAR1B	0.701104	3.54E-05	0.001164	4.182731	Up	protein kinase cAMP-dependent type I regulatory subunit beta
NMNAT3	0.641441	4.03E-05	0.001305	4.151903	Up	nicotinamide nucleotide adenylyltransferase 3
TSPAN13	0.656865	4.05E-05	0.00131	4.150707	Up	tetraspanin 13
POLR3G	0.862253	4.19E-05	0.001346	4.143028	Up	RNA polymerase III subunit G
TMEM158	0.832551	4.39E-05	0.0014	4.131626	Up	transmembrane protein 158 (gene/pseudogene)
CYTOR	0.669042	4.41E-05	0.001403	4.130782	Up	cytoskeleton regulator RNA
FN3K	0.715739	4.44E-05	0.001411	4.128739	Up	fructosamine 3 kinase
CENPU	0.685833	4.48E-05	0.001421	4.126825	Up	centromere protein U
ANXA3	0.642891	4.52E-05	0.001431	4.124872	Up	annexin A3

PGLYRP1	0.743358	4.53E-05	0.001432	4.124178	Up	peptidoglycan recognition protein 1
LINC00853	0.886342	4.73E-05	0.001482	4.113907	Up	long intergenic non-protein coding RNA 853
C21orf58	0.673046	5E-05	0.001552	4.10054	Up	chromosome 21 open reading frame 58
PHACTR3	0.768701	5.12E-05	0.001582	4.094798	Up	phosphatase and actin regulator 3
CYSTM1	0.639491	6.02E-05	0.001809	4.055347	Up	cysteine rich transmembrane module containing 1
E2F1	0.689528	6.28E-05	0.001867	4.045197	Up	E2F transcription factor 1
CTNS	0.723506	6.31E-05	0.001876	4.043771	Up	cystinosin, lysosomalcystine transporter
LUZP6	0.784849	6.33E-05	0.00188	4.043183	Up	leucine zipper protein 6
LY6G6F-LY6G6D	0.697512	6.82E-05	0.002	4.024994	Up	LY6G6F-LY6G6D readthrough
DRC7	0.641026	6.97E-05	0.00203	4.019452	Up	dynein regulatory complex subunit 7
SPINT2	0.716213	7.44E-05	0.002142	4.003447	Up	serine peptidase inhibitor, Kunitz type 2
TST	0.653129	8.57E-05	0.002428	3.968702	Up	thiosulfate sulfurtransferase
PBLD	0.728909	9.82E-05	0.002708	3.934854	Up	phenazine biosynthesis like protein domain containing
COL6A3	0.800552	0.000106	0.002866	3.916014	Up	collagen type VI alpha 3 chain
SMYD3	0.658545	0.00011	0.002954	3.906774	Up	SET and MYND domain containing 3
SEPTIN4	0.678613	0.000113	0.003014	3.900217	Up	septin 4
ADAM32	0.660263	0.000114	0.003032	3.898284	Up	ADAM metallopeptidase domain 32
ADH1B	0.683312	0.000115	0.003044	3.896241	Up	alcohol dehydrogenase 1B (class I), beta polypeptide
TTLL7	0.772356	0.000116	0.003081	3.892908	Up	tubulin tyrosine ligase like 7
ME1	0.679181	0.000119	0.003134	3.887332	Up	malic enzyme 1
PADI4	0.638723	0.000119	0.00315	3.885738	Up	peptidyl arginine deiminase 4
CIDECP1	0.65588	0.000123	0.003226	3.877866	Up	cell death inducing DFFA like effector c pseudogene 1
CD151	0.680244	0.000133	0.003439	3.859108	Up	CD151 molecule (Raph blood group)
ETV4	0.762875	0.000137	0.003518	3.851736	Up	ETS variant transcription factor 4
MYOM1	0.712787	0.000141	0.003611	3.843573	Up	myomesin 1
MSANTD3-TMEFF1	0.694055	0.000161	0.00403	3.810035	Up	MSANTD3-TMEFF1 readthrough
GLA	0.768164	0.000169	0.004193	3.797347	Up	galactosidase alpha
TRHDE	0.673175	0.000173	0.004275	3.791127	Up	thyrotropin releasing hormone degrading enzyme
CCT6P3	0.64622	0.000176	0.00433	3.786849	Up	chaperonin containing TCP1 subunit 6 pseudogene 3
DNAH14	0.67538	0.000197	0.004737	3.757991	Up	dynein axonemal heavy chain 14
PLEKHA8P1	0.678922	0.000198	0.004758	3.756381	Up	pleckstrin homology domain containing A8 pseudogene 1
MIR646HG	0.725938	0.0002	0.004796	3.753511	Up	MIR646 host gene
TMEFF1	0.71416	0.000213	0.005026	3.73756	Up	transmembrane protein with EGF like and two follistatin like domains 1
DPY19L2	0.678632	0.000214	0.005044	3.736377	Up	dpy-19 like 2
ERC2	0.640215	0.000232	0.005396	3.715528	Up	ELKS/RAB6-interacting/CAST family member 2
PLA2G4A	0.672732	0.000232	0.005396	3.715504	Up	phospholipase A2 group IVA
ZC3HAV1L	0.67853	0.000241	0.005556	3.705049	Up	zinc finger CCCH-type containing, antiviral 1 like
AQP10	0.702387	0.000255	0.005825	3.690433	Up	aquaporin 10
PRTFDC1	0.732046	0.000266	0.006032	3.67956	Up	phosphoribosyltransferase domain containing 1
SERPINE2	0.708281	0.000278	0.006263	3.667198	Up	serpin family E member 2

PRR16	0.647548	0.000365	0.007821	3.594668	Up	proline rich 16
ACER2	0.714054	0.000441	0.009068	3.543878	Up	alkaline ceramidase 2
THEM5	0.68475	0.000632	0.012136	3.44491	Up	thioesterase superfamily member 5
MS4A3	0.669703	0.000713	0.013422	3.41125	Up	membrane spanning 4-domains A3
CLEC2L	0.667059	0.000745	0.013903	3.398829	Up	C-type lectin domain family 2 member L
TRPC6	0.669122	0.000816	0.014941	3.373194	Up	transient receptor potential cation channel subfamily C member 6
LINC01089	0.641558	0.00098	0.017284	3.320844	Up	long intergenic non-protein coding RNA 1089
GRB14	0.73252	0.001457	0.023689	3.205476	Up	growth factor receptor bound protein 14
MYEOV	0.66784	0.001553	0.024891	3.186553	Up	myeloma overexpressed
TNNC2	0.681795	0.001798	0.027848	3.142855	Up	troponin C2, fast skeletal type
PLAAT1	0.716924	0.001991	0.030092	3.112202	Up	phospholipase A and acyltransferase 1
INKA2-AS1	0.64851	0.002272	0.033302	3.072049	Up	INKA2 antisense RNA 1
DEFA1	0.710406	0.002482	0.035699	3.044927	Up	defensin alpha 1
LYPLAL1-DT	0.653678	0.00251	0.035991	3.041436	Up	LYPLAL1 divergent transcript
G0S2	0.666254	0.003148	0.04269	2.970966	Up	G0/G1 switch 2
LOC105371967	0.715866	0.00336	0.044907	2.950485	Up	uncharacterized LOC105371967
FBXO7	-1.02578	4.57E-31	2.47E-26	-12.6471	Down	F-box protein 7
CD44	-0.77354	1.37E-24	3.7E-20	-10.9533	Down	CD44 molecule (Indian blood group)
BNIP3L	-1.11652	7.58E-24	1.37E-19	-10.7506	Down	BCL2 interacting protein 3 like
ITGA4	-0.7155	7.16E-22	6.46E-18	-10.202	Down	integrin subunit alpha 4
SRRM2	-0.7545	2.82E-21	1.74E-17	-10.0332	Down	serine/arginine repetitive matrix 2
IL7R	-0.9167	3.22E-21	1.74E-17	-10.0169	Down	interleukin 7 receptor
HLA-DRA	-0.72512	6.41E-21	2.89E-17	-9.93149	Down	major histocompatibility complex, class II, DR alpha
AHNAK	-1.08285	1.37E-20	5.71E-17	-9.83691	Down	AHNAK nucleoprotein
SESN3	-0.83384	3.7E-20	1.34E-16	-9.71209	Down	sestrin 3
BTG1	-0.67464	8.57E-20	2.9E-16	-9.606	Down	BTG anti-proliferation factor 1
TCF7	-1.05537	9.82E-20	3.13E-16	-9.58878	Down	transcription factor 7
PTPRC	-0.79038	1.95E-19	5.55E-16	-9.50153	Down	protein tyrosine phosphatase receptor type C
STK17B	-0.6627	8.27E-19	1.95E-15	-9.31582	Down	serine/threonine kinase 17b
IKZF3	-0.84512	4.27E-18	9.64E-15	-9.10211	Down	IKAROS family zinc finger 3
OGT	-0.85075	8.43E-18	1.83E-14	-9.01274	Down	O-linked N-acetylglucosamine (GlcNAc) transferase
MALAT1	-1.15502	1.98E-17	4.04E-14	-8.89988	Down	metastasis associated lung adenocarcinoma transcript 1
MBNL3	-0.85006	2.01E-17	4.04E-14	-8.89733	Down	muscleblind like splicing regulator 3
TXNIP	-0.69647	3.04E-17	5.67E-14	-8.8425	Down	thioredoxin interacting protein
SLC38A1	-0.674	7.23E-17	1.22E-13	-8.72615	Down	solute carrier family 38 member 1
NCKAP1L	-0.66777	7.45E-17	1.22E-13	-8.72221	Down	NCK associated protein 1 like
PAX5	-1.15676	2.44E-16	3.67E-13	-8.56139	Down	paired box 5
TNRC6B	-0.80631	3.35E-16	4.86E-13	-8.51801	Down	trinucleotide repeat containing adaptor 6B
ATM	-0.65967	4.2E-16	5.83E-13	-8.48699	Down	ATM serine/threonine kinase
HLA-DPA1	-0.67781	1.41E-15	1.82E-12	-8.31961	Down	major histocompatibility complex, class II, DP alpha 1
FAM102A	-0.76298	1.5E-15	1.89E-12	-8.31093	Down	family with sequence similarity 102

						member A
DYRK2	-0.69741	1.54E-15	1.89E-12	-8.30769	Down	dual specificity tyrosine phosphorylation regulated kinase 2
STRADB	-0.88854	2.32E-15	2.7E-12	-8.24996	Down	STE20 related adaptor beta
RNF213	-0.78696	2.36E-15	2.7E-12	-8.2476	Down	ring finger protein 213
RPL10	-0.68279	2.4E-15	2.7E-12	-8.24564	Down	ribosomal protein L10
EEF1A1	-0.93399	4.56E-15	4.75E-12	-8.15527	Down	eukaryotic translation elongation factor 1 alpha 1
RPL23A	-0.69095	5.13E-15	5.14E-12	-8.13875	Down	ribosomal protein L23a
RPL37	-0.68343	6.21E-15	5.9E-12	-8.11176	Down	ribosomal protein L37
HBB	-1.18457	1.01E-14	9.1E-12	-8.04285	Down	hemoglobin subunit beta
CAMK4	-1.1638	1.36E-14	1.17E-11	-8.00017	Down	calcium/calmodulin dependent protein kinase IV
TENT5C	-0.78619	1.47E-14	1.24E-11	-7.98892	Down	terminal nucleotidyltransferase 5C
BACH2	-1.06422	1.5E-14	1.24E-11	-7.98579	Down	BTB domain and CNC homolog 2
TBCEL	-0.64594	1.51E-14	1.24E-11	-7.98482	Down	tubulin folding cofactor E like
WDFY4	-0.99635	2.23E-14	1.75E-11	-7.9292	Down	WDFY family member 4
RPL27A	-0.6388	2.37E-14	1.83E-11	-7.92052	Down	ribosomal protein L27a
AAK1	-0.65765	4.11E-14	2.89E-11	-7.8413	Down	AP2 associated kinase 1
MS4A1	-0.95361	4.31E-14	2.96E-11	-7.8342	Down	membrane spanning 4-domains A1
DCAF12	-0.7593	5.05E-14	3.3E-11	-7.81122	Down	DDB1 and CUL4 associated factor 12
KMT2D	-0.87707	5.94E-14	3.83E-11	-7.78757	Down	lysine methyltransferase 2D
OPA1	-0.62121	6.75E-14	4.3E-11	-7.76907	Down	OPA1 mitochondrial dynamin like GTPase
CAMK1D	-0.67422	1.2E-13	6.98E-11	-7.68504	Down	calcium/calmodulin dependent protein kinase ID
FAM117B	-0.73486	1.2E-13	6.98E-11	-7.68502	Down	family with sequence similarity 117 member B
BCL11B	-0.71547	1.26E-13	7.28E-11	-7.67723	Down	BAF chromatin remodeling complex subunit BCL11B
HBA1	-1.28343	1.39E-13	7.86E-11	-7.66283	Down	hemoglobin subunit alpha 1
SEC16A	-0.63051	2.06E-13	1.07E-10	-7.60474	Down	SEC16 homolog A, endoplasmic reticulum export factor
NOTCH2	-1.02848	3.2E-13	1.62E-10	-7.53985	Down	notch receptor 2
SLC25A37	-0.97321	3.22E-13	1.62E-10	-7.53857	Down	solute carrier family 25 member 37
BCL9L	-0.7821	3.41E-13	1.67E-10	-7.53032	Down	BCL9 like
RCAN3	-0.67723	3.62E-13	1.75E-10	-7.52118	Down	RCAN family member 3
RALGPS2	-0.81589	4.58E-13	2.08E-10	-7.48622	Down	Ral GEF with PH domain and SH3 binding motif 2
SOX6	-1.09995	5.44E-13	2.43E-10	-7.46032	Down	SRY-box transcription factor 6
TRANK1	-0.70118	6.86E-13	2.99E-10	-7.4255	Down	tetratricopeptide repeat and ankyrin repeat containing 1
IL10RA	-0.80857	7.25E-13	3.11E-10	-7.41713	Down	interleukin 10 receptor subunit alpha
TCP11L2	-0.85596	8.16E-13	3.42E-10	-7.39924	Down	t-complex 11 like 2
TMC8	-0.90771	8.95E-13	3.69E-10	-7.38532	Down	transmembrane channel like 8
HBA2	-1.1918	1.49E-12	5.84E-10	-7.30802	Down	hemoglobin subunit alpha 2
ZBTB20	-0.68652	2.37E-12	8.9E-10	-7.23703	Down	zinc finger and BTB domain containing 20
CTSB	-0.68749	3.44E-12	1.27E-09	-7.17953	Down	cathepsin B
NSUN3	-0.97469	3.57E-12	1.3E-09	-7.17397	Down	NOP2/Sun RNA methyltransferase 3
MARCHF8	-0.64518	4.02E-12	1.45E-09	-7.15528	Down	membrane associated ring-CH-type finger 8

BLK	-0.93113	4.45E-12	1.6E-09	-7.13963	Down	BLK proto-oncogene, Src family tyrosine kinase
LEF1	-0.72094	5.64E-12	1.97E-09	-7.10302	Down	lymphoid enhancer binding factor 1
TLCD4	-0.94983	5.98E-12	2.04E-09	-7.09373	Down	TLC domain containing 4
CBLB	-0.62042	6.13E-12	2.06E-09	-7.08996	Down	Cbl proto-oncogene B
IFIT1B	-1.14286	7.54E-12	2.43E-09	-7.05769	Down	interferon induced protein with tetratricopeptide repeats 1B
NLRP1	-0.70059	8.94E-12	2.81E-09	-7.03094	Down	NLR family pyrin domain containing 1
SORL1	-0.74274	1.46E-11	4.32E-09	-6.95383	Down	sortilin related receptor 1
IGF2R	-0.81797	1.48E-11	4.34E-09	-6.95175	Down	insulin like growth factor 2 receptor
PLEC	-0.76357	1.63E-11	4.68E-09	-6.93634	Down	plectin
EEF2	-0.65473	1.63E-11	4.68E-09	-6.93587	Down	eukaryotic translation elongation factor 2
AFF3	-0.87612	1.65E-11	4.71E-09	-6.93416	Down	AF4/FMR2 family member 3
YOD1	-0.88888	1.72E-11	4.78E-09	-6.92773	Down	YOD1 deubiquitinase
SFT2D2	-0.63701	2E-11	5.49E-09	-6.90414	Down	SFT2 domain containing 2
NIBAN3	-0.99082	2.03E-11	5.5E-09	-6.90116	Down	niban apoptosis regulator 3
POU2F2	-0.62862	2.43E-11	6.49E-09	-6.87264	Down	POU class 2 homeobox 2
BCL11A	-0.69858	3.3E-11	8.52E-09	-6.82374	Down	BAF chromatin remodeling complex subunit BCL11A
CLEC17A	-0.81849	3.72E-11	9.42E-09	-6.80453	Down	C-type lectin domain containing 17A
ARL4A	-0.79887	3.94E-11	9.88E-09	-6.79545	Down	ADP ribosylation factor like GTPase 4A
TLCD4-RWDD3	-0.96826	4.03E-11	1E-08	-6.79186	Down	TLCD4-RWDD3 readthrough
SCARNA21B	-1.42152	4.37E-11	1.07E-08	-6.77868	Down	small Cajal body-specific RNA 21B
RANBP10	-0.73457	5.18E-11	1.22E-08	-6.75141	Down	RAN binding protein 10
BMF	-0.79975	6.24E-11	1.46E-08	-6.72111	Down	Bcl2 modifying factor
CLEC2D	-0.68117	9.34E-11	2.09E-08	-6.65559	Down	C-type lectin domain family 2 member D
CIITA	-0.75359	1.01E-10	2.25E-08	-6.64292	Down	class II major histocompatibility complex transactivator
TTN	-1.14193	1.17E-10	2.57E-08	-6.61882	Down	titin
SLC4A1	-1.02319	1.56E-10	3.25E-08	-6.57166	Down	solute carrier family 4 member 1 (Diego blood group)
VSTM2A	-0.78114	1.64E-10	3.41E-08	-6.56331	Down	V-set and transmembrane domain containing 2A
FGL2	-0.65079	1.81E-10	3.71E-08	-6.54693	Down	fibrinogen like 2
RORA	-0.65858	1.96E-10	3.99E-08	-6.53369	Down	RAR related orphan receptor A
TNFRSF13C	-0.91687	2.97E-10	5.64E-08	-6.46456	Down	TNF receptor superfamily member 13C
EP400	-0.66759	3.19E-10	5.96E-08	-6.45231	Down	E1A binding protein p400
PER1	-0.85447	3.87E-10	7.05E-08	-6.42021	Down	period circadian regulator 1
MPEG1	-0.67212	5.39E-10	9.42E-08	-6.3641	Down	macrophage expressed 1
MGAT4A	-0.65772	5.49E-10	9.55E-08	-6.36127	Down	alpha-1,3-mannosyl-glycoprotein 4-beta-N-acetylglucosaminyltransferase A
OSBPL10	-0.76921	6.1E-10	1.04E-07	-6.34334	Down	oxysterol binding protein like 10
SLC2A1	-1.01788	6.65E-10	1.13E-07	-6.32861	Down	solute carrier family 2 member 1
PLAGL2	-0.65128	7.62E-10	1.27E-07	-6.30558	Down	PLAG1 like zinc finger 2
WDFY2	-0.69295	7.76E-10	1.29E-07	-6.30233	Down	WD repeat and FYVE domain containing 2
SLC14A1	-0.82792	7.81E-10	1.29E-07	-6.30132	Down	solute carrier family 14 member 1 (Kidd blood group)
VIPR1	-0.76825	8.51E-10	1.37E-07	-6.28656	Down	vasoactive intestinal peptide receptor 1

TFRC	-0.80086	8.7E-10	1.39E-07	-6.28281	Down	transferrin receptor
AGPAT4	-0.83329	9.33E-10	1.48E-07	-6.27089	Down	1-acylglycerol-3-phosphate O-acyltransferase 4
COBLL1	-0.72259	1.01E-09	1.59E-07	-6.25677	Down	cordon-bleu WH2 repeat protein like 1
SPOCK2	-0.89285	1.11E-09	1.74E-07	-6.24084	Down	SPARC (osteonectin), cwcv and kazal like domains proteoglycan 2
FECH	-0.79692	1.35E-09	2.03E-07	-6.20743	Down	ferrochelatase
HLA-DMB	-0.71841	1.47E-09	2.19E-07	-6.19232	Down	major histocompatibility complex, class II, DM beta
MXI1	-0.66288	1.67E-09	2.43E-07	-6.17102	Down	MAX interactor 1, dimerization protein
TRAK2	-0.99989	1.9E-09	2.73E-07	-6.14798	Down	trafficking kinesin protein 2
TSPAN5	-0.68028	3.29E-09	4.34E-07	-6.05219	Down	tetraspanin 5
SPTA1	-1.01751	4.06E-09	5.21E-07	-6.01532	Down	spectrin alpha, erythrocytic 1
SCARNA10	-1.16787	4.37E-09	5.55E-07	-6.00252	Down	small Cajal body-specific RNA 10
CXCR5	-0.91719	5.95E-09	7.25E-07	-5.9476	Down	C-X-C motif chemokine receptor 5
KLK1	-0.94232	6.66E-09	8.03E-07	-5.92739	Down	kallikrein 1
CTC1	-0.70188	8.37E-09	9.87E-07	-5.88644	Down	CST telomere replication complex component 1
ALDH5A1	-0.71117	9.58E-09	1.11E-06	-5.86216	Down	aldehyde dehydrogenase 5 family member A1
YIPF4	-0.68858	9.91E-09	1.14E-06	-5.85599	Down	Yip1 domain family member 4
SZT2	-0.73017	1.03E-08	1.18E-06	-5.84867	Down	SZT2 subunit of KICSTOR complex
MIAT	-0.63403	1.18E-08	1.33E-06	-5.82457	Down	myocardial infarction associated transcript
LENG8	-0.63693	1.58E-08	1.72E-06	-5.7713	Down	leukocyte receptor cluster member 8
SLC7A6	-0.77445	1.83E-08	1.94E-06	-5.74413	Down	solute carrier family 7 member 6
PLBD2	-0.83269	1.94E-08	2.05E-06	-5.73332	Down	phospholipase B domain containing 2
RPL13A	-0.62991	2.15E-08	2.21E-06	-5.71499	Down	ribosomal protein L13a
TNFRSF13B	-0.94543	2.39E-08	2.41E-06	-5.6953	Down	TNF receptor superfamily member 13B
CD22	-0.67168	2.5E-08	2.49E-06	-5.68696	Down	CD22 molecule
SERINC5	-0.73923	2.52E-08	2.5E-06	-5.6859	Down	serine incorporator 5
GPRASP1	-0.81967	2.57E-08	2.55E-06	-5.68227	Down	G protein-coupled receptor associated sorting protein 1
ADA2	-0.73878	2.61E-08	2.58E-06	-5.67885	Down	adenosine deaminase 2
CCR7	-0.82793	2.73E-08	2.68E-06	-5.67111	Down	C-C motif chemokine receptor 7
SCARNA6	-0.77803	2.88E-08	2.81E-06	-5.66069	Down	small Cajal body-specific RNA 6
CNKSR2	-0.75294	3.18E-08	3.06E-06	-5.64253	Down	connector enhancer of kinase suppressor of Ras 2
VCAN	-0.73858	3.74E-08	3.52E-06	-5.61242	Down	versican
SLC24A4	-0.87802	4.35E-08	4.03E-06	-5.58396	Down	solute carrier family 24 member 4
LINC00926	-0.87511	4.52E-08	4.17E-06	-5.57692	Down	long intergenic non-protein coding RNA 926
ACSL6	-0.82878	4.81E-08	4.39E-06	-5.56537	Down	acyl-CoA synthetase long chain family member 6
TTC14	-0.89136	4.84E-08	4.41E-06	-5.5642	Down	tetratricopeptide repeat domain 14
FCRL1	-0.86187	5.34E-08	4.82E-06	-5.54543	Down	Fc receptor like 1
SLC25A39	-0.68018	5.46E-08	4.91E-06	-5.54135	Down	solute carrier family 25 member 39
LY9	-0.76456	5.66E-08	5.08E-06	-5.53456	Down	lymphocyte antigen 9
GOLGA8A	-0.83441	7.01E-08	6.08E-06	-5.49414	Down	golgin A8 family member A
ATP2B1	-0.62628	7.37E-08	6.37E-06	-5.48451	Down	ATPase plasma membrane Ca2+ transporting 1

PWAR5	-0.75691	8.03E-08	6.79E-06	-5.46817	Down	PraderWilli/Angelman region RNA 5
MRC2	-0.81976	9.06E-08	7.63E-06	-5.44524	Down	mannose receptor C type 2
SPIB	-0.63152	9.37E-08	7.82E-06	-5.43865	Down	Spi-B transcription factor
GRINA	-0.65332	1.01E-07	8.28E-06	-5.42515	Down	glutamate ionotropic receptor NMDA type subunit associated protein 1
LRP1	-0.84115	1.01E-07	8.28E-06	-5.42512	Down	LDL receptor related protein 1
ADAM28	-0.81306	1.11E-07	9.02E-06	-5.40656	Down	ADAM metallopeptidase domain 28
TRABD2A	-0.7573	1.16E-07	9.42E-06	-5.39715	Down	TraB domain containing 2A
PIEZO1	-0.74385	1.17E-07	9.44E-06	-5.39644	Down	piezo type mechanosensitive ion channel component 1
ADAM19	-0.68425	1.47E-07	1.15E-05	-5.35189	Down	ADAM metallopeptidase domain 19
PARP15	-0.71333	2.02E-07	1.5E-05	-5.29026	Down	poly(ADP-ribose) polymerase family member 15
CD27	-0.71993	2.07E-07	1.53E-05	-5.28562	Down	CD27 molecule
NELL2	-0.67846	2.21E-07	1.62E-05	-5.27231	Down	neural EGFL like 2
CD79A	-0.74535	2.38E-07	1.73E-05	-5.2578	Down	CD79a molecule
ANKRD52	-0.63287	2.6E-07	1.87E-05	-5.24037	Down	ankyrin repeat domain 52
DNHD1	-0.7211	2.8E-07	1.98E-05	-5.22571	Down	dynein heavy chain domain 1
NEURL1	-0.74572	2.93E-07	2.06E-05	-5.21673	Down	neuralized E3 ubiquitin protein ligase 1
CRTC1	-0.68306	3.27E-07	2.25E-05	-5.1949	Down	CREB regulated transcription coactivator 1
GOLGA8B	-0.84973	3.8E-07	2.56E-05	-5.16529	Down	golgin A8 family member B
ZNF860	-0.72407	3.83E-07	2.58E-05	-5.16356	Down	zinc finger protein 860
P2RX5	-0.67155	3.84E-07	2.58E-05	-5.16328	Down	purinergic receptor P2X 5
BTLA	-0.73832	3.96E-07	2.65E-05	-5.15708	Down	B and T lymphocyte associated
OBSCN	-0.80054	4.42E-07	2.91E-05	-5.13505	Down	obscurin, cytoskeletal calmodulin and titin-interacting RhoGEF
SEMA7A	-0.6976	4.47E-07	2.94E-05	-5.13259	Down	semaphorin 7A (John Milton Hagen blood group)
IFFO1	-0.65589	4.96E-07	3.2E-05	-5.11184	Down	intermediate filament family orphan 1
SLC38A5	-0.75551	5.64E-07	3.56E-05	-5.0858	Down	solute carrier family 38 member 5
LINC02273	-0.70556	5.67E-07	3.57E-05	-5.08477	Down	long intergenic non-protein coding RNA 2273
DNAH1	-0.7411	6.47E-07	4.02E-05	-5.05819	Down	dynein axonemal heavy chain 1
NEU3	-0.70715	7.2E-07	4.4E-05	-5.03638	Down	neuraminidase 3
POLM	-0.67693	7.44E-07	4.53E-05	-5.02954	Down	DNA polymerase mu
RPS6KA5	-0.67198	8.28E-07	4.96E-05	-5.00771	Down	ribosomal protein S6 kinase A5
PDE3B	-0.68318	8.73E-07	5.17E-05	-4.99695	Down	phosphodiesterase 3B
COL7A1	-0.7674	9.21E-07	5.42E-05	-4.98585	Down	collagen type VII alpha 1 chain
HEPACAM2	-0.65213	1.02E-06	5.93E-05	-4.96469	Down	HEPACAM family member 2
CELSR1	-0.64047	1.12E-06	6.39E-05	-4.94638	Down	cadherin EGF LAG seven-pass G-type receptor 1
ZBTB39	-0.67388	1.13E-06	6.46E-05	-4.94372	Down	zinc finger and BTB domain containing 39
MOB3B	-0.68472	1.25E-06	7.03E-05	-4.92272	Down	MOB kinase activator 3B
RHAG	-0.8349	1.26E-06	7.06E-05	-4.92115	Down	Rh associated glycoprotein
CR1	-0.65192	1.32E-06	7.32E-05	-4.91176	Down	complement C3b/C4b receptor 1 (Knops blood group)
DBP	-0.65426	1.38E-06	7.62E-05	-4.90202	Down	D-box binding PAR bZIP transcription factor
TUBGCP6	-0.66735	1.55E-06	8.4E-05	-4.8776	Down	tubulin gamma complex associated protein 6

ZNF549	-0.69296	1.59E-06	8.58E-05	-4.87232	Down	zinc finger protein 549
CSF1R	-0.63553	1.62E-06	8.71E-05	-4.86868	Down	colony stimulating factor 1 receptor
EPB42	-0.87201	1.73E-06	9.24E-05	-4.85526	Down	erythrocyte membrane protein band 4.2
SCARNA7	-0.63099	1.87E-06	9.88E-05	-4.83874	Down	small Cajal body-specific RNA 7
GNG7	-0.66304	1.98E-06	0.000104	-4.82656	Down	G protein subunit gamma 7
ZNF589	-0.63146	2E-06	0.000105	-4.82428	Down	zinc finger protein 589
GCNT2	-0.69581	2.01E-06	0.000105	-4.82357	Down	glucosaminyl (N-acetyl) transferase 2 (I blood group)
GPR146	-0.72697	2.04E-06	0.000106	-4.82048	Down	G protein-coupled receptor 146
QSOX2	-0.66298	2.14E-06	0.000109	-4.8106	Down	quiescin sulfhydryl oxidase 2
SNORA53	-0.92118	2.21E-06	0.000113	-4.80308	Down	small nucleolar RNA, H/ACA box 53
SCARNA13	-0.77859	2.26E-06	0.000115	-4.79894	Down	small Cajal body-specific RNA 13
ITGB2-AS1	-0.62011	3.09E-06	0.000151	-4.73185	Down	ITGB2 antisense RNA 1
ESPN	-0.78256	3.11E-06	0.000152	-4.73085	Down	espin
NEAT1	-0.72879	3.35E-06	0.000162	-4.71479	Down	nuclear paraspeckle assembly transcript 1
FHDC1	-0.93149	3.52E-06	0.000169	-4.70423	Down	FH2 domain containing 1
ZC3H12D	-0.64158	3.53E-06	0.000169	-4.70345	Down	zinc finger CCCH-type containing 12D
ABCD2	-0.6691	3.76E-06	0.000178	-4.6898	Down	ATP binding cassette subfamily D member 2
MCOLN1	-0.69108	3.83E-06	0.000181	-4.68576	Down	mucolipin 1
NR4A1	-0.64016	4.23E-06	0.000196	-4.66458	Down	nuclear receptor subfamily 4 group A member 1
SLC25A42	-0.63249	4.54E-06	0.000209	-4.64904	Down	solute carrier family 25 member 42
GYPA	-0.73764	5.3E-06	0.000239	-4.61504	Down	glycophorin A (MNS blood group)
SCARNA2	-0.67524	6.79E-06	0.000297	-4.5607	Down	small Cajal body-specific RNA 2
FAM167A	-0.65735	7.44E-06	0.000319	-4.54065	Down	family with sequence similarity 167 member A
ALDH6A1	-0.6308	8.11E-06	0.000345	-4.52128	Down	aldehyde dehydrogenase 6 family member A1
CD4	-0.62279	8.14E-06	0.000345	-4.52057	Down	CD4 molecule
ABCA2	-0.6866	9.04E-06	0.000378	-4.49716	Down	ATP binding cassette subfamily A member 2
BEND4	-0.64725	9.32E-06	0.000388	-4.49036	Down	BEN domain containing 4
CENPF	-0.7335	1.03E-05	0.000422	-4.46818	Down	centromere protein F
CD6	-0.65075	1.03E-05	0.000423	-4.46737	Down	CD6 molecule
KLHL3	-0.63143	1.15E-05	0.000465	-4.44229	Down	kelch like family member 3
GYPB	-0.73759	1.45E-05	0.00056	-4.39099	Down	glycophorin B (MNS blood group)
ABCC13	-0.70835	1.46E-05	0.000566	-4.38865	Down	ATP binding cassette subfamily C member 13 (pseudogene)
ATP13A1	-0.61946	1.58E-05	0.000606	-4.3702	Down	ATPase 13A1
MYO15B	-0.6612	1.65E-05	0.000624	-4.36062	Down	myosin XVB
CD5	-0.65427	1.89E-05	0.000697	-4.32962	Down	CD5 molecule
DUSP2	-0.64467	1.91E-05	0.000702	-4.32778	Down	dual specificity phosphatase 2
SCML4	-0.63141	1.91E-05	0.000702	-4.32734	Down	Scmpolycomb group protein like 4
PIK3IP1	-0.62444	3.82E-05	0.001247	-4.16463	Down	phosphoinositide-3-kinase interacting protein 1
ALAS2	-0.66726	5.72E-05	0.001735	-4.06777	Down	5'-aminolevulinate synthase 2
RMRP	-0.64882	8.71E-05	0.002461	-3.96458	Down	RNA component of mitochondrial RNA processing endoribonuclease
RNF182	-0.84789	0.000111	0.00298	-3.90357	Down	ring finger protein 182

RNA5-8SN2	-1.28453	0.000116	0.003077	-3.89329	Down	RNA, 5.8S ribosomal N2
SELENBP1	-0.63971	0.000122	0.003212	-3.87967	Down	selenium binding protein 1
LINC01857	-0.67006	0.000136	0.003506	-3.85285	Down	long intergenic non-protein coding RNA 1857
SCARNA5	-0.67276	0.00026	0.005928	-3.68493	Down	small Cajal body-specific RNA 5
HBM	-0.66252	0.001557	0.024934	-3.18581	Down	hemoglobin subunit mu
TUBB1	-0.63203	0.002292	0.033535	-3.06938	Down	tubulin beta 1 class VI

Table 3 The enriched GO terms of the up and down regulated differentially expressed genes

GO ID	CATEGORY	GO Name	P Value	FDR B&H	FDR B&Y	Bonferroni	Gene Count	Gene
Up regulated genes								
GO:0016050	BP	vesicle organization	3.92E-07	8.10E-04	7.19E-03	1.58E-03	40	LAPTM4B,CEACAM6,PTGER3,DEFA1,MAGI2,SERPINE2,GLA,PTPRN,HP,VNN1,SPHK1,FGA,FGB,HRG,PLA2G4A,LOXL3,FGG,RAB32,WASF1,VEGFC,UNC13B,PGLYRP1,SEPTIN4,ANXA3,GRK4,APOA2,APOB,LCN2,APOH,DERA,SCARF1,TGFB3,ORM1,TIMP1,MS4A3,CYSTM1,CD63,ERC2,CD151,MCEMP1
GO:0046903	BP	secretion	5.39E-06	1.17E-03	1.04E-02	2.18E-02	38	MYOM1,MAOB,CEACAM6,MDK,PTGER3,DEFA1,SERPINE2,GLA,PTPRN,HP,VNN1,SPHK1,FGA,FGB,HRG,PLA2G4A,FGG,FKBP1B,VEGFC,UNC13B,PGLYRP1,SEPTIN4,ANXA3,ICA1,APOA2,LCN2,APOH,DERA,ARG2,TGFB3,ORM1,OXTR,TIMP1,MS4A3,CYSTM1,CD63,ERC2,MCEMP1
GO:0099503	CC	secretory vesicle	1.01E-08	4.90E-06	3.31E-05	4.90E-06	32	CEACAM6,DEFA1,SERPINE2,GLA,PTPRN,HP,VNN1,SPHK1,FGA,FGB,HRG,PLA2G4A,FGG,VEGFC,UNC13B,PGLYRP1,SEPTIN4,ANXA3,ICA1,RABAC1,LCN2,APOH,DERA,TGFB3,MAL2,O

								RM1,TIMP1,MS4A3, CYSTM1,CD63,SMP D1,MCEMP1
GO:0098805	CC	whole membrane	2.77E-03	3.64E-02	2.47E-01	1.00E+00	29	TSPAN15,MAOB,LA PTM4B,CEACAM6,F UNDC1,PTPRN,MAP 1LC3B2,VNN1,SPHK 1,GOLIM4,HRG,RAB 32,WASF1,UNC13B,S EPTIN4,ANXA3,ICA1 ,TOM1L1,AP1M2,GR B14,APOB,RET,SCA RF1,MAL2,MS4A3,C YSTM1,CD63,CTNS, MCEMP1
GO:0046983	MF	protein dimerization activity	4.40E-04	9.54E-02	6.73E-01	2.86E-01	30	TPM1,TPM2,PADI4, MYOM1,MAOB,TRP C6,ACOT7,CEACAM 6,ARNTL2,PRTFDC1, TYMS,H2AC13,H2BC 17,GLA,HP,H4C14,MI TF,PKD2,FGG,H2BC 11,TPST1,SEPTIN4,I CA1,H4C15,GRB14,E 2F1,APOA2,LCN2,TG FB3,H2AJ
GO:0005102	MF	signaling receptor binding	4.71E-03	2.10E-01	1.00E+00	1.00E+00	30	MDK,MTRNR2L2,M AGI2,SERPINE2,GLA ,PKD2,FGA,FGB,HR G,FGG,FHL2,FKBP1 B,VEGFC,PROK2,PG LYRP1,CMTM2,GRB 14,LAMB2,APOA2,A POB,ADAMTS5,CXC L3,ADAM22,CCNB1, TGFB1I1,TGFB3,BC AP31,IGFBP2,TIMP1, CD151
				Down regulated genes				
GO:0046649	BP	lymphocyte activation	1.37E-15	5.40E-12	4.78E-11	5.40E-12	40	HLA-DMB,HLA-DPA1,SPTA1,BCL11 A,ITGA4,FGL2,CXC R5,FCRL1,PTPRC,ZC 3H12D,FBXO7,CCR7, NOTCH2,TCF7,IKZF 3,POLM,CAMK4,PO U2F2,BTLA,CR1,CBL B,SLC4A1,TFRC,BCL 11B,CD4,CD5,CD6,M S4A1,CD22,CD27,CD 44,TNFRSF13C,TNFR SF13B,CD79A,RORA, ATM,LY9,LEF1,IL7R, NCKAP1L
GO:0010941	BP	regulation of cell death	9.53E-05	6.03E-03	5.34E-02	3.75E-01	40	STK17B,OBSCN,ITG A4,NR4A1,STRADB, BNIP3L,PTPRC,BTG1 ,TMC8,FBXO7,PLAG L2,CCR7,NOTCH2,T CF7,IKZF3,OGT,CA MK1D,BMF,NLRP1, GRINA,OPA1,EEF1A 1,TXNIP,BCL11B,IGF 2R,CSF1R,CD27,NEU RL1,CD44,LRP1,AT M,HBA1,HBA2,HBB, CTSB,LEF1,RPL10,IL 7R,SORL1,NCKAP1L
GO:0009986	CC	cell surface	2.02E-09	3.10E-07	2.08E-06	9.30E-07	35	ADAM19,HLA-DPA1,HLA-

								DRA,ITGA4,CXCR5, FCRL1,PTPRC,CIITA ,MRC2,CCR7,NOTCH 2,SEMA7A,BTLA,CR 1,SLC4A1,TFRC,CD4, CD5,IGF2R,CD6,CSF 1R,MS4A1,CLEC17A, CD22,CD27,GYPA,V CAN,CD44,CLEC2D, TNFRSF13C,TNFRSF 13B,CD79A,LY9,CTS B,IL7R
GO:0031226	CC	intrinsic component of plasma membrane	5.35E-07	4.11E-05	2.76E-04	2.47E-04	43	HLA-DPA1,HLA-DRA,SPTA1,SLC38A 5,ITGA4,SLC38A1,C XCR5,PTPRC,SLC24 A4,TMC8,NOTCH2,V IPR1,TRABD2A,SEM A7A,BTLA,SLC7A6, CR1,MCOLN1,SLC2 A1,TSPAN5,RHAG,S LC4A1,TFRC,CELSR 1,CD4,CD5,IGF2R,CD 6,CSF1R,P2RX5,MS4 A1,SLC14A1,CD22,C D27,GYPA,GYPB,CD 44,CLEC2D,LRP1,TN FRSF13B,ATP2B1,SO RL1,NCKAP1L
GO:0016772	MF	transferase activity, transferring phosphorus-containing groups	9.72E-04	4.32E-02	3.09E-01	6.92E-01	35	ZBTB20,RPS6KA5,ST K17B,OBSCN,TENT5 C,TTN,PIK3IP1,BLK, STRADB,PTPRC,CIIT A,FBXO7,CCR7,DYR K2,OGT,CAMK1D,C TC1,POLM,CAMK4, DUSP2,AAK1,CBLB, SLC4A1,EEF1A1,RM RP,CD4,IGF2R,CSF1 R,NEURL1,CD44,LR P1,ATM,SERINC5,SO RL1,NCKAP1L
GO:0008144	MF	drug binding	1.15E-02	1.55E-01	1.00E+00	1.00E+00	30	ABCA2,RPS6KA5,ST K17B,OBSCN,TTN,B LK,STRADB,CIITA,A LAS2,ABCD2,DYRK 2,DNHD1,ACSL6,CA MK1D,EP400,ATP13 A1,CAMK4,AAK1,N LRP1,EEF1A1,DNAH 1,CSF1R,P2RX5,ATM ,HBA1,HBA2,HBM,H BB,ATP2B1,EPB42

Biological Process(BP), Cellular Component(CC) and Molecular Functions (MF)

Table 4 The enriched pathway terms of the up and down regulated differentially expressed genes

Pathway ID	Pathway Name	P-value	FDR B&H	FDR B&Y	Bonferroni	Gene Count	Gene
Up regulated genes							
1269340	Hemostasis	4.28E-06	7.47E-04	5.11E-03	2.24E-03	22	GNG8,TRPC6,CEACAM 6,CABLES1,SERPINE2, FGA,KCNMB1,FGB,HR G,PLA2G4A,MMP1,FG G,VEGFC,GRB14,APOB ,APOH,ZFPM2,TGFB3,

							ORM1,TIMP1,CD63,PRKAR1B
1269741	Cell Cycle	8.91E-04	2.12E-02	1.45E-01	4.67E-01	17	CETN2,MND1,MCM10,GINS1,TYMS,H2BC17,H4C14,BUB1,H2BC11,UBE2C,H4C15,CENPU,E2F1,CCNB1,DMC1,CENPI,H2AJ
1269507	Signaling by Rho GTPases	1.14E-02	8.42E-02	5.76E-01	1.00E+00	11	PPP1R14A,TAX1BP3,H2BC17,H4C14,BUB1,WASF1,H2BC11,H4C15,CENPU,CENPI,H2AJ
1269203	Innate Immune System	7.89E-02	2.91E-01	1.00E+00	1.00E+00	21	CEACAM6,DEFA1,GLA,HP,VNN1,FGA,FGB,FGG,WASF1,PGLYRP1,APOB,RET,LCN2,POLR3G,DERA,ORM1,MS4A3,CYSTM1,CD63,PRKAR1B,MCEMP1
1270001	Metabolism of lipids and lipoproteins	1.52E-01	3.82E-01	1.00E+00	1.00E+00	13	ACER2,ACOT7,ME1,GLA,SPHK1,PLA2G4A,FHL2,PLAAT1,G0S2,THEM5,APOA2,APOB,SMPD1
1268677	Metabolism of proteins	3.37E-01	5.01E-01	1.00E+00	1.00E+00	21	GNG8,CETN2,FN3K,H2AC13,H2BC17,VNN1,SPHK1,H4C14,MITF,FGA,MMP1,RAB32,METTL22,DYNC1I1,H2BC11,ADAMTS1,UBE2C,H4C15,ADAMTS5,IGFBP2,AOPEP
			Down regulated genes				
1269171	Adaptive Immune System	1.59E-03	8.64E-02	5.87E-01	7.96E-01	20	HLA-DMB,HLA-DPA1,HLA-DRA,TNRC6B,ITGA4,NR4A1,BLK,KLHL3,PTPRC,MRC2,FBXO7,RNF213,BTLA,CBLB,CD4,CD22,CLEC2D,CD79A,CTSB,RNF182
1269903	Transmembrane transport of small molecules	1.39E-02	1.95E-01	1.00E+00	1.00E+00	15	ABCA2,SLC38A5,SLC38A1,SLC24A4,ABCD2,GNG7,ATP13A1,SLC7A6,MCOLN1,SLC2A1,RHAG,SLC4A1,TFRC,SLC14A1,ATP2B1
1269203	Innate Immune System	8.82E-02	4.76E-01	1.00E+00	1.00E+00	21	RPS6KA5,SPTA1,TNRC6B,NR4A1,ADA2,FGL2,PTPRC,CAMK4,DUSP2,NLRP1,CNKSR2,CR1,EEF1A1,TXNIP,EEF2,CD4,IGF2R,CD44,HBB,CTSB,NCKAP1L
1269876	Vesicle-mediated transport	1.54E-01	5.50E-01	1.00E+00	1.00E+00	11	SPTA1,SEC16A,COL7A1,AAK1,TFRC,CD4,IGF2R,LRP1,HBA1,HBA2,HBB
1268854	Disease	3.21E-01	6.43E-01	1.00E+00	1.00E+00	12	RPL23A,RPL27A,RPL37,NR4A1,NOTCH2,CNKSR2,EEF2,CD4,VCAN,NEURL1,RPL13A,RPL10
1268677	Metabolism of proteins	5.53E-01	7.60E-01	1.00E+00	1.00E+00	19	RPL23A,RPL27A,RPL37,SPTA1,MGAT4A,NEU3,ADA2,TUBB1,YOD1,SEC16A,GNG7,KLK1,COL7A1,OGT,EEF1A1,EEF2,RPL13A,RPL10,SORL1

Table 5 Topology table for up and down regulated genes.

Regulation	Node	Degree	Betweenness	Stress	Closeness
Up	EZH2	350	0.076224	81130962	0.349924
Up	DBN1	256	0.049032	39941040	0.348151
Up	CCNB1	158	0.024471	43653864	0.313488
Up	FHL2	158	0.031673	16397718	0.336762
Up	E2F1	151	0.025971	16601668	0.333208
Up	TPM1	134	0.022043	16976362	0.329604
Up	KRT18	132	0.018793	17362522	0.338383
Up	TPM2	126	0.021531	17717608	0.323503
Up	FGB	115	0.021143	15804232	0.298889
Up	PTGER3	113	0.019531	25585198	0.284342
Up	SPINT2	108	0.023415	14310762	0.303448
Up	BUB1	102	0.018982	9083534	0.319527
Up	PTPRN	93	0.015139	21217898	0.283912
Up	BCAP31	91	0.017733	11925460	0.323825
Up	MAP1B	91	0.011535	22589676	0.310858
Up	KRT8	79	0.009251	9231600	0.332081
Up	TMEM67	76	0.014065	4982016	0.290838
Up	RABAC1	74	0.013172	9708740	0.293098
Up	APOB	72	0.011818	15182272	0.302587
Up	UBE2C	69	0.00877	8892764	0.298716
Up	SPHK1	68	0.011494	4951244	0.325666
Up	TOM1L1	66	0.00895	6727694	0.305124
Up	RET	66	0.009723	10964184	0.305199
Up	WASF1	65	0.010329	14175172	0.29873
Up	KRT19	64	0.008418	5490710	0.32224
Up	CENPU	61	0.011081	3633098	0.296468
Up	DTL	61	0.006526	9721978	0.297152
Up	CETN2	60	0.009249	16418248	0.269586
Up	MCM10	59	0.007694	9107150	0.300602
Up	DYNC1I1	58	0.007347	6841812	0.299279
Up	PLA2G4A	57	0.006497	7102868	0.307673
Up	TYMS	55	0.008254	2898568	0.306378
Up	MDK	54	0.007633	2641060	0.307322
Up	GOLIM4	45	0.009056	6535396	0.299091
Up	TGFB1I1	43	0.00576	2542056	0.317363
Up	PKD2	42	0.006903	2134988	0.290538
Up	FGA	41	0.004439	1801264	0.293153
Up	PRKAR1B	41	0.004763	4851900	0.299424
Up	ACOT7	39	0.00511	6777086	0.287968
Up	FGG	37	0.002736	1188570	0.282125
Up	AP1M2	37	0.007088	9431672	0.281894
Up	MITF	36	0.006067	5049390	0.308118
Up	SMYD3	35	0.006122	1971838	0.303776
Up	ACTR3B	35	0.002767	5762182	0.273907
Up	CTPS2	34	0.004516	1656234	0.297352
Up	HP	33	0.004002	2476788	0.299743
Up	MYL6B	33	0.001721	1494552	0.303835
Up	LAMB2	33	0.003266	3787290	0.283015
Up	ME1	32	0.00497	5458746	0.266142
Up	FKBP1B	31	0.002492	3149134	0.263535
Up	EAF2	31	0.003666	3614748	0.273181
Up	CD63	30	0.002963	1542292	0.278807
Up	TMEFF1	29	0.004306	1459454	0.277382
Up	PHACTR3	29	0.003235	6793662	0.273205
Up	MMP1	28	0.004131	1062610	0.285972
Up	RAB32	28	0.004125	3089688	0.273326
Up	NT5DC2	27	0.003149	4016356	0.290497
Up	LAPTM4B	26	0.003861	1308630	0.280985
Up	LCN2	26	0.003047	3293226	0.261121
Up	GRB14	26	0.001737	2102726	0.272171
Up	PRTFDC1	26	0.003559	2778424	0.248364
Up	SERPINE2	25	0.003606	2767974	0.266199
Up	APOA2	24	0.003639	1777538	0.282035
Up	CNN1	24	0.002696	1398988	0.281984

Up	MAGI2	24	0.003636	4072986	0.273277
Up	PADI4	24	0.001853	2786250	0.285457
Up	ARNTL2	23	0.004537	2736046	0.276156
Up	MAL2	23	0.004035	3057928	0.266555
Up	TAX1BP3	22	0.00296	2483404	0.27773
Up	APOH	22	0.002261	1011952	0.294759
Up	GLA	22	0.002185	2812520	0.25131
Up	KRT7	22	0.002247	3354252	0.283132
Up	ROBO1	22	0.002997	2829202	0.285181
Up	ADAMTS1	21	0.003523	2991386	0.249044
Up	OXTR	21	0.003005	1885024	0.254274
Up	ADAM32	21	0.002751	2226220	0.244362
Up	TSPAN15	20	0.002903	1636154	0.248684
Up	DMC1	20	0.001518	1667540	0.255218
Up	EPDR1	20	0.00263	955076	0.289735
Up	LACTB2	20	0.003285	3861294	0.241888
Up	UNC13B	19	0.003409	6715552	0.228252
Up	ERC2	19	0.002956	2368572	0.246592
Up	HRG	19	0.002437	1023636	0.273991
Up	SMPD1	19	0.00236	2063048	0.275125
Up	ZFPM2	19	0.001198	1822000	0.266153
Up	METTL22	19	0.001598	2257038	0.269023
Up	ORM1	18	0.001349	1072266	0.255461
Up	ZC3HAV1L	18	0.001054	1624786	0.281202
Up	STAC	18	0.001798	2388538	0.275578
Up	POLR3G	17	0.003237	9664174	0.229055
Up	DDAH1	17	0.003704	1699018	0.290824
Up	TIMP1	17	0.002047	1211820	0.264888
Up	DERA	17	0.001512	1709944	0.240983
Up	TGFB3	16	0.001732	1135010	0.26056
Up	ANXA3	16	0.002306	3218636	0.263928
Up	ETV4	16	0.00158	1430402	0.286767
Up	RND3	16	0.001618	1798784	0.267963
Up	FUNDC1	16	0.001881	5031262	0.246033
Up	PPP1R14A	16	0.001348	1468196	0.269398
Up	ADAM22	16	9.66E-04	1467492	0.278092
Up	TRHDE	16	0.002417	2718244	0.265571
Up	AOPEP	15	5.09E-04	455628	0.281778
Up	LOXL3	15	0.002245	2647672	0.272735
Up	TST	15	0.002644	2760934	0.24058
Up	CENPI	15	6.90E-04	213372	0.26143
Up	TRPC6	15	0.002982	3195972	0.236597
Up	MSANTD3	14	0.001423	599870	0.282602
Up	DCBLD2	14	0.001863	1414006	0.280806
Up	ICA1	14	0.001837	1818980	0.253566
Up	CABLES1	14	4.42E-04	448806	0.275222
Up	GTF3C6	13	0.001446	393772	0.300413
Up	AVEN	13	7.46E-04	364352	0.294788
Up	PBLD	13	0.001491	1062854	0.235839
Up	CD151	13	0.001883	1879220	0.264662
Up	YIF1B	13	0.001267	1419634	0.263917
Up	C5orf30	13	0.001783	1452154	0.265582
Up	FRMD3	11	8.55E-04	686546	0.235579
Up	FAH	11	0.001509	1294972	0.259587
Up	HTATIP2	11	0.00148	1272602	0.261231
Up	CYSTM1	11	0.002293	1438306	0.2152
Up	MAP1LC3B2	10	0.001139	1052378	0.240608
Up	MYEOV	2	5.45E-05	24642	0.227079
Up	DNAH14	1	0	0	0.212349
Up	MYOM1	1	0	0	0.247539
Down	HEPACAM2	496	0.004088	4614336	0.259565
Down	HLA-DPA1	443	0.021345	6656236	0.294395
Down	DCAF12	359	0.002195	1838728	0.28738
Down	POLM	259	6.45E-05	60748	0.246809
Down	TUBB1	231	0.017014	13445244	0.31686
Down	KMT2D	211	0.004121	6143304	0.276119
Down	TNFRSF13B	208	0.004558	7473486	0.25441
Down	SEC16A	199	0.024345	23456762	0.332778
Down	AHNAK	158	0.012868	12992410	0.339572
Down	OGT	151	0.02538	23785672	0.321486

Down	TRAK2	148	0.005447	1889278	0.291359
Down	PER1	143	0.007889	3343992	0.297667
Down	TXNIP	142	0.005831	3723272	0.3011
Down	GPRASP1	140	0.011046	5269570	0.284316
Down	CTSB	139	0.011516	5746824	0.316973
Down	ITGA4	132	0.110358	99169576	0.373747
Down	CBLB	131	0.011859	9651222	0.31117
Down	LEF1	111	0.008924	3863000	0.305275
Down	PLEC	110	0.025923	21209448	0.346999
Down	BNIP3L	110	0.005843	2394548	0.292184
Down	CAMK1D	109	0.007993	5854240	0.294255
Down	NR4A1	99	0.024611	10885038	0.333639
Down	OPA1	94	0.007387	5152054	0.317804
Down	EEF2	83	0.037887	47075150	0.354698
Down	SEMA7A	82	0.00308	4153990	0.271146
Down	RPS6KA5	78	0.010004	5767566	0.321653
Down	STK17B	78	0.00446	1356036	0.284918
Down	P2RX5	75	0.003754	3579124	0.255008
Down	SLC2A1	68	0.003791	2359116	0.318622
Down	GYPB	66	0.007619	6671358	0.262863
Down	HBB	65	0.01032	10858208	0.304059
Down	CD22	64	0.001809	1124092	0.279752
Down	CD4	64	0.018753	14195846	0.322845
Down	CD44	63	0.031474	16859342	0.344469
Down	TFRC	63	0.019104	17774714	0.337221
Down	PTPRC	62	0.012352	6796924	0.316681
Down	CD5	62	0.00189	1129318	0.283456
Down	HLA-DRA	61	0.009348	4428892	0.287995
Down	HLA-DMB	60	0.002503	1238774	0.277344
Down	CELSR1	60	0.003079	1745004	0.272928
Down	MS4A1	58	0.0017	1236694	0.276378
Down	SPTA1	55	0.007158	4511084	0.30275
Down	IL7R	54	0.027811	45141856	0.327043
Down	GYPA	53	8.14E-04	390278	0.260045
Down	SLC4A1	53	0.002142	1341058	0.273169
Down	EPB42	52	0.002323	1787000	0.260879
Down	RHAG	49	0	0	0.214566
Down	CD79A	49	0.008789	4491848	0.293056
Down	CD6	48	0	0	0.220862
Down	CSF1R	48	0.002723	5503564	0.281868
Down	IKZF3	48	0.021447	15624140	0.316487
Down	POU2F2	46	0.002814	4242740	0.262773
Down	IGF2R	45	0.005336	8354606	0.300049
Down	NSUN3	45	0	0	0.226647
Down	BLK	44	0.009001	4827382	0.309644
Down	VCAN	44	0.00605	2854094	0.288546
Down	ADAM28	41	0	0	0.272076
Down	RPL27A	41	0.009338	13186584	0.337921
Down	RPL23A	39	0.022449	25286012	0.35326
Down	EEF1A1	37	0.098882	1.23E+08	0.370457
Down	RPL13A	37	0.009659	13645424	0.339386
Down	RPL10	35	0.066934	69760500	0.352275
Down	NOTCH2	35	0.009449	4095454	0.307291
Down	ATP2B1	35	0.00508	5650696	0.303835
Down	SLC38A1	35	0.008346	5880382	0.292709
Down	QSOX2	35	0.00527	3561792	0.291167
Down	SORL1	34	0.01017	6644994	0.299569
Down	LRP1	34	0.030447	29146796	0.321269
Down	SRRM2	34	0.044661	52105132	0.347662
Down	ABCC13	34	0	0	0.250182
Down	ATM	33	0.040568	31808618	0.330997
Down	FECH	33	0.007383	3340210	0.299511
Down	CD27	32	0.004882	2960412	0.278142
Down	VIPR1	32	0.004948	5472644	0.278694
Down	AGPAT4	32	1.70E-05	28760	0.230987
Down	CIITA	32	0.003427	3117716	0.289328
Down	EP400	31	0.007237	9601258	0.288196
Down	RORA	31	0.004548	1396286	0.302558
Down	SOX6	31	0.001788	1768940	0.255661
Down	CENPF	30	0.008068	6644598	0.297681

Down	FAM167A	29	0.008587	3540932	0.276168
Down	MXI1	28	0.001985	3293278	0.269504
Down	ALDH5A1	27	0.003494	4468018	0.270813
Down	RPL37	27	0.001913	3460916	0.29617
Down	TSPAN5	26	0.01221	9998796	0.2873
Down	PIEZO1	26	0	0	0.223188
Down	BTG1	25	0.002334	3106952	0.271777
Down	SPIB	25	0.001073	679476	0.280679
Down	ALDH6A1	25	0.00345	3839804	0.246053
Down	COL7A1	25	0.003621	3830672	0.277705
Down	PAX5	25	0.008408	15230588	0.288317
Down	DUSP2	24	0.003694	4774362	0.262573
Down	IFFO1	24	0.004108	2648480	0.262006
Down	COBLL1	24	0.00318	3800612	0.267373
Down	DBP	24	0.00207	2593884	0.258708
Down	SELENBP1	24	0.011965	15173332	0.275259
Down	DYRK2	23	0.00992	5736550	0.313918
Down	PDE3B	23	0.005858	5188848	0.268242
Down	ABCA2	22	0.002246	1887488	0.270647
Down	TTN	22	0.022803	22179002	0.328956
Down	AAK1	22	0.001768	1776702	0.306636
Down	CAMK4	21	0.001804	1122842	0.282382
Down	ANKRD52	21	0.004706	3610412	0.290251
Down	OBSCN	21	0.002307	1424536	0.295125
Down	YOD1	21	0.003727	4452540	0.278581
Down	RNF213	21	0.003281	4225796	0.28073
Down	HBM	21	0.003971	2893622	0.211891
Down	FAM117B	20	0.002939	3060242	0.274465
Down	RANBP10	20	0.010162	16110914	0.263344
Down	RALGPS2	20	0.008034	10752578	0.280386
Down	CNKSR2	19	0.003716	4283878	0.253753
Down	MYO15B	19	0.001548	1850770	0.253763
Down	BMF	18	0.002348	3575424	0.266842
Down	WDFY2	18	0.004928	3808614	0.241237
Down	LENG8	18	0.006353	9944066	0.270896
Down	TUBGCP6	18	0.00405	3821222	0.278155
Down	NELL2	17	0.005907	5985122	0.250435
Down	YIPF4	17	0.002754	3249620	0.263928
Down	OSBPL10	17	0.002471	663904	0.287727
Down	BACH2	16	0.002632	2910574	0.257534
Down	NLRP1	16	0.003929	3755972	0.280691
Down	BCL11B	2	0.001184	2467486	0.258362
Down	STRADB	2	0.001267	1783952	0.276898
Down	BCL11A	1	0.004017	6158386	0.273664
Down	RCAN3	1	0	0	0.233006
Down	KLHL3	1	0.003155	2811806	0.280551
Down	CLEC2D	1	0.015351	13153684	0.270766
Down	TNRC6B	1	0.010638	19725384	0.302365
Down	FBXO7	1	0.011435	14645282	0.298528
Down	MOB3B	1	0	0	0.202401
Down	ZNF549	1	0	0	0.230523
Down	VSTM2A	1	0	0	0.220343
Down	CTC1	1	0	0	0.200285
Down	MRC2	1	0.002911	3908206	0.26787
Down	TTC14	1	0	0	0.257985
Down	ADA2	1	0	0	0.257985

Table 6 miRNA - target gene and TF - target gene interaction

Regulation	Target Genes	Degree	MicroRNA	Regulation	Target Genes	Degree	TF
Up	COL1A1	178	hsa-mir-4492	Up	IRF4	10	NFATC2
Up	IRF4	140	hsa-mir-4319	Up	LCK	10	YY1
Up	MYBL2	83	hsa-mir-637	Up	RET	10	NR2C2
Up	PRKCB	81	hsa-mir-1261	Up	MAP1LC3C	10	MAX
Up	IL2RB	54	hsa-mir-4300	Up	IL2RB	8	PDX1
Up	CCR5	50	hsa-mir-5193	Up	GRAP2	8	ELK1
Up	GRAP2	41	hsa-mir-3681-5p	Up	MYBPC2	7	RELA

Up	MDFI	41	hsa-mir-4441	Up	MDFI	6	TFAP2A
Up	RET	17	hsa-mir-129-2-3p	Up	MYBL2	6	GATA2
Up	IKZF1	16	hsa-mir-3607-3p	Up	CD247	5	SREBF1
Up	BTK	13	hsa-mir-4667-3p	Up	COL1A1	5	NFYA
Up	LCK	6	hsa-mir-210-3p	Up	PRKCB	4	IRF2
Up	MYBPC2	6	hsa-mir-214-3p	Up	IKZF1	4	E2F6
Up	CD247	4	hsa-mir-346	Up	BTK	2	SOX5
Up	MAP1LC3C	2	hsa-mir-27a-3p	Up	CCR5	1	EGR1
Down	JUN	144	hsa-mir-3943	Down	ATF3	19	TP53
Down	EGR1	132	hsa-mir-548e-3p	Down	EGR1	16	ARID3A
Down	ZFP36	130	hsa-mir-6077	Down	JUNB	15	SRF
Down	FOS	105	hsa-mir-5586-5p	Down	FOS	13	CREB1
Down	DUSP1	97	hsa-mir-4458	Down	PTPRO	12	NR3C1
Down	JUNB	85	hsa-mir-3065-5p	Down	NR0B2	11	USF1
Down	MME	54	hsa-mir-922	Down	MME	9	BRCA1
Down	NR4A2	50	hsa-mir-29b-2-5p	Down	JUN	9	SP1
Down	ATF3	48	hsa-mir-5000-5p	Down	DUSP1	9	STAT3
Down	NR4A1	43	hsa-mir-107	Down	NR4A1	9	HINFP
Down	PCK1	38	hsa-mir-1185-1-3p	Down	NR4A2	7	NR2E3
Down	PTPRO	18	hsa-mir-203a-3p	Down	PCK1	6	NR2F1
Down	APOB	17	hsa-mir-548p	Down	ZFP36	5	TFAP2C
Down	ALB	10	hsa-mir-492	Down	APOB	4	FOXA1
Down	NR0B2	5	hsa-mir-141-3p	Down	ALB	4	STAT1

Table 7. Docking results of designed molecules on CCNB1 and FHL2

Sl. No/ Code	CCNB1						FHL2					
	PDB: 1H0V			PDB: 4Y72			PDB: 2D8Z			PDB: 2EHE		
	Total Score	Crash (-Ve)	Polar	Total Score	Crash (-Ve)	Polar	Total Score	Crash (-Ve)	Polar	Total Score	Crash (-Ve)	Polar
IM 1	7.239	0.5252	4.194	6.229	1.1758	1.3468	5.1488	1.0826	2.402	3.9597	1.1337	1.1388
IM 2	3.9559	3.76	1.2296	7.7753	1.5013	3.1751	6.8491	0.7865	3.1253	5.3884	0.7304	3.2443
IM 3	7.1917	1.469	4.9203	7.3727	2.1681	1.9271	5.4126	0.9455	1.6539	4.5339	0.7044	0.9497
IM 4	4.1974	3.568	4.3031	6.8188	2.006	2.4134	5.6181	0.9326	1.7125	3.5135	0.7458	1.0505
IM 5	4.5533	1.6492	2.0927	8.4227	0.344	2.1941	6.0708	0.8126	1.7745	5.5747	0.8468	3.3308
IM 6	6.3787	1.9626	3.3289	9.0333	1.8462	3.2587	6.6937	0.6986	1.7217	5.1739	0.7641	3.8671
IM 7	6.1374	4.1751	3.5386	9.6167	1.1087	3.9025	5.225	1.4565	2.041	4.6648	1.4029	3.3006
IM 8	8.5712	2.8957	5.1053	7.0482	1.1147	1.7475	5.8786	2.3548	4.3253	6.2485	0.9775	7.501
IM 9	7.2601	1.6697	4.5599	11.1159	3.4644	4.6657	7.1497	0.8496	2.7825	4.8018	1.1365	3.8469
IM 10	7.1162	1.8814	4.5343	8.442	3.5097	1.9408	7.7546	3.7166	5.382	4.9785	0.8538	3.1734
IM 11	7.8374	2.1808	5.6745	9.5941	0.7735	2.1344	5.2956	1.1168	2.1061	3.9556	1.1707	0.6484
IM 12	4.4123	3.1644	0.1694	5.6246	1.2211	5.4648	5.6561	0.5109	1.6096	3.7807	1.5365	2.3817
IM 13	4.8829	1.641	0.8781	8.0134	1.4762	1.0656	5.2993	1.3644	0.5235	3.7134	1.1631	2.6632
IM 14	6.0738	2.1599	1.0809	7.2224	2.4795	2.1333	6.0942	1.3044	0.9106	3.6364	0.7145	0
IM 15	4.1335	1.6663	0.6394	7.8573	1.0353	1.397	5.1601	2.6366	2.7824	4.9877	0.7211	1.2175
IM 16	4.7049	2.8785	0.8354	4.754	1.9003	2.3893	5.8987	3.4229	2.683	3.811	0.9693	2.5824
TZ17	4.7263	2.4231	1.618	7.2734	1.358	0.053	5.1753	1.1334	2.2964	2.938	1.0363	0.9651
TZ 18	2.802	3.145	0.7759	6.8537	3.0008	1.6321	7.8024	2.4086	2.4203	4.6169	1.5742	3.205
TZ 19	5.2455	4.8167	3.4624	5.6781	2.5738	1.298	5.1226	2.2316	1.0413	3.4199	1.0615	2.0714
TZ 20	4.2031	2.0537	1.495	6.1116	2.1732	3.8228	6.2266	0.6144	1.7861	2.938	1.0363	0.9651
TZ 21	3.0014	4.7503	2.5662	6.8135	1.9569	0.1433	6.5063	2.1789	3.6709	5.7655	1.6648	2.5621
TZ 22	3.7751	3.6506	1.0649	3.7896	0.9741	1.2645	6.1962	3.8971	2.3063	4.0152	1.5781	2.7668
TZ 23	5.1601	2.6366	2.7824	8.5232 -	1.5576	1.447	5.1729	0.7908	0.0547	2.6522	1.3858	1.0325
TZ 24	2.9866	4.5065	3.6118	3.7807	1.5325	1.1317	6.9491	1.9739	4.849	5.6246	1.2211	5.4648
TZ 25	4.8039	2.7509	4.8277	7.5881	1.5654	2.7715	6.8022	1.7602	1.3582	4.6179	0.8504	3.0354
TZ 26	4.6867	5.5789	4.0836	4.082	0.8257	1.2626	5.6376	1.0268	0.6945	6.1116	2.1732	3.8228
TZ 27	5.0617	0.919	3.0108	8.2356	5.0255	2.733	6.9041	1.2875	1.3144	4.0538	2.6973	2.4686
TZ 28	4.754	1.9003	2.3893	3.7807	1.5365	2.3817	6.2017	0.8992	2.0979	2.8957	2.2563	1.1849
TZ 29	3.8498	3.1807	2.6601	8.0953	2.9258	0.0118	5.0893	1.1718	1.9465	4.0316	1.4654	2.5085
TZ 30	2.1031	2.8504	0.4643	3.7644	2.6181	0.8861	4.971	3.1573	1.1485	2.8812	1.0498	0.0078
TZ 31	3.5097	3.5835	1.0165	6.7706	0.5308	0.0066	4.9571	1.2321	1.1728	2.7919	2.5153	1.8636
TZ 32	2.9901	3.3732	1.7976	2.041	4.6648	1.4029	6.2178	0.9615	1.6287	3.6108	1.261	2.2254

PU33	5.0124	2.6209	1.6596	8.3705	2.4455	1.8383	5.1058	2.8533	2.1314	4.082	0.8257	1.2626
PU 34	1.8876	3.1575	1.8876	2.9186	1.7769	0.7803	6.2293	0.79	4.1623	5.7541	0.8169	2.2649
PU 35	4.2415	0.9639	1.4337	8.5453	0.7988	0.3678	5.993	1.1302	1.6123	3.7896	0.9741	1.2645
PU 36	3.7644	2.6181	0.8861	3.4946	1.6854	2.8474	5.5186	0.8034	1.7233	4.2415	0.9639	1.4337
PU 37	2.2051	3.0552	1.6443	8.8008	1.667	3.5679	6.3895	1.7399	2.0389	5.0617	0.919	3.0108
PU 38	5.2735	4.1465	2.4599	4.754	1.9003	2.3893	4.2415	0.9639	1.4337	3.4946	1.6854	2.8474
PU 39	5.0617	0.919	3.0108	7.8157	1.3292	0.2824	5.0617	0.919	3.0108	4.2155	0.823	3.9682
PU 40	4.8638	5.448	1.8878	4.2415	0.9639	1.4337	3.2316	1.6854	2.8474	4.7646	1.6643	4.7161
PU 41	7.1661	3.1588	5.0991	10.3389	4.9022	4.0552	3.2121	0.823	3.9682	5.2192	1.3596	1.3065
PU 42	5.278	1.1462	3.3261	4.754	1.9003	2.3893	5.4326	1.6643	4.7161	4.9542	3.6876	3.8272
PU 43	5.2192	1.3596	1.3065	10.8916	2.8239	2.464	4.0152	1.5781	2.7668	3.9964	1.1219	0.8063
PU 44	4.8815	3.9606	2.9386	6.5063	2.1789	3.6709	3.9964	1.1219	0.8063	4.3649	0.7553	3.4696
PU 45	3.4541	3.3428	1.9008	8.3081	0.3422	2.9369	3.9597	1.1337	1.1388	4.2415	0.9639	1.4337
PU 46	3.5097	3.5835	1.0165	6.0942	1.3044	0.9106	3.9556	1.1707	0.6484	5.0617	0.919	3.0108
PU 47	3.7807	1.5365	2.3817	7.5477	2.2832	2.7503	4.0152	1.5781	2.7668	3.4946	1.6854	2.8474
PU 48	3.6402	3.5929	1.2563	4.2415	0.9639	1.4337	3.9964	1.1219	0.8063	4.2155	0.823	3.9682

Figures

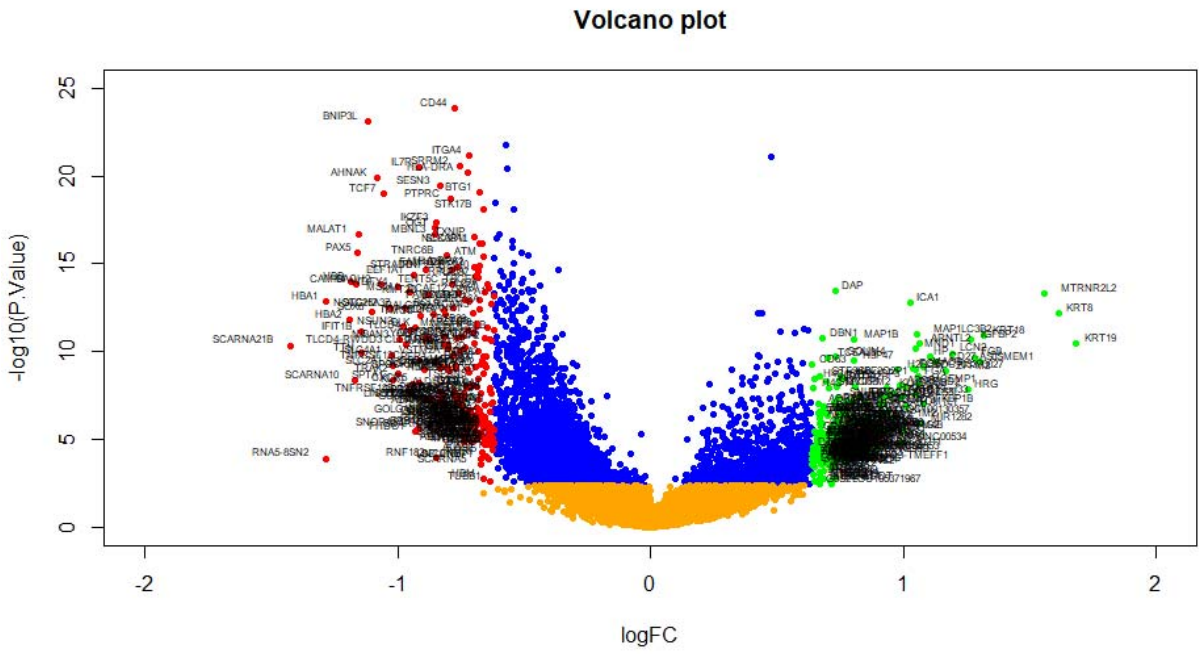

Fig. 1. Volcano plot of differentially expressed genes. Genes with a significant change of more than two-fold were selected. Green dot represented up regulated significant genes and red dot represented down regulated significant genes.

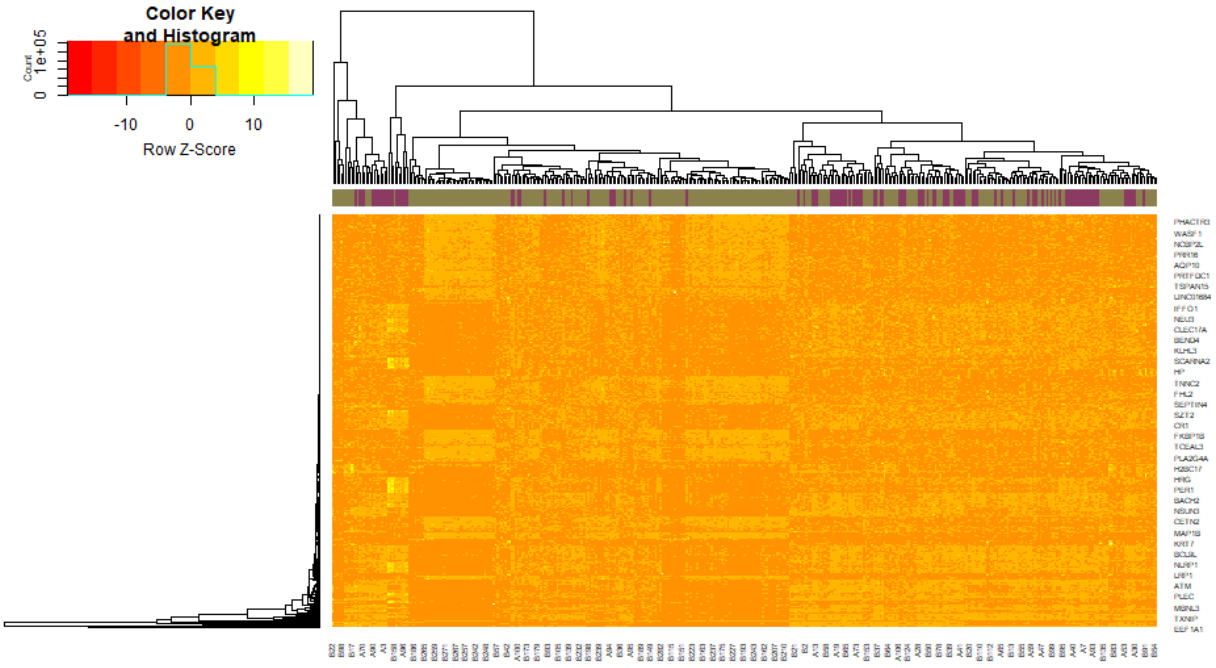

Fig. 2. Heat map of differentially expressed genes. Legend on the top left indicate log fold change of genes. (A1 – A114 = normal control samples; B1 – B284 = PDAC samples)

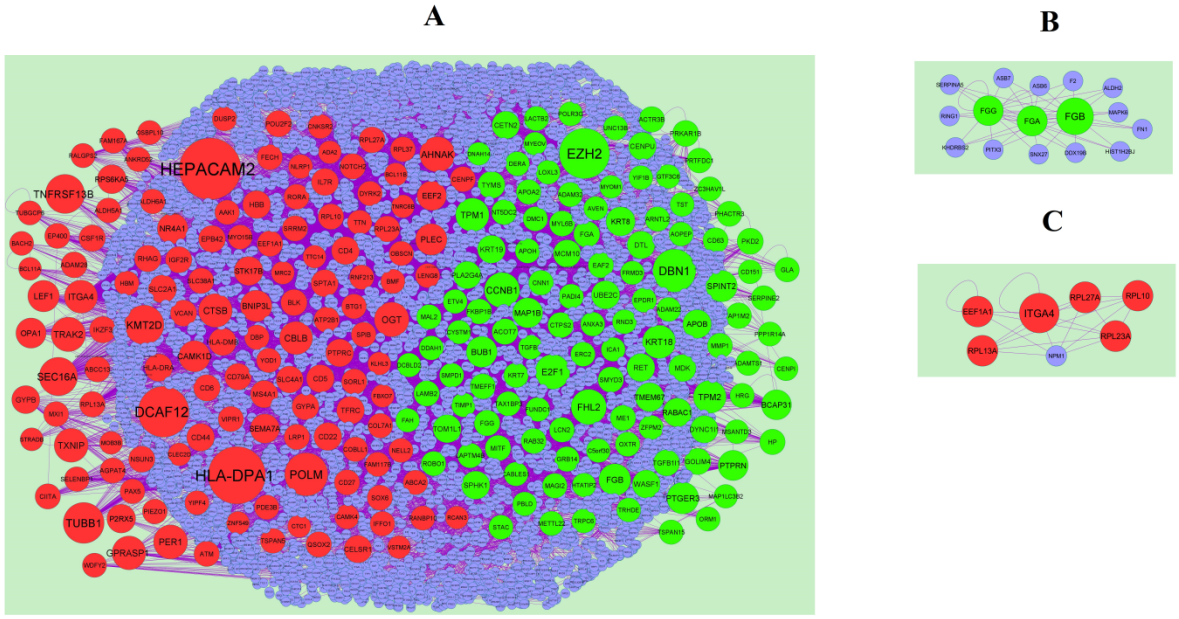

Fig. 3. PPI network and the most significant modules of DEGs. (A) The PPI network of DEGs was constructed using Cytoscape (B) The most significant module was obtained from PPI network with 16 nodes and 44 edges for

up regulated genes (C) The most significant module was obtained from PPI network with 6 nodes and 20 edges for up regulated genes. Up regulated genes are marked in green; down regulated genes are marked in red

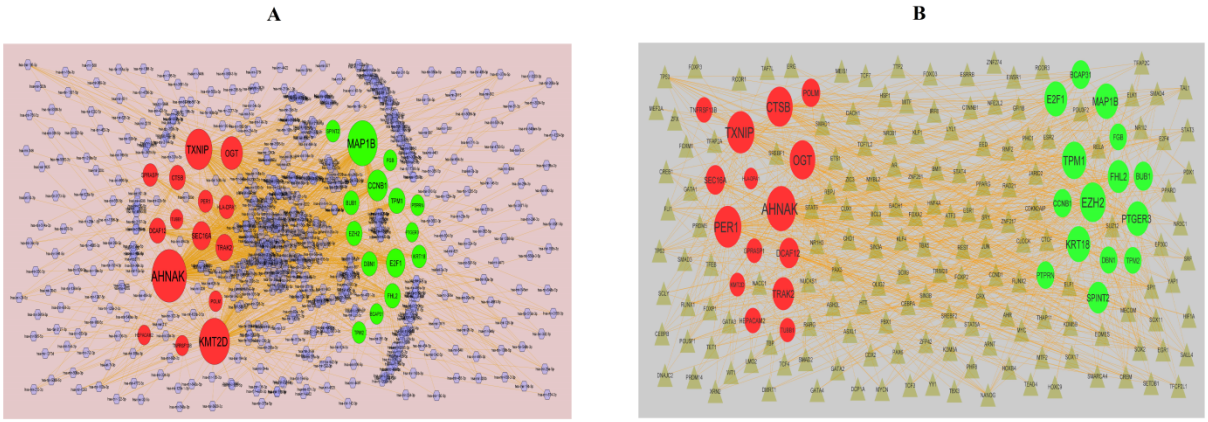

Fig. 4. (A) Target gene - miRNA regulatory network between target genes and miRNAs (B) Target gene - TF regulatory network between target genes and TFs. Up regulated genes are marked in green; down regulated genes are marked in red; The blue color diamond nodes represent the key miRNAs; the gray color triangle nodes represent the key TFs

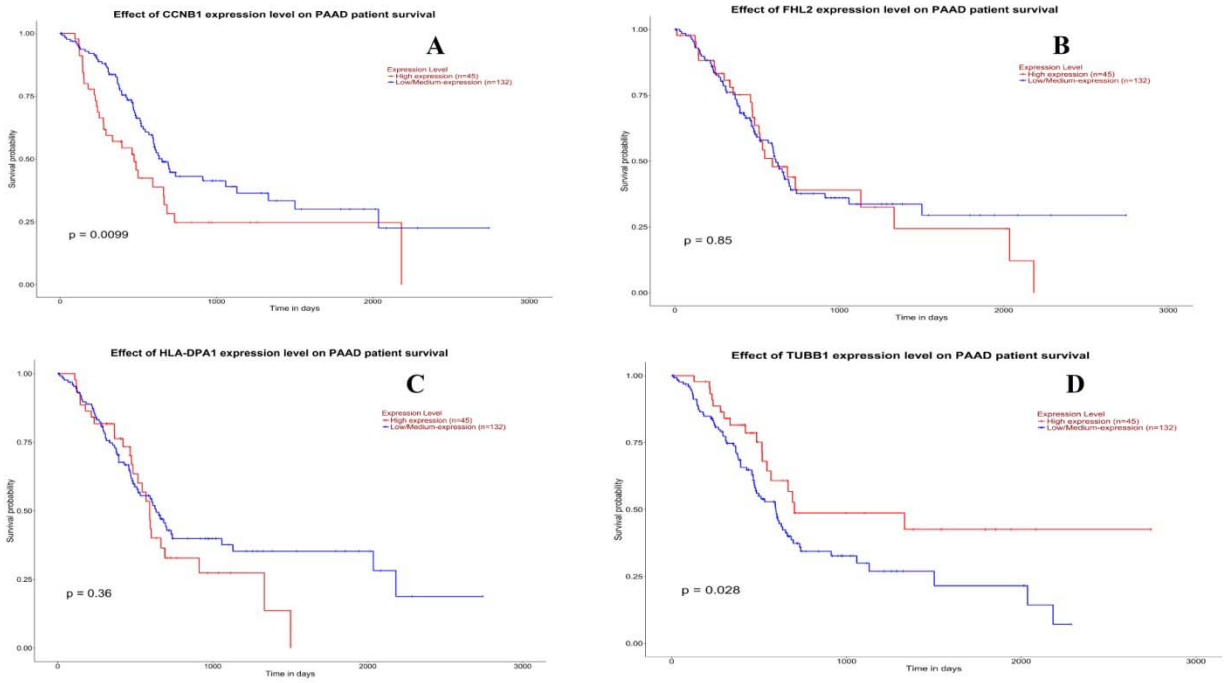

Fig. 5. Overall survival analysis of hub genes. Overall survival analyses were performed using the UALCAN online platform. Red line denotes - high expression; Blur line denotes – low expression. A) CCNB1 B) FHL2 C) HLA-DPA1 D) TUBB1

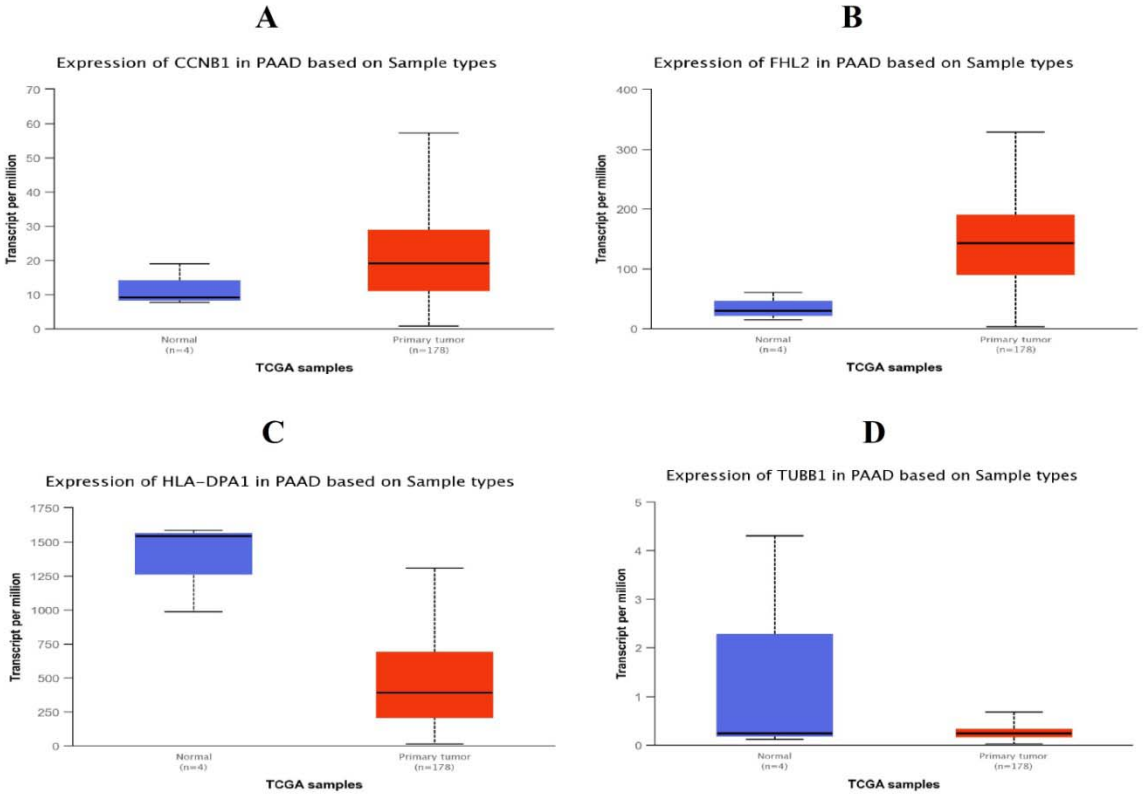

Fig. 6. Box plots (expression analysis) hub genes were produced using the UALCAN platform. A) CCNB1 B) FHL2 C) HLA-DPA1 D) TUBB1

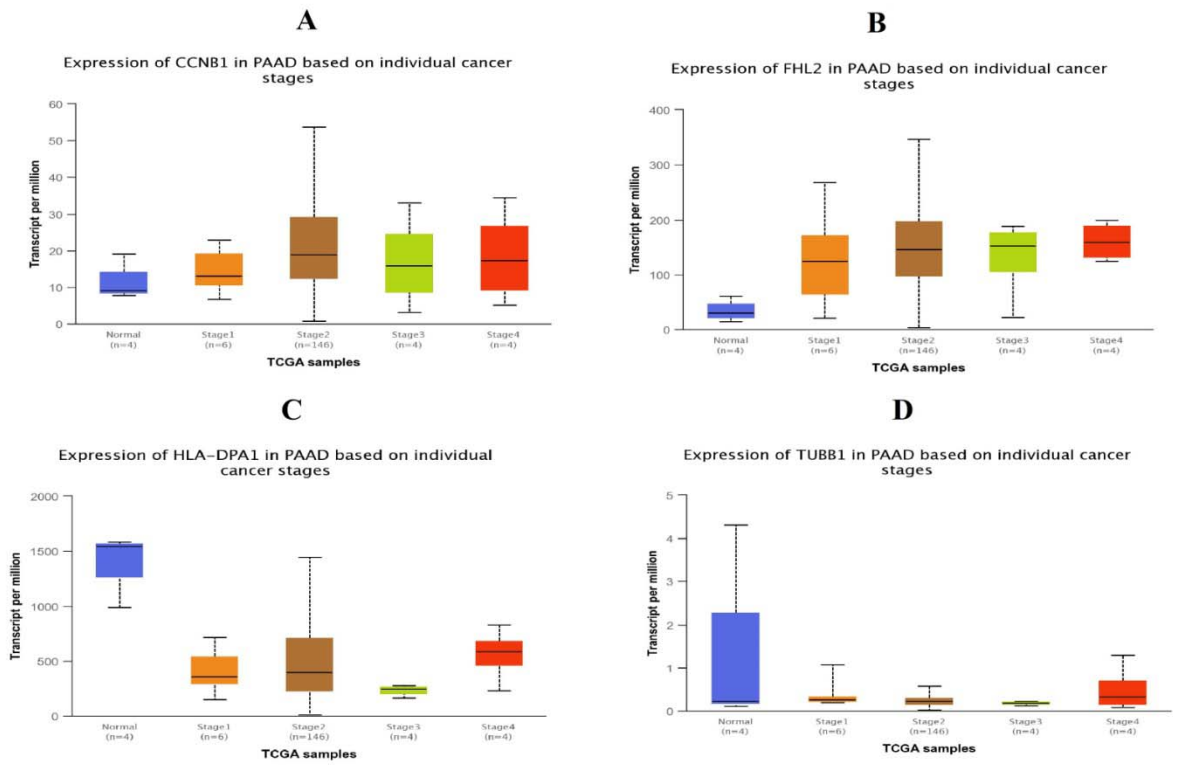

Fig. 7. Box plots (clinical stage analysis) hub genes were produced using the UALCAN platform. A) CCNB1 B) FHL2 C) HLA-DPA1 D) TUBB1

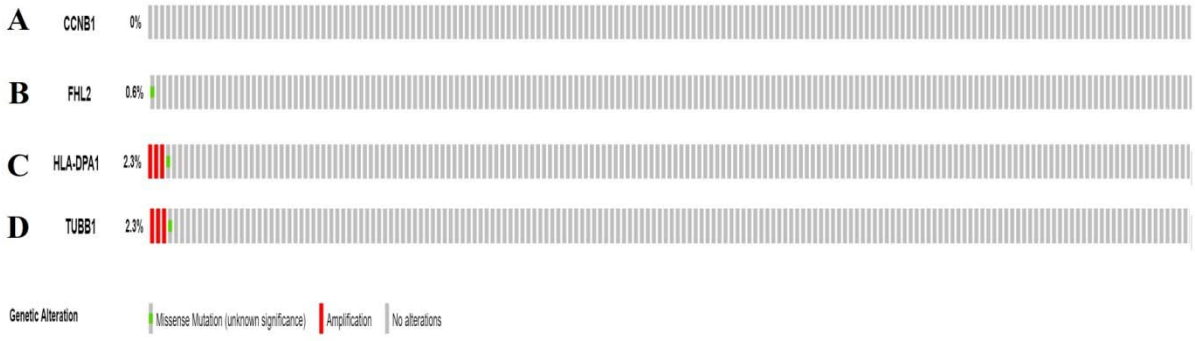

Fig. 8. Mutation analyses of hub genes were produced using the CbioPortal online platform. A) CCNB1 B) FHL2 C) HLA-DPA1 D) TUBB1

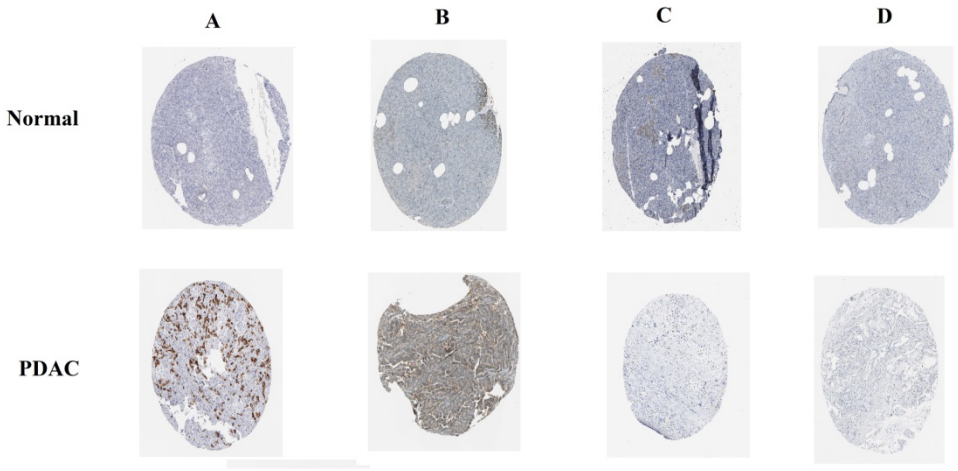

Fig. 9. Immunohisto chemical (IHC) analyses of hub genes were produced using the human protein atlas (HPA) online platform. A) CCNB1 B) FHL2 C) HLA-DPA1 D) TUBB1

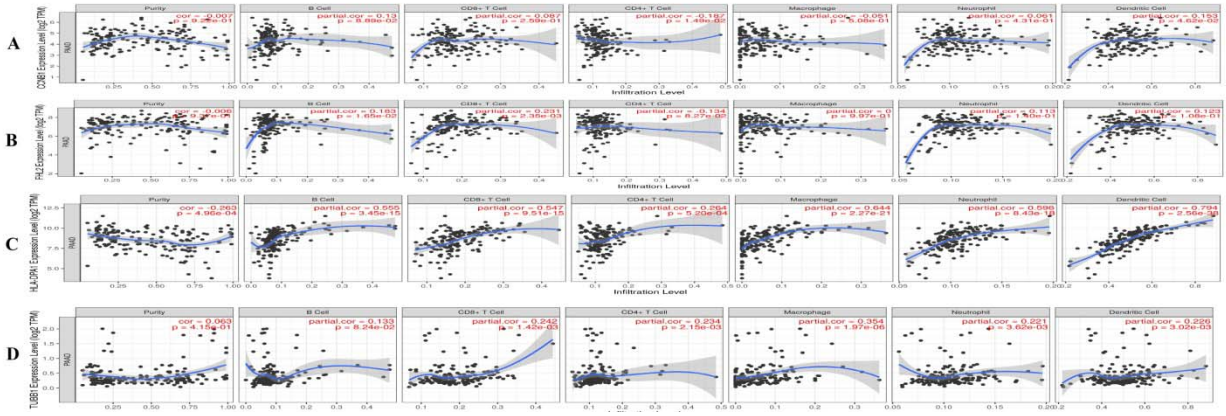

Fig. 10. Scatter plot for immune infiltration for hub genes. A) CCNB1 B) FHL2 C) HLA-DPA1 D) TUBB1

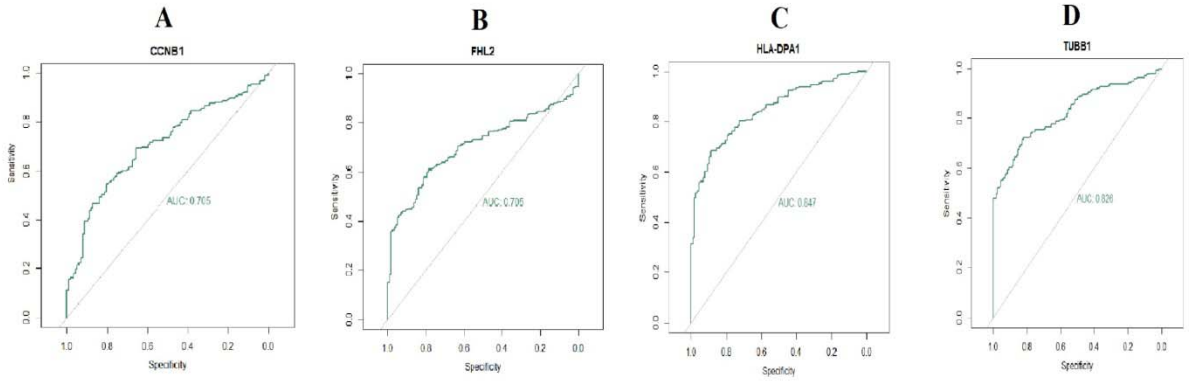

Fig. 11. ROC curve validated the sensitivity, specificity of hub genes as a predictive biomarker for PDAC prognosis. A) CCNB1 B) FHL2 C) HLA-DPA1 D) TUBB1

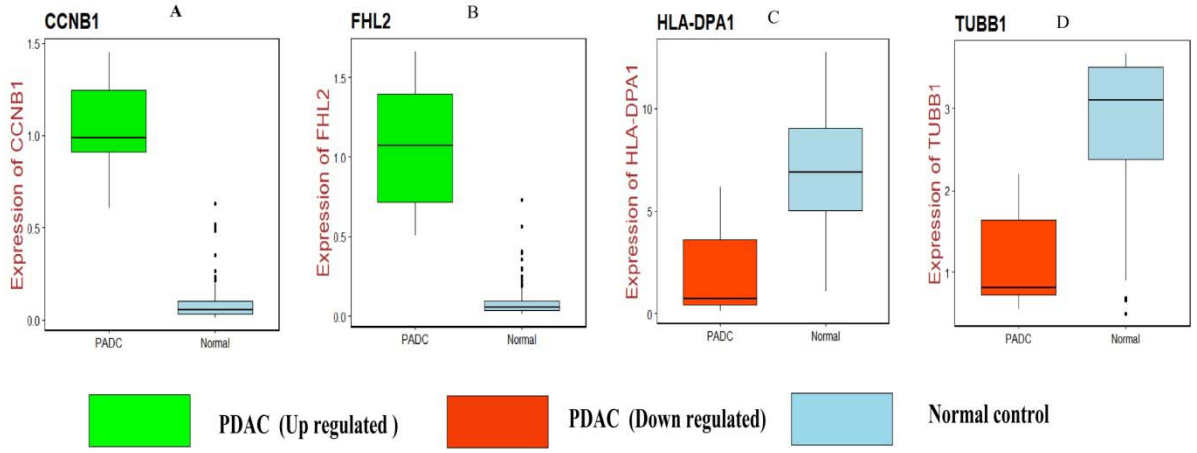

Fig. 12. Validation of hub genes by RT- PCR. A) CCNB1 B) FHL2 C) HLA-DPA1 D) TUBB1

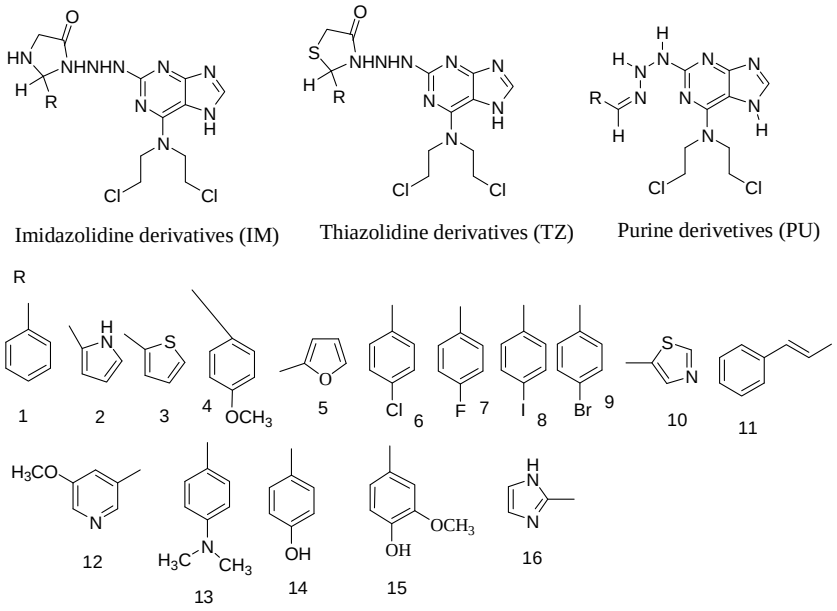

Fig. 13. Structures of Designed Molecules

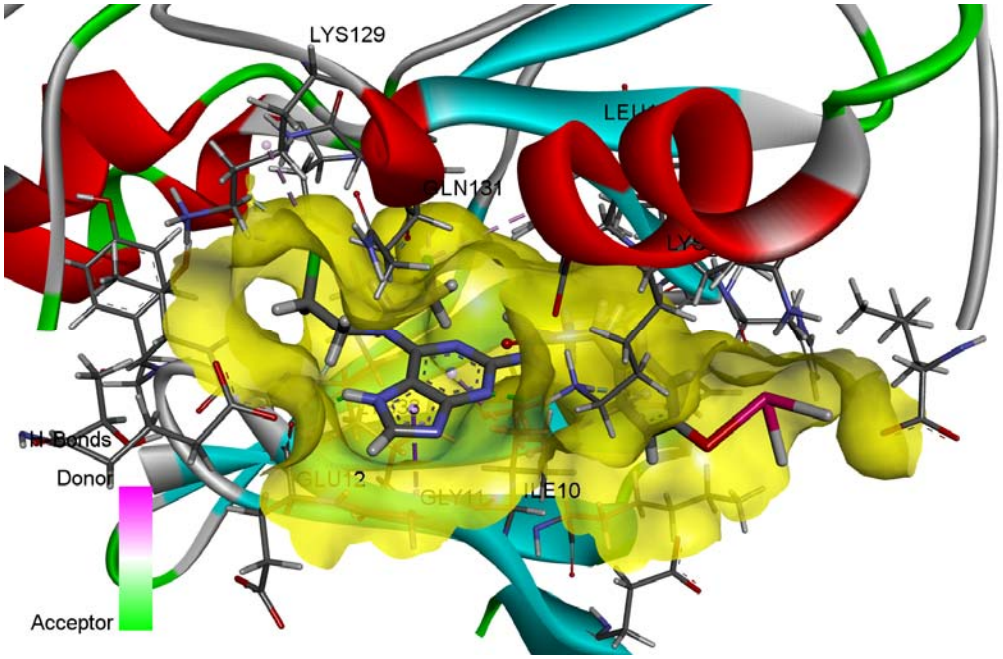

Fig.14. 3D Binding of Molecule IM 8 with 1H0V

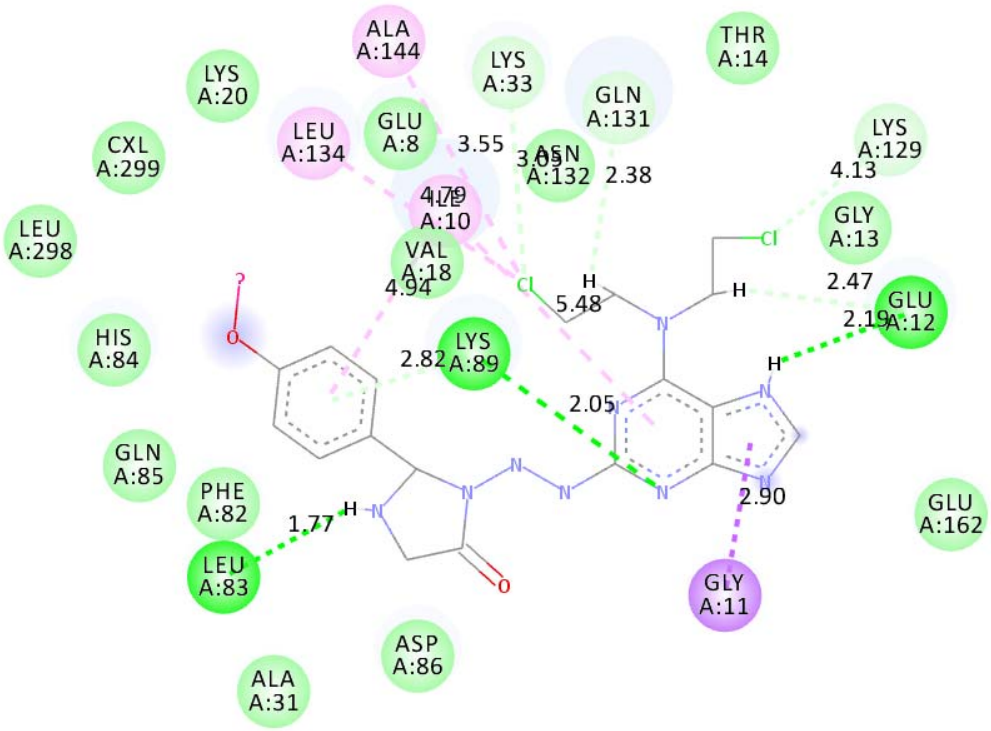

Fig. 15. 2D Binding of Molecule IM 8 with 1H0V